Fraunhofer
IPT

FRAUNHOFER INSTITUTE FOR PRODUCTION TECHNOLOGY IPT

DISCUSSION PAPER

THE RELEVANCE OF FUEL CELLS FOR MOBILITY APPLICATIONS

EXECUTIVE SUMMARY

As energy conversion systems, Fuel Cells (FCs) enable zero emission mobility and have advantages compared to battery-based powertrains for electric vehicles with high payload and high range requirements. Currently high system costs due to low volume production and technological uncertainty hold back a widespread market distribution.

Developments of production technologies and manufacturing processes for high production volumes are needed to establish competitiveness and market diffusion of the FC technology. Also, technological and regulatory issues have to be addressed. Aiming at economies of scale, an upscaling of the production volume is one leverage for reducing the manufacturing costs. Therefore, the topic of FC production has high potential for many different industries. Plant engineering as well as manufacturing industry may give efficient technological solutions to given problems by adapting common und well known processes. This projection of available knowledge may lead to quick improvements in manufacturing as well as improved value generation.

This study was conducted and published in two parts. The first part, covered in the previously published discussion paper "Future Energy Storage Systems for Mobility Applications" provides an overview of potential solutions for the manufacturing industry regarding energy storage and conversion systems. Those solutions were shown with regards to principle of operation and design, possible markets and manufacturing technology of specific energy systems. In particular, it emphasizes the potential of the promising FC technology for mechanical and plant engineering. The second part of the study, covered in this document, proposes a reference process chain for FC manufacturing and analyses it in the light of possible use cases, their economic feasibility and their technological suitability. This example aims to help manufacturing as well as plant engineering industry to conceptualize, optimize and scale up their FC stack production facilities by lowering technological uncertainties. The description and assessment of production technologies is done for the single components Bipolar Plate (BPP), Membrane Electrode Assembly (MEA) and Gasket for a planar stack design, in which these components are stacked on top of each other in an assembly process. The reference chain and the technology descriptions serve as a quick orientation for manufacturing companies in a very dynamic and complex technological field. The market diffusion of energy conversion and storage systems may thereby be amplified through new, more efficient and upscaled production processes.

By investigating both, market-oriented customer demands and technological perspectives in terms of state-of-the-art vehicles, a broad range of relevant use cases in commercial vehicles are identified and evaluated for their feasibility of FC applications. Key enabling factors for FC mobility solutions are the current technological limitations of battery electric drivetrains and political conditions for the reduction of Carbon-Dioxide (CO_2) emissions.

Due to their long range, dynamic payloads feasibility and extended uptime, coaches and distribution trucks shipping goods from logistic hubs to retail stores, hereinafter referred to as heavy duty trucks for hub store delivery, have been identified to be the most promising use cases. Their requirements profiles create suitable boundary conditions for the market entrance of FC technology in commercial vehicles. The market analysis indicates scalable design options and promising production volumes. We show that both use cases have sufficient market potential to outline technology concepts and share synergies among their driving profiles in terms of velocity, acceleration cycles and uptime.

The main components of a Proton Exchange Membrane Fuel Cell stack (PEMFC stack), namely BPP and MEA, are in the focus of the technical analysis for production. By analyzing technological concepts in terms of design, material and processes, multiple manufacturing technologies are discussed. The investigation and description of limiting factors are displayed in a theoretical process chain. The different production processes have been compared regarding advantages in cost, quality, and ease of production. Based on these technological and financial considerations, a process chain is proposed by Fraunhofer Institute for Production Technology IPT (Fraunhofer IPT). This chain involves manufacturing a metallic BPP by applying embossing as the forming technology and by coating with carbon in a Physical Vapor Deposition (PVD) process. For joining, laser welding is used and mechanical shear cutting for the cutting process. The proposed technology for manufacturing the MEA is a slot die coating procedure combined with an indirect Catalyst Coated Membrane (CCM) process. After the following FC stack assembly, End of Line (EoL) tests may be carried out which could be insulation or leakage tests. In addition to technological assessments, manufacturing has been analyzed from an economic point of view by developing a cost estimation tool for the analysis of upscaled production scenarios.

The analysis of possible use cases, the transparent overview about manufacturing technologies and production chains with a cost estimation aim to help identifying possible potentials for individual companies. Finally, the results are of relevance for manufacturing planning and optimization of the economies of scale in FC stack production giving a guideline to companies for profitable decisions on a new strategic alignment and investment.

Fraunhofer IPT is deeply committed to enhance the development of energy storage and conversion system technology and its production to facilitate the change to clean energy consumption. With more than 35 years of experience in applied research and development in manufacturing technologies and processes both in energy and mobility sectors, Fraunhofer IPT is well placed to achieve this ambitious goal through in-depth research and industry cooperation. Fraunhofer IPT uses this knowledge to develop solutions for production upscaling and to reduce technological uncertainty for industries by developing and investing in new production lines for FC systems. One way to lower uncertainty is to explain technologies and energy systems in more detail to enable manufacturers to project their knowledge onto energy system manufacturing.

TABLE OF CONTENTS

CONTENT OVERVIEW

DISCUSSION PAPER I
FUTURE ENERGY STORAGE SYSTEMS FOR MOBILITY APPLICATIONS

Motivation

High availability and **reasonable prices** of renewable energies as well as regulatory constraints are the main drivers of the **demand for energy storage technologies**.

Technology Selection

Analysis of the different energy storage technologies regarding their **suitability for deployment** in different **mobility applications**.

Energy Storage Solutions

Comparison of the **most relevant energy storage technologies** regarding their principle of operation, design, market potential and required manufacturing technologies.

Technology: PEMFC

Identification of the **key components** and the **manufacturing processes** required for their production as a basis for technical development.

DISCUSSION PAPER II
THE RELEVANCE OF FUEL CELLS FOR MOBILITY APPLICATIONS

REVIEW OF THE PRELIMINARY DISCUSSION PAPER AND INTRODUCTION

The shifting focus to electric power generation drives a rapidly evolving industry that is tailored around the design of new energy storage technologies. Therefore a comprehensive study on energy storage and system solutions was conducted. Its results are published in two parts. The first part, covered in the previously published discussion paper "Future Energy Storage Systems for Mobility Applications" serves as a quick guide for directors and managers in mechanical and plant engineering as well as manufacturing industry. It provides an overview of the most relevant technologies such as FCs, Lithium-Ion Batteries (LIBs) and Solid-State Batteries (SSBs) and, Supercapacitors (SCs). In-depth, the paper covers insights into these promising energy storage and system solutions their principle of operation and design, market potential and manufacturing technology. Key takeaways composed for manufacturing companies can be utilized in order to make profitably targeted decisions on new strategic alignment and investment.

Study Design

The introduced technological options for energy storage are examined regarding their suitability for application in several mobility scenarios. For the use in commercial vehicles, LIBs and FCs are evaluated based on their favorable technical characteristics in energy density and Technology Readiness Level (TRL). However, the costs of LIB packs show an exponential dependence on range capability. In contrast to LIBs, the investment costs for Fuel Cell Electric Vehicles (FCEV) develops approximately linear with an increasing range. This makes FCs the clearly preferable option in commercial vehicles such as long-range buses and trucks.

Main Takeaways

Among all of the evaluated FC technologies, the PEMFC shows the highest potential for application in commercial vehicles due to the low operation temperature, high electrical efficiency and high energy density. Core components of the stack are the MEA for chemical reactions and proton conductivity as well as the BPP for the distribution of the reactants and electrical contacts. Several technical challenges such as degradation of BPP and MEA materials exist. Another hurdle are the currently high production costs. Main cost drivers, namely production costs of MEAs and BPPs and potential levers are pointed out in the first paper. To address these challenges, upscaling of the production volumes and advances in manufacturing technologies are of great interest.

Challenges in Production Technology

Therefore, the second part of the study, whose results are covered in this discussion paper, deepens the analysis of production concepts and identification of potential levers specifically for the PEMFC. In order to define a best possible production processes, it needs to be customized to the design specifications of the FC. For determining these specifications, firstly possible applications in the mobility sector for PEMFC based drives were analyzed and the most promising ones selected. For this selection, the current situation of hydrogen infrastructure is considered an important factor. Secondly, the technical specifications of the FC stack were determined based on the requirements to the drive system of the selected applications. Based on these technical specifications, different production technologies were evaluated in detail. Furthermore, a production cost analysis complements the technical analysis. The study results, presented in this discussion paper, are intended to expand and deepen both understanding and knowledge about FC stack production of companies in the automotive industry and its suppliers, as well as companies in the mechanical and plant engineering industry.

IDENTIFICATION OF PEMFC USE CASES FOR COMMERCIAL VEHICLES

As a basis for selecting particularly appropriate production processes, an understanding of the specific technical requirements to PEMFCs for different applications is required. Therefore, potential vehicle types and operational scenarios (use cases) were identified and those of particular interest preselected for further investigation of technical requirements. This chapter provides a holistic overview of potential use cases of PEMFCs in the commercial vehicle sector that are evaluated by both quantitative and qualitative criteria and complemented by high-level market estimations. The outcome of this analysis and evaluation are two selected use cases which are presented in detail.

Use Case Overview and Method of Selection

This study examines a total of 20 potential commercial use cases of vehicles in commercial applications. An overview of the investigated use cases is given in Fig. 1. These use cases have been identified by systematically assessing the industry and its currently used vehicles. For further evaluation, they were organized in two dimensions. Vehicle types, in particular buses, trucks, as well as special purpose vehicles are shown on the horizontal axis and the predetermined application spaces, namely urban, regional and long-distance, are shown on the vertical axis.

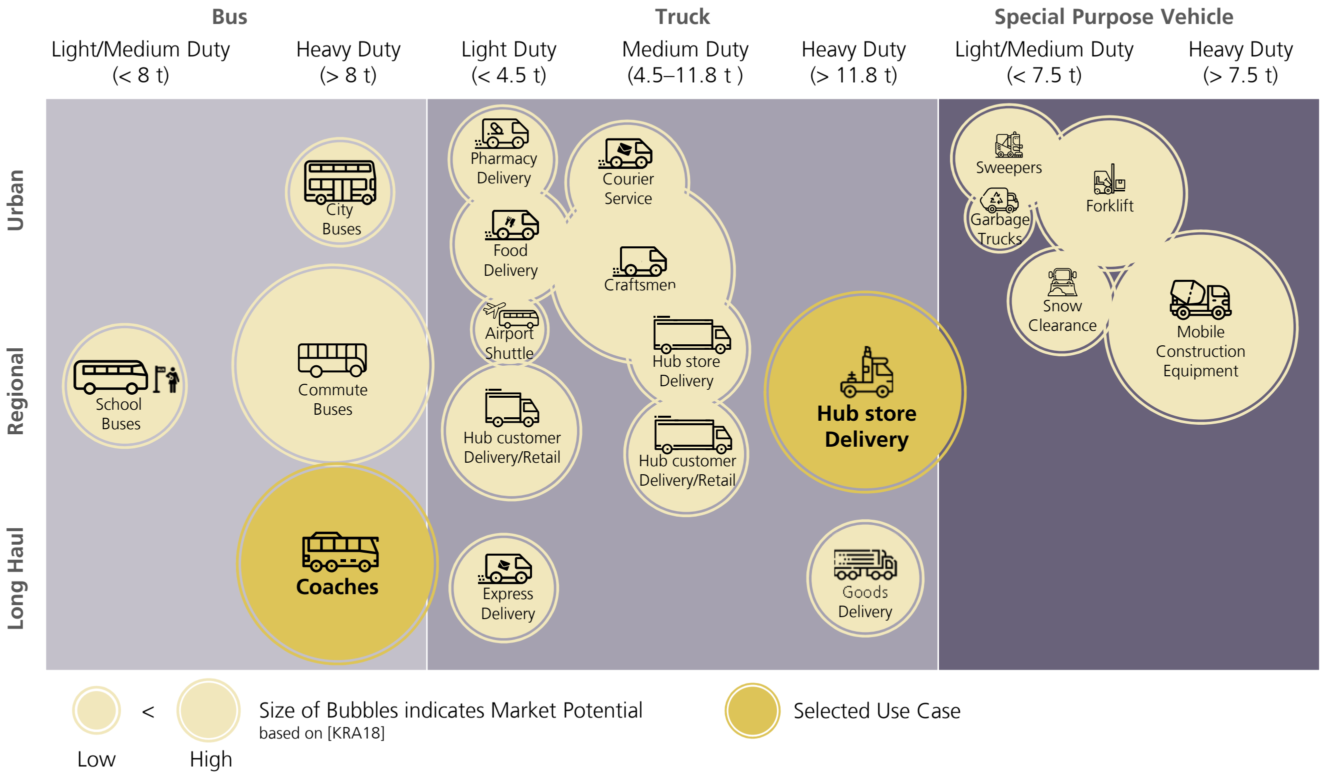

Fig. 1: Overview of Potential Use Cases for PEMFC Applications

Clearly the grade of suitability of FCs differs between the use cases. In order to identify the most promising of the 20 preselected use cases for FC application, firstly a description and specification of each use case was established. Secondly, a systematic comparison of the use cases on basis of identified customer needs, corresponding technology requirements as well as defined and weighted evaluation criteria (key indicators) was conducted. The quantitative evaluation of FC-suitability to customer and technology requirements was complemented by market sizing and concluded by a qualitative discussion of factors such as fueling infrastructure setup. As a result, the most suited and promising two of the 20 use cases for FC implementation were identified.

In addition to determining promising use cases for FC technology, another aim of this study is to avoid over-performing FC systems for the different use cases by identifying the use cases' minimal technical requirements based on a proceeding evaluation of the customer requirements. In this way, an economic optimum for the PEMFC application can be determined, which is an important condition to enable competitiveness in the market as soon as possible.

Evaluation Criteria

The key indicators range, power, uptime and emissions were defined and weighted to allow for a systematic analysis and evaluation of the use cases aptitude to FC technology. A brief definition of these four key indicators is provided in Fig. 2.

Range
The range is the average distance traveled during the uptime per day and per vehicle [km/d]. Values are based on the demand to driving distance, independent of current limitations to fuel quantity.
Source: [REU17]

Power
Power is the sum of the power need of the drive system and, if required, the power demand of cooling and heating units per vehicle [kW]. Drive system power is derived from data outlined by manufacturers of comparable vehicle types that have been specified by defined declaration modes, such as the European Union Directive guidelines for power measurement.
Sources: [EVO12], [DEL16]

Uptime
Uptime is the daily time share during which the vehicle is operated measured in hours [h]. Due to availability of data, assumptions on uptime are based on operating times of drivers per shift with multiple shifts and breaks per day. Uptime is typically restricted by locally varying legislative constraints regarding driver shift length.
Sources: [DHL20], [KUN17], [DUR13]

Emissions
Emissions include CO_2 emissions as well as noise emissions. CO_2 emission evaluation is based on the EU proposal of 2018. Noise emission measurements are compared for accelerating the vehicle at 50 km/h at full–load according to European standards.
Sources: [FUE20], [EUR18], [EUR70]

Fig. 2: Evaluation Dimensions of Use Case Selection

Use Case Specification

To specify customer requirements, an in-depth literature and market research was conducted. Major sources are data sheets of existing vehicles on the one hand and studies examining the actual application of vehicles according to each use case on the other hand. Assuming that current vehicle specifications give insights into requirements to future FC-powered vehicles, data from current vehicles and operational scenarios is utilized.

As an additional source, driving profiles were considered. An analysis and subsequent evaluation of use case-specific driving profiles was conducted. The driving profiles are visualized in the form of speed as a function of time or distance traveled. The data were obtained from the Vehicle Energy Consumption Calculation Tool (VECTO). Key indicators, such as average speed, were derived from the available data. [REX17]

The research resulted in a comparable set of values and information for each category (range, power, etc.) and every use case. This information is summarized in use case-specific portfolios as shown by example in Fig. 3, such as Fig. 5 and Fig. 7.

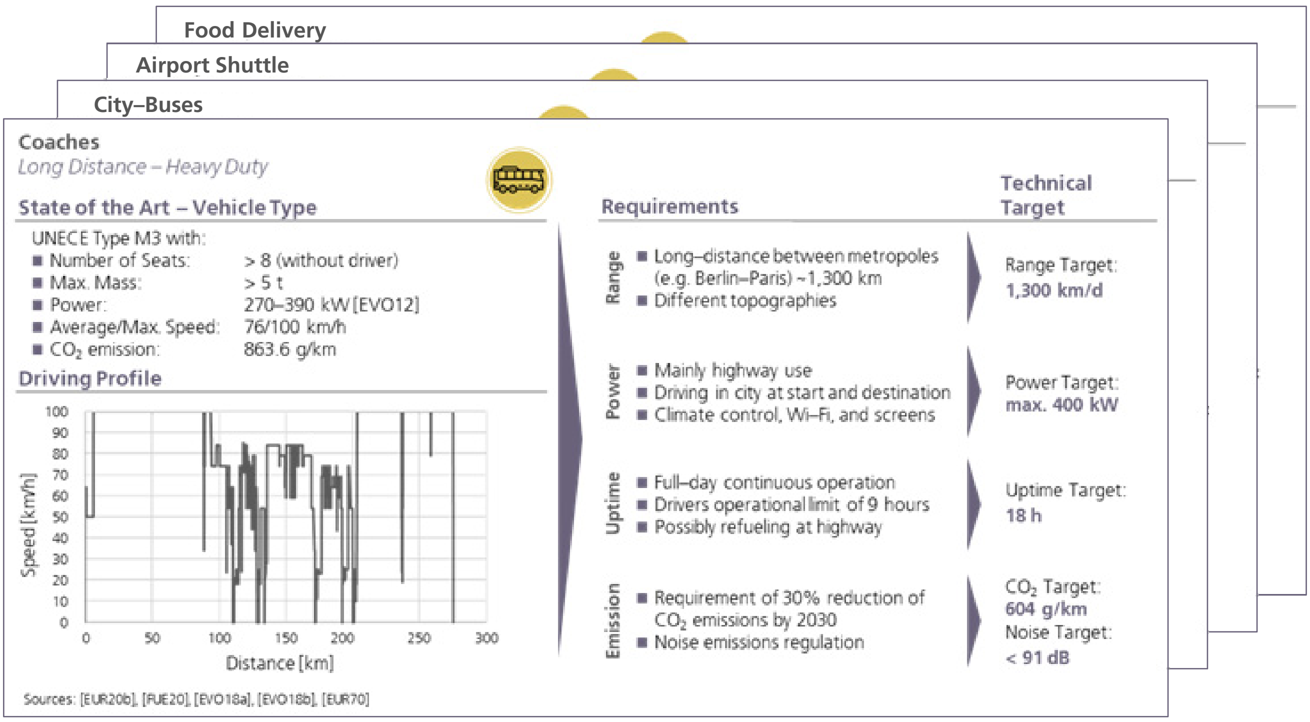

Fig. 3: Analyzed Vehicle Profiles per Criteria

Use Case Selection

Following the detailed description of the applications, they are evaluated in the above mentioned four dimensions to select those that are particularly favorable for FC electrification in terms of market demand and technical feasibility. All 20 use cases (see Fig. 1) are compared with each other on the basis of the acquired data. In order to achieve a selection even in the case of an ambiguous result, the criteria are weighted according to their relevance and in descending order. Only the most suitable applications are further pursued for each criterion.

To determine the weighting of the criteria, they are compared in pairs. Range is regarded as the most important criterion and is therefore rated with the weighting factor five of five. In this consideration, the range also depends on the driving times and the velocity of the vehicles according to their driving profile. Power and uptime are attributed the weighting factors five and four of five, respectively. Local noise and CO_2 emission reduction is a great future benefit of all FC driven vehicles as well as Battery Electric Vehicle (BEV) solutions. Emissions are less differentiating feature of FC powered vehicles and as a result, this indicator's impact on the evaluation of the use cases plays a minor role and therefore has the weight value three of five.

By structurally analyzing each criterion, a consistent focus on the most suitable application cases is achieved. The approach and results are outlined in Fig. 4.

Range

Regarding the range of each use case, it becomes clear that in-city applications are out of scope because their limited demand in range will preliminary be covered by BEVs as they are more suitable for short range application with a range of a few 100 km [BAU20]. Following this approach, the city-bus with FC-substitutes of catenary wires and BEV-applications are considered to be outside the scope. Similarly, the use case of a craftsman is not part of the further analysis. Their driving profile shows back-and-forth routes to customers in the nearby city where distances can be assumed as being not more than 80 km per day. Delivery services including the listed cases of pharma, food, and courier services are also outside the scope: a typical courier service, for example, delivers 200 parcels per day [RIC17], with a total of 90 stops per 100 km. This equals to an average distance of 225 km per day. Due to this relatively short range requirement combined with stop and go operation within the city and the possibility of night-time charging, common understanding is that BEVs are better suited in this context.

Power

The combined requirement of high range and high power cannot currently be addressed by any ecological-friendly alternative to conventional combustion-engines, e.g. BEVs have the issue of leaping battery weight with extended power and range. High power and energy requirements are primarily related to heavy duty vehicles. The resulting high weight of the battery is especially relevant for transportation-vehicles such as (heavy duty) hub store delivery because the high battery weight reduces the effective payload and thus significantly increases the operating cost per payload. The implementation of FC technology is therefore particularly attractive for these applications. Light and medium duty vehicles are considered out of scope due to reduced payload-sensitivity and current high feasibility of battery-powered vehicles. In this regard, the school bus is left out of further considerations due to the low power demands, complemented by the previously examined limited range of 120 km. Also, airport shuttle, express-delivery, light duty hub customer delivery and, medium duty hub store delivery are not considered due to reduced vehicle size and weight, which limits the payload sensitivity in relation to the heavier vehicle types.

Uptime

Long uptime with short refueling times is identified to be beneficial for the application of FCEVs compared to BEVs. Following this logic, the use case of medium duty hub customer delivery/retail is found to be out of scope due to an estimated uptime of 10 h and overnight runtime. Commute buses have a comparatively long uptime ranging between 10–20 h, but the downtimes in the depot and longer stops at terminal stations are predominantly adequate for recharging batteries. Additionally, the reduced power and range result in a rather unattractive use case for FCEVs.

Emissions

Based on the criteria of reducing CO_2 emissions, the entire area of special-purpose vehicles is excluded due to their special emission requirements, which are not comparable to the

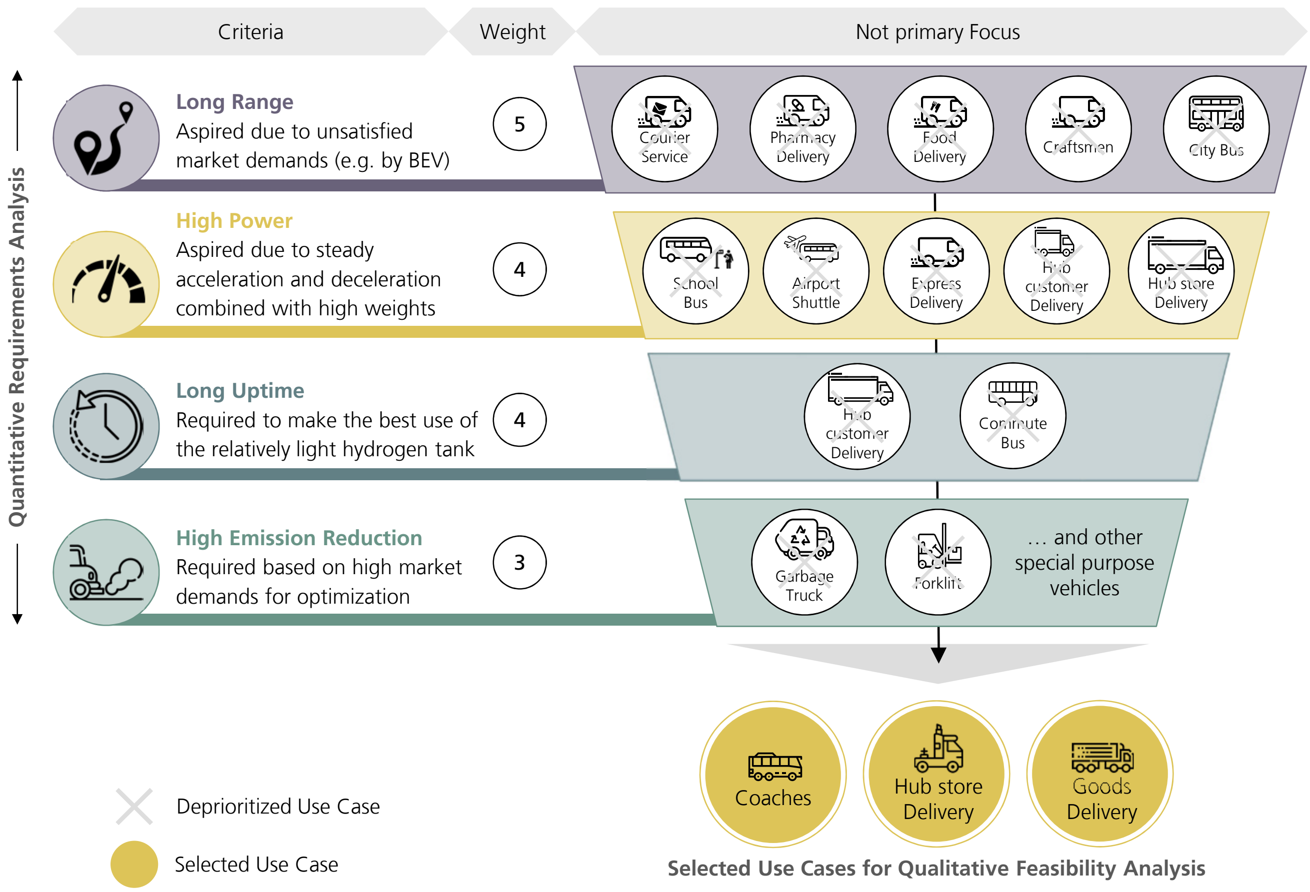

Fig. 4: Overview of Selection Criteria and Quantitative Evaluation

other applications. CO_2 emission targets with low reduction potential (< 126 g/km) are considered to be out of scope because of their limited impact on the overall weighted scoring. Furthermore, driving restrictions will most certainly be installed for vehicles with a high level of CO_2 emissions thus underlining the importance to focus on use cases indicating high reduction potentials. FCEVs share the advantage of low engine noise with BEV. Particularly in urban areas, these vehicles have significantly reduced noise emissions, since engine noise has a significant impact on noise levels at low speeds.

Market Estimation

Furthermore, market estimations enrich the information base for the use case selection. As no information on exact market sizes for the investigated use cases were available, a market estimation was conducted. The method for market estimation and excerpts of the results are described in the further course and also shown in Fig. 6 and Fig. 8.

The data is based on the German market in 2017 and was gathered and structured by a standard methodology. The key scale variable – from which next to other assumptions the market shares are deduced – is drawn from the reports of the Kraftfahrt-Bundesamt (KBA) under the category "Besitzumschreibungen". This term is defined as a transfer of ownership of two parties (consumer-to-consumer and business-to-consumer), i.e., selling used vehicles but also selling new vehicles preliminary owned by the manufacturer) [KRA18]. Secondary data, i.e., market shares and market sizes are predominantly drawn from Statista complementing the assumptions made per hierarchy level. Market shares for the specific use cases are deduced based on numbers available in relation to e.g., the average size of the industry, the weight of vehicle tailored to use case, the number of seats. A logical tree with assumptions per hierarchical level serves as the guiding framework throughout this estimation.

The results of the market sizing approach show considerable differences, as indicated in Fig. 1. For example, the airport shuttle use case is comparatively small due to the small-scale applications. On the opposite end, a high number of units of craftsmen vehicles are sold annually [WAG20]. Also, mobile construction machinery has a high annual demand which is due to a wide range of different vehicle types (crawler excavator, low loader, wheel loader, shovel excavator) and shorter life span.

Preliminary Use Case Selection

Those use cases that are particularly suitable for FC application in terms of market demand and technical feasibility have been selected. As previously described, the vast number of use-cases is considered of minor importance. The excluded use cases are displayed in Fig. 4 according to the key indicator, which had the most negative impact on FC-suitability. The preliminary selected use cases are coaches and hub store delivery (with and without cooling) as well as goods delivery vehicles. They will be further analyzed by a qualitative discussion.

Despite the large number of FC driven forklifts on the market, this application is left out of the further analysis. One focus of this study is the evaluation of FCs for the reduction of emissions. As this is not relevant for the operation of forklifts, this study concentrates on the cases coaches and hub store delivery.

Subsequent to the evaluation on basis of the four defined key indicators as well as the market analysis, further qualitative factors shaping the ecosystem of each use case were considered and are briefly described in the following.

The hydrogen refueling infrastructure was part of the consideration, due to its high relevance for success of hydrogen vehicles. Regarding the use case evaluation, the currently insufficient international hydrogen refueling infrastructure, as there are various routes across borders and countries without fixed hubs, and destinations are frequently served during operating hours, shipping in international long-distance operation with and without cooling (use case goods delivery) are considered a slightly less promising use case. In the Excursion: Hydrogen-Infrastructure, the status quo and influence of refueling infrastructure on the establishment of FC long-distance heavy duty trucks are presented and current developments and possible solutions are pointed out.

By contrast, for FC-based coaches and heavy duty hub store delivery, the general infrastructure setup is feasible as these vehicles frequently travel between the same hubs. For example, a coach bus travels the same routes over and over again, or the hub store delivery truck frequently travels between defined hubs and stores. It is assumed, that the installation of Hydrogen Refueling Stations (HRS`s) at frequently traveled locations is economically reasonable which mitigates one major customer concern of non-manageable infrastructure. Thus, FC-application is still evaluated suitable and promising for both use cases.

Also, regulatory aspects were considered for the use case selection. The ambitious CO_2 reduction targets require direct measures and actions especially for 4x2 truck-trailer combinations. This fact makes the heavy duty hub store delivery use case even more promising.

In the following, both finally selected use cases coaches and hub store delivery with and without cooling are described in more detail regarding their requirements and their market share.

Detailed View on Selected Use Cases and Market Estimation

Coaches

The use case of coaches can be described as the typical long-distance transport of passengers between metropoles. It is predominantly used for group tours as well as complementary inter-city tours by travel companies. The driving profile within the use case description serves as a basis for uptime, range, and power estimations. For the coaches, the customer requirements reflect a driving profile that combines city traffic and highway drives characterized by high-speed-intervals. The overall power demand includes additional electronic devices such as e.g., air conditioning. Further technical details, requirements of e.g. customers, and the technical targets are shown in Fig. 5. As the FC capabilities meet the requirements of the use case well compared to Internal Combustion Engine-Based Vehicles (ICEVs) and BEVs, this use case was chosen.

The market breakdown in Fig. 6 is based on the findings from the KBA study of new vehicle registrations in Germany [KRA18]. The total number of buses resold in 2017 serves as a key scale variable and stands at approximately 6,300 vehicles. The buses that are not sold within the transportation-industry, marked as "Other Industries", are excluded from the scope. The vehicle weight serves as another differentiating factor to further detail the market estimations. Buses of lower weight are assumed to be school buses. Moreover, the number of seats is another indicator to split up market volumes. The

Coaches

Long Distance – Heavy Duty

State of the Art – Vehicle Type

UNECE Type M3 with:

- Number of Seats: > 8 (without driver)
- Max. Mass: > 5 t
- Power: 270–390 kW [EVO12]
- Average/Max. Speed: 76/100 km/h
- CO_2 emission: 863.6 g/km

Driving Profile

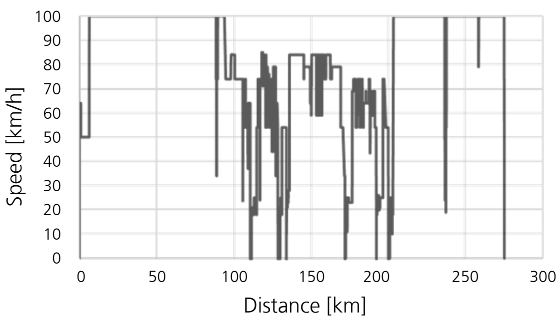

Sources: [EUR20b], [FUE20], [EVO18a], [EVO18b], [EUR70]

	Requirements	Technical Target
Range	■ Long–distance between metropoles (e.g. Berlin–Paris) ~1,300 km ■ Different topographies	Range Target: **1,300 km/d**
Power	■ Mainly highway use ■ Driving in city at start and destination ■ Climate control, Wi–Fi, and screens	Power Target: **max. 400 kW**
Uptime	■ Full–day continuous operation ■ Drivers operational limit of 9 hours ■ Possibly refueling at highway	Uptime Target: **18 h**
Emission	■ Requirement of 30% reduction of CO_2 emissions by 2030 ■ Noise emissions regulation	CO_2 Target: **604 g/km** Noise Target: **< 91 dB**

Fig. 5: Use Case Analysis Description Including Derived Technical Targets for Coaches

share in annual market volumes of school and city-buses is split from the total number of buses in the transport industry by the listed table of seats. To differentiate between regional commute buses and coaches, the share of the public and private sector is applied. Based on this approach the market for coaches comprises around 1,800 vehicles.

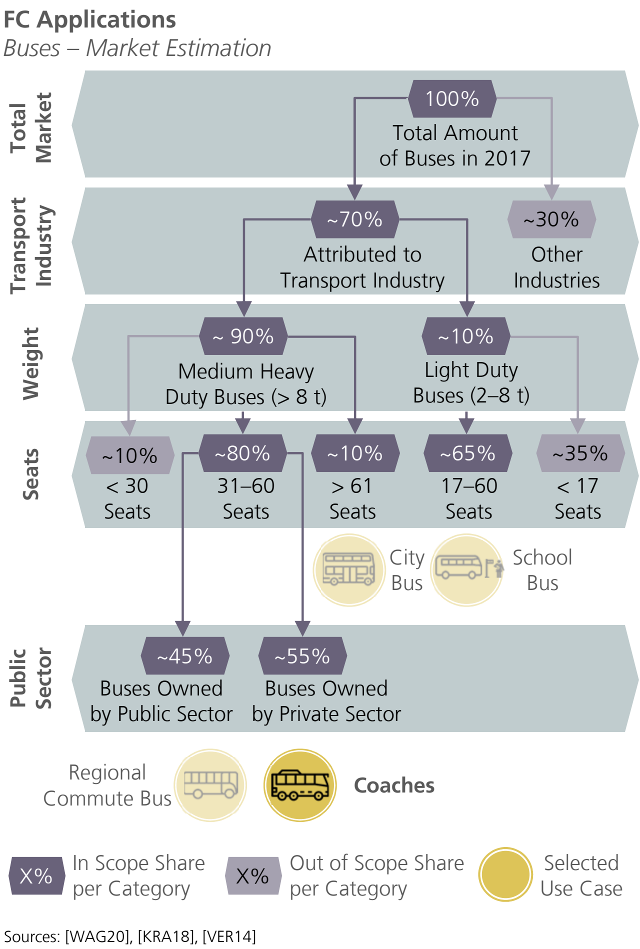

Fig. 6: Exemplary Market Analysis for Coaches

Heavy Duty Hub store Delivery

The use case of heavy duty trucks for hub store delivery in Fig. 7 refers to the daily delivery of goods from logistic hubs to stores within a city.

The presented driving profile reflects inner-city and highway repeating routes. Additional cooling is required and needs to be provided by the power unit of such a vehicle. The estimated yearly range of 130,000 km is broken down to at least 200 days of usage. Given a regulatory uptime of 8–9 h per driver, two-shift operation allows a total uptime of 16 h per vehicle. Taking loading and unloading into consideration, the daily distance of about 650 km is realized within around 9–10 h net driving time. Subsequently, the daily distance of about 650 km can be realized within the uptime of 8–9 h which is regulated by law. Additional time for loading such as shared vehicles among two different drivers allows uptimes of 16 h. These requirements are well met by FC capabilities unlike Internal ICEs and Batteries capabilities. Thus, this use case was assessed as suitable and promising for deployment of FCEVs.

Hub store Delivery

Regional Distance – Heavy Duty

State of the Art – Vehicle Type

Tractor–trailer combinations with

■ GVW*/Max. Payload:	36.3–40/19.3–25.5 t [ROD18, DEL16]
■ Power:	322 kW [RIC17]
■ Average/Max. Speed:	60/90 km/h [FUE20, REX17]
■ CO_2 emission:	937.9 g/km (35.7 l/100 km) [RIC17]

Driving Profile

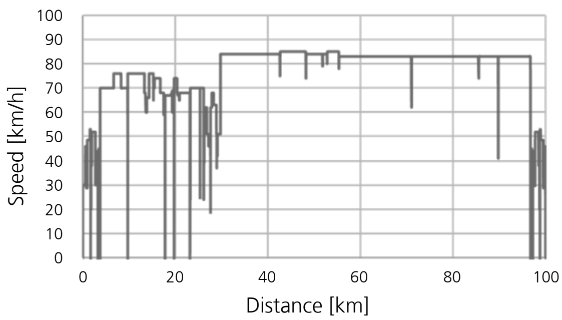

*Gross Vehicle Weight

Sources: [FUE20], [ROD18], [RIC17], [REX17], [DEL16], [EUR70]

	Requirements	Technical Target
Range	■ Daily driving distance: 650 km ■ Annual activity range: 130,000 km Repeating inter/inner–city highway	Range Target: **650 km/d**
Power	■ Transport heavy freight, large volume ■ Additional power for cooling required ■ Middle average speed	Power Target: **max. 325 kW**
Uptime	■ High utilization demanded ■ Easily available refueling stations ■ Middle stop time to meet schedules	Uptime Target: **16 h**
Emission	■ Requirement of 30% reduction of CO_2 emissions by 2030 ■ Noise emissions regulation	CO_2 Target: **657 g/km** Noise Target: **< 91 dB**

Fig. 7: Use Case Analysis Description Including Derived Technical Targets for Heavy Duty Hub store Delivery

In analogy to the market size estimation for coaches, a market estimation for hub store delivery is estimated. The determined market shares are shown in Fig. 8 and the market is found to be equally significant. The total market of around 350,000 leads to approximately 1,300 heavy duty hub store delivery trucks.

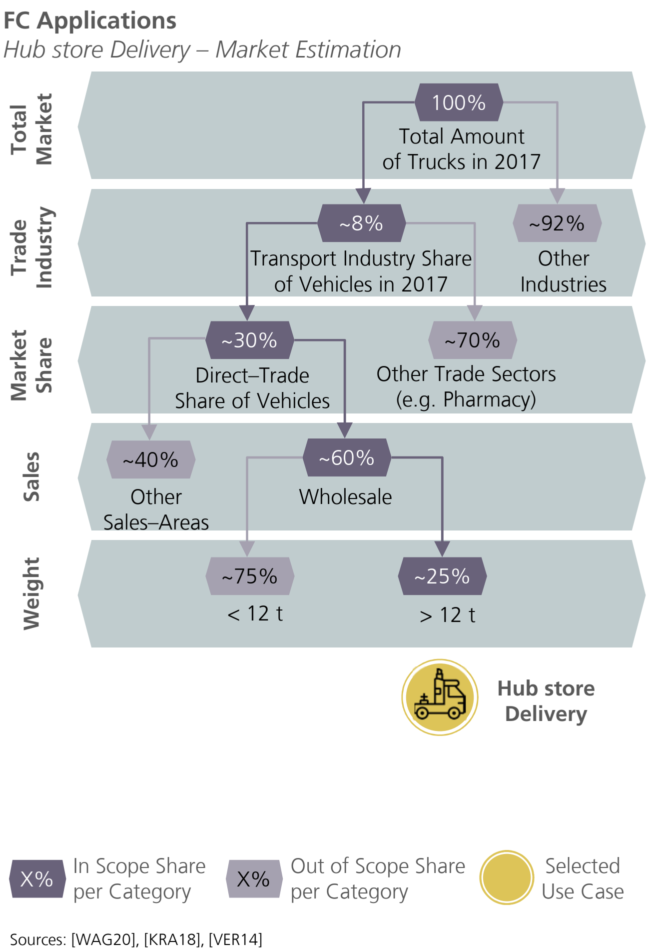

Fig. 8: Exemplary Market Analysis for Heavy Duty Hub store Delivery

EXCURSION: HYDROGEN-INFRASTRUCTURE

Influence of the Infrastructure on FCEV Technology Establishment

FCEVs in analogy to ICEVs and BEVs need recharging. Recharging of BEVs can take place at public stations as well as private electrical outlets at home. The existing electric infrastructure can be utilized. However, significant investments for extending the existing infrastructure are required for a wide electrification of the mobility sector. On the contrary, hydrogen refueling inevitably requires an entirely new infrastructure to be provided. Due to this imperative, commercialization success of FCEVs is largely dependent on the availability and convenience of hydrogen refueling to the user. Furthermore, as a part of the Total Cost of Ownership (TCO), refueling must be provided at a reasonable price. These requirements to the design of the network of HRS's significantly vary depending on the driving profile and vehicle type of the use case (see description of use cases chapter "Identification of Potential Use Cases").

Requirements to the HRS Network Regarding Spatial Distribution, Total Capacity and Refueling Protocols

In contrast to short-distance and locally operated trucks and buses, an extensive public HRS network is required for long-distance heavy duty trucks and buses due to their non-return-to-base nature [KLU19].

In addition to the driving profile, hydrogen tank systems vary for different vehicle segments as displayed in Fig. 9. Passenger cars and light duty vehicles typically use SAE J2601 (Society of Automotive Engineers) standards for fueling protocols. Storage initially took place at 350 bar, but has shifted to a 700 bar standard, which enables longer ranges being applied [EHR19]. For medium duty and heavy duty vehicles, there is currently no existing standard. The 350 bar storage currently used by munic-

Vehicle Segment	Passenger Cars & Light Duty Vehicles		Medium & Heavy Duty Vehicles	
Pressure	350 bar	700 bar	350 bar	700 bar
Standard	SAE TIR J2601		No standard*	No standard
Max. Allowed Tank Capacity	6 kg Hydrogen	10 kg Hydrogen	N/a (Assumption**: ≈60 kg Hydrogen)	
Hydrogen Specific Volume (@ 300 K)	0.04 m^3/kg	0.025 m^3/kg	0.04 m^3/kg	0.025 m^3/kg
Hydrogen Volume (@ 300 K)	0.24 m^3	0.25 m^3	2.6 m^3	1.6 m^3
Charging Time (A-Type Dispenser)	6 kg/min	2 kg/min	6 kg/min	2 kg/min

* Only guideline for buses
** Users require approximately 60 kg Hydrogen for Long-Haul

Source: [KLU19]

Fig. 9: Characteristics of Hydrogen Tank Systems for Different Vehicle Segments

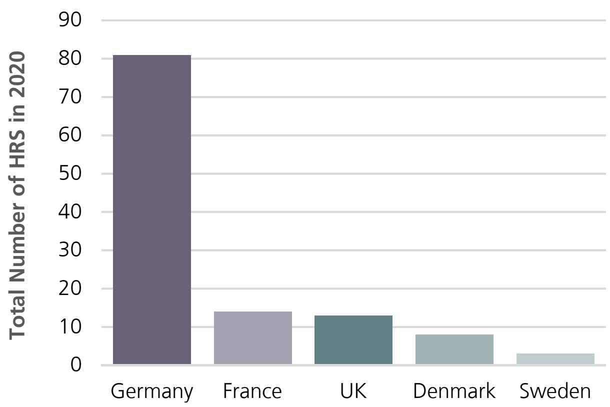

Source: [FUE20]

Fig. 10: Total Number of HRS's for the Top Five Countries in Europe in 2020

ipal vehicles and city buses might not be suitable for heavy duty vehicles with high capacity on-board tanks (>50 kg hydrogen) as these tanks would become very large and therefore would take away valuable cargo space [EUR19, KLU19].

In general, requirements for refueling differ between passenger cars and light duty to medium duty, and heavy duty vehicles among others due to incompatible dispenser and compressed hydrogen storage system capacities. Long-haul heavy duty vehicles require tank capacities up to approximately 60 kg hydrogen compared to 6–10 kg hydrogen of passenger cars and light duty vehicles. Therefore, HRS's intended for passenger cars cannot immediately be used for heavy duty vehicles. However, technical upgrading is feasible and reasonable under certain conditions (compare note on optimal location below).

HRS for Passenger Cars **HRS for Buses & Trucks**

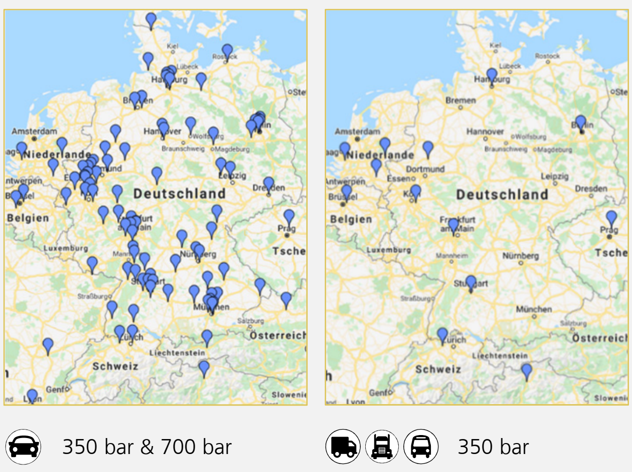

Source: [EUR20a]

Fig. 11: HRS's for Passenger Cars (350 and 700 bar) (left) in Comparison to Buses and Trucks (350 bar) (right)

Current Network of HRS's and Planned Developments

Countries across the world are starting to drive hydrogen-based mobility by national policies, subsidies and push by OEMs. Japan and South Korea are two key countries driving the development of hydrogen-based mobility. South Korea currently leads the global market for FCEV, while Japan is the country with the most HRS's in place (111 in 2019). So far, FCEV have not played a significant role in China, however this is expected to change quickly. In the long term it is going to be the country with the largest amount of HRS's in the region and the adaption will be driven primarily by commercial vehicles. California is leading the FCEV market as well as the infrastructure expansion in North America. In Europe, the development is led by Germany, where the largest infrastructure can be found and the hydrogen economy is strongly aided by the government. [GLO20]

434 HRS's currently exist worldwide (status as of 2020) [LUD20]. Of these, about 350 HRS's are public while the others are reserved for closed user groups or vehicle types such as buses. Of these 434 stations worldwide, 148 are currently in operation in Europe and most of these in Germany (see Fig. 10). [TÜV19] Most of these stations in Germany are for passenger cars (see Fig. 11).

To close existing gaps in the HRS's infrastructure for passenger cars, several strategies have been developed and commitments been made. One of the most eminent solutions is the so-called "hydrogen highway", which projects refueling stations at main routes and highways and additionally HRS clusters in major metropolitan areas. [H2M20] In Germany, six companies (Air Liquide, Daimler, Linde, OMV, Shell and Total) have established the joint venture H2 MOBILITY Deutschland GmbH & Co. KG. The project is government-sponsored and supported and advised by Original Equipment Manufacturers (OEMs) such as BMW and Toyota. The H2 MOBILITY roadmap comprises up to ten stations in each of the six urban regions of

Hamburg, Berlin, Rhine-Ruhr, Frankfurt, Stuttgart and Munich as well as hydrogen corridors along the connecting highways. In total 400 HRS's are planned to ensure the development of a complete national hydrogen infrastructure network for passenger cars in Germany by 2023. [NOW20] In Europe, a compound annual growth rate of 35 % till 2027 in HRS's for passenger cars is estimated for the case that all current plans are realized (see high scenario in Fig. 12) [LUD17].

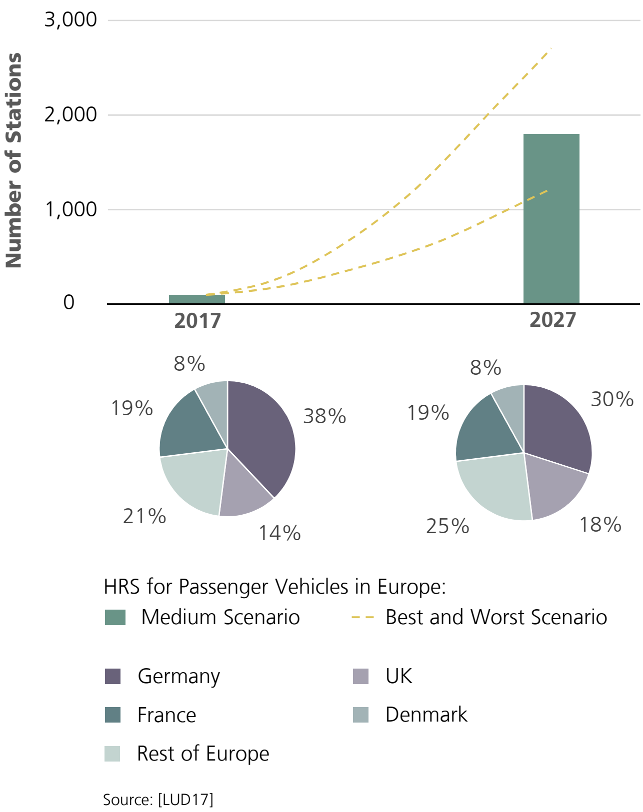

Fig. 12: Projected Development of Number of HRS's for Passenger Cars in Europe (Low, Medium and High Scenario)

In 2018, worldwide already over 10,000 Fuel Cell Electric (FCE) cars have been in circulation. FCE buses are today in the phase of early commercialization, while FC-powered trucks of various payload classes are mostly being developed and tested with a view to market launch in the near future. [EHR19] However, first FCE trucks have recently entered the market. Thus, more and more FCE buses, FCE trucks or FCE range extenders are deployed. More than 400 FCE buses are operating today in the United States, Europe and China [SUS19]. In 2018 over 500 FCE trucks have been deployed in China [BAL18]. In contrast to Europe and other countries, China has targeted buses and small delivery trucks first. In the past years, increasing activities in the use of hydrogen as fuel for trucks have also been visible in countries outside China. In the USA for example, Nikola Motor, Hyundai, and Toyota have been working on FC-powered trucks and their refueling infrastructure and Hyundai has agreed to supply 1,000 hydrogen FCE trucks to Switzerland from 2019 to 2024 [LEA19, TÜV19].

While the HRS network for passenger cars is projected (based on commitments and current state) to be well developed as described above, only few HRS's exist for buses and trucks (with 350 bar systems) (see Fig. 11) [EUR20a]. Furthermore, it needs to be stated, that while in California, USA, many stations have been built to be able to serve both passenger and heavy commercial vehicles, this is not the case in general. Therefore, refueling infrastructure of long-haul heavy duty FCEVs is practically non-existent and needs to be urgently arranged. [HAL19]

Infrastructure Long-Haul Heavy Duty Buses and Trucks

Dependent on the type and use case, vehicles have different driving profiles as described above. While commercial short-distance freight vehicles or buses mostly return to a depot where these fleets can be refueled, long-haul heavy duty vehicles are commonly driven 650 to 1,600 km per day, and cannot be refueled in a depot in a centralized way but require a broad HRS network. [HAL19] Current heavy duty FCE trucks have ranges of more than 320 km (Hyunday XClient (in production)) to 1,200 km (Nikola Motors Two (announced for 2021) [WAT20]) which require an adjusted frequency of HRS's occurring on their routes.

Kluschke et al. estimate heavy duty traffic intensity is locally resolved and, on this basis, the total number and optimal locations for HRS's for Germany is based on an optimization model. The result is 90 HRS's with a volume of around 1,000 to 66,000 vehicles per day. As regulations and approval procedures increase when operators store above 30 t hydrogen, a second proposition with this limit has been developed, where the required number of HRS's increases to 125. Currently existing HRS's (mainly passenger cars) are displayed in Fig. 13 as white dots. In both investigated cases, the distribution of the necessary HRS's locations appear to be quite different from the existing station locations (see Fig. 13). [KLU19]

Potential Station Locations without Capacity Limit

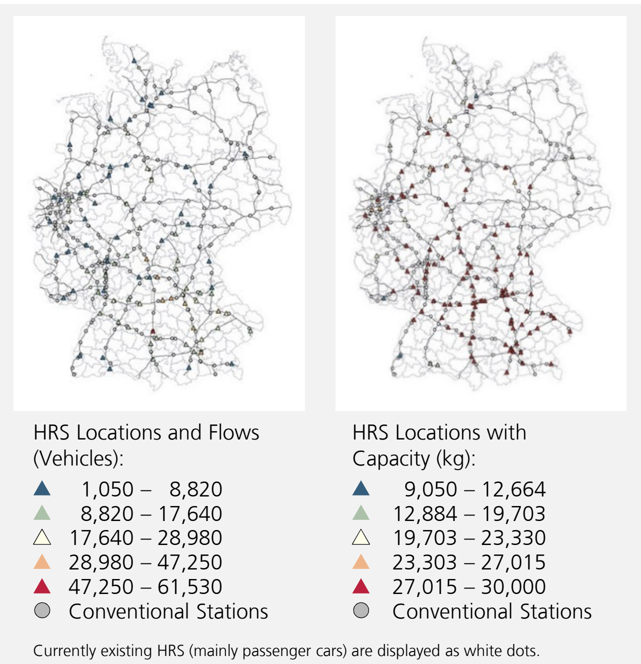

Source: [KLU19]

Fig. 13: Estimation of Optimal Number of Locations of HRS's in Germany without (left) and with (right) Restriction of Maximal 30 t Capacity

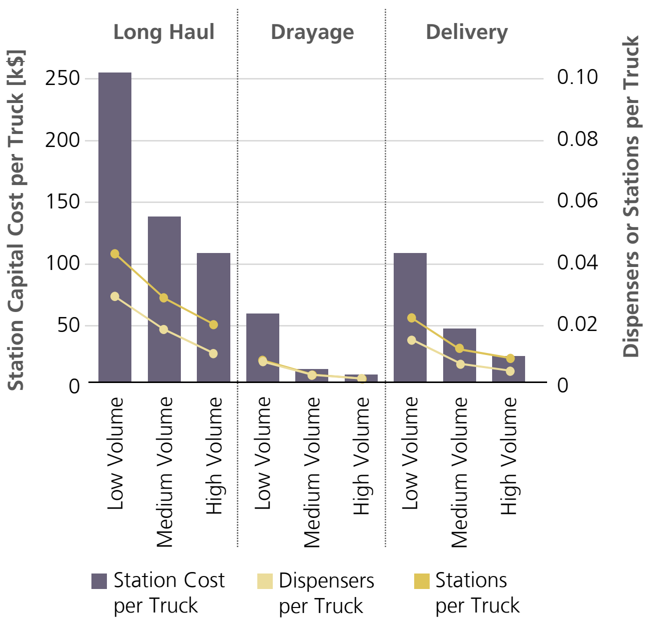

Source: [HAL19]

Fig. 14: HRS Cost Depending on Volume and Truck Type

Refueling Costs as Part of TCO

For a successful technology to be established, cost of fuel and HRS infrastructure as part of the TCO need to be competitive. Today, most hydrogen is produced from fossil fuels and a change to green hydrogen is impeded due to higher production costs. As of this date, renewable hydrogen produced from electrolysis costs approximately 6 USD/kg and could drop to 2–3 USD/kg by 2030 under average conditions. Besides production costs, hydrogen costs at the pump also include distribution and delivery at a HRS. [HYD20] Centralized, large-scale production is cost-efficient but requires additional distribution. Hydrogen is typically distributed as pressured gas in trucks or gas pipelines as well as liquefied for long-distance transport. A pipeline network is related to high initial investment cost [HYD17], while road transport of hydrogen is associated with regulatory hurdles (e.g. in vehicles on bridges and tunnels). Provision at HRS's make up for the largest share, currently contributing about 5–6 USD/kg [HYD20].
Costs per HRS mainly depend on capacity (kg/d), pressure and hydrogen production site (delivery or on-site production). Cost for a HRS currently amount to about 2–3 million USD. A reduction of HRS costs to a price comparable to conventional refueling stations is anticipated. [BAR19]

The station costs per vehicle scale mainly with the number of stations per vehicle. In 2018, worldwide over 10,000 FCE passenger cars have been in circulation which corresponds to an average utilization of stations of more than 0.1 stations per car (in Germany) and less than 0.01 stations per car in the United States [ANT19]. A realistic future scenario of 1*10-3 stations per passenger car and the current price per station would then result in infrastructure related costs of 150–1,000 USD per passenger car.

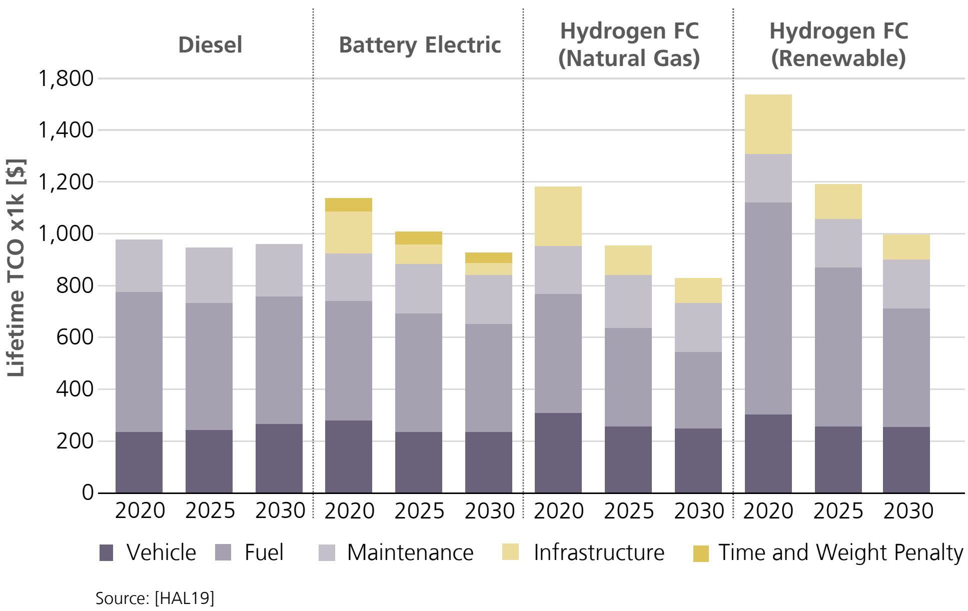

Fig. 15: Share of Infrastructure and Fuel Related Cost and Other as Part of the TCO for Diesel, Electric, and Hydrogen FC Long-Haul Tractor-Trailers

However, the number of heavy duty trucks and buses is currently significantly lower than the number of passenger cars. In 2019, Hall and Lutsey investigated costs associated with the required hydrogen infrastructure for three applications (long haul, drayage and delivery trucks) and three deployment scenarios: low-, medium-, and high-volume namely the deployment of the first 100, 1,000 and 10,000 trucks, respectively [HAL19]. Station costs for long haul high duty trucks decrease from about 250,000 USD in a low volume scenario (0.04 stations per truck) to 100,000 USD for a high volume scenario (0.015 stations per truck) (see Fig. 14). Costs decline similarly for the other two applications with increased number of trucks. However, especially for long haul trucks, infrastructure-associated costs stay at a high level. In Fig. 15, these infrastructure related costs are set in relationship to the other costs making up for the TCO. A high volume infrastructure scenario as well as lowered hydrogen production costs (from renewable energy) are significant factors besides the selling price of the vehicle for reaching TCO comparable to ICEVs and BEVs in 2030. This makes funding and fiscal incentives even more important, so that the vehicles do not fully bear to these associated infrastructure costs as assumed in the report by Hall and Lutsy [HAL19].

Regulations Concerning Green Hydrogen Production and Refueling Infrastructure Costs

As the German government is convinced that hydrogen will play a vital role in order to reduce CO_2 emissions by 55 % by 2030 and up to 95 % by 2050 in all energy consumption sectors it elaborated its National Hydrogen Strategy (NHS) in 2020 [FED20]. The sustainable, efficient, reliable and affordable production of green hydrogen is one of the central goals of this strategy. Concrete measures to reach this goal are defined in the NHS. One central measure is to embed the use of green hydrogen as an alternative renewable from the EU Renewable Energy Directive (REDII) into German law. Furthermore, an introduction of CO_2 pricing for fossil fuels in transport is foreseen as part of an improved framework for the use of electricity from renewables. According to a study by PwC, CO_2 pricing will be a key guiding instrument in order to establish hydrogen as an alternative energy carrier [NEU20]. Additionally, a reduction of the surcharge defined in the German Renewable Energy Sources Act (EEG) is planned. In addition, it is taken into consideration to exempt electricity used for the production of green hydrogen from taxes, levies and surcharges. Overall, the business environment shall be attractive for companies operating plants for the production of green hydrogen. Furthermore, considerable funding is provided. Funding from the Energy Climate Fund (ECF) and the National Innovation Programme for Hydrogen and Fuel Cell Technology (NIP) are available for all technologies including hydrogen applications until 2023. 1.1 billion EUR from the ECF will be provided for the development of and funding for the production of electricity-based fuels. Additionally, 3.4 billion EUR from the ECF will be granted for the construction of a refueling and charging infrastructure. [FED20] Thus, chances for significantly lower production costs of hydrogen from renewable energy as well as for refueling infrastructure in the near future seem high.

Conclusion

Long-haul road-freight transports are responsible for a large share of greenhouse gas emissions. The substitution of diesel heavy duty vehicles for long-distance road transport is a large lever. In contrast to FCE passenger cars and buses, FCE heavy duty trucks have only recently been deployed with a still small total number. Nevertheless, the number of FCE heavy duty trucks is believed to be significantly on the rise in the next years. However, a sufficient HRS infrastructure has not yet been established for these trucks.

As the commercialization success of FCEVs is strongly dependable on the availability of a cost-effective hydrogen fueling infrastructure, vehicle manufacturers, hydrogen providers and government need to work together to create a sufficient infrastructure. Due to the recently passed NHS among other regulations and programmes, a significant reduction of green hydrogen production cost in the near future appears probable. Partnership among these players has been extending the light duty hydrogen network in Germany (e.g. H2 Mobility). This strategy may also be useful for the heavy duty market.

The existing HRS infrastructure for passenger cars and short-distance commercial vehicles might be technically adapted to be able to serve heavy duty trucks and buses where reasonable. Furthermore, the government needs to lower regulatory barriers that slow down new HRS's built up (as well as hydrogen transport). Furthermore, first-movers, who build up HRS's are faced with high initial costs and a high risk. These circumstances need to be addressed by e.g. governmental financial support.

In addition, hydrogen and HRS costs are significant levers for TCO reduction. For a high volume scenario, TCO are projected to be comparable to diesel and BEVs.

DERIVATION OF TECHNICAL REQUIREMENTS FOR THE FC SYSTEM

The desired FC performance is a relevant technical requirement to be considered in order to guarantee the operation feasibility of the use cases selected in the previous chapters. However, the power output itself cannot be considered isolated to fit the driving and load profile requirements. Additional boundaries like the desired operation strategies (dynamic properties), auxiliaries, regulations, etc. need to be included. Thus, by identifying the most suitable level of power output per FC to be applied in synergetic use cases corresponding to the requirements and market demands, the quantitative production targets for the FC can be determined (i.e. number of BPPs, MEAs required). These requirements serve as input variables for a final layout of the production line in the later process.

In this chapter the following aspects are derived sequentially: firstly, the most suitable operation strategy (dynamic FC, static FC, plug-in / range extender) predominantly defined by range and power necessities will be identified. Furthermore, most feasible power demand depending on the previously defined operating strategy per FC will be determined in order to serve the most promising market demands in synergetic pre-selected applications. Finally, the previous considerations are used to deduce a quantitative estimation for the production of FCs (MEA, BPP) and auxiliary components.

The considerations in the chapter above outlined that specifically the selected cases of long-distance coaches and heavy duty hub store delivery showed similar driving profiles in terms of range, velocity and acceleration frequency. The preselected use case of hub store delivery and coaches both show city usage with frequent stop-and-go portions, complementary payload fluctuations by passenger or freight, but also highway drives at constant high speed. Power demand is here not completely steady but peak power is barely necessary and comparable to the average power (see Fig. 5 and Fig. 6). Optional additional power for thermal systems leave a bandwidth of power requirements of 325–340 kW for hub store delivery and 370–400 kW for long-distance coaches.

The performance considerations and furthermore the operation strategies have been treated only marginally and therefore are examined in more detail in this section.

Three operation strategies of FC driven vehicles are possible: dynamic FC approach, static FC approach, plug-in or range extender approach (see Fig. 16). They all differ in the share

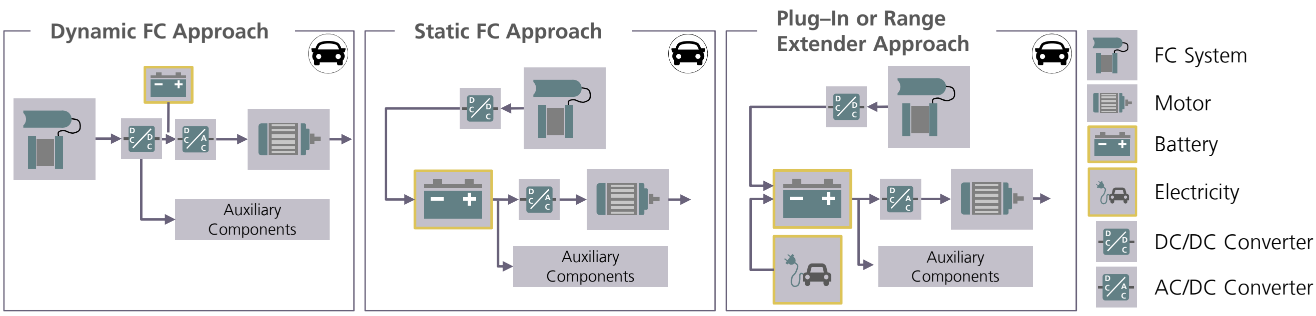

Source: [WIL17]

Fig. 16: FCEV Architectures

of FC and battery and offer up- and downsides with regards to peak power, range, useability and durability. The main difference between battery and FC is the ability to quickly adapt to high gradients of electric currents. Batteries are able to deliver high currents without preparation nor is cutting of electricity a problem. Gravitational power density is higher for hydrogen which is why ranges of FCEV are higher than similarly heavy BEVs. Combining the different technology specific features, the already mentioned strategies may be derived. None of those need to be analyzed for which strategy suits best for the specific case. In the dynamic FC approach, the electric drive motor is majorly fed by the FC stack. A small battery is installed for the vehicle start-up or for peak power supply. In this configuration, the FC operation must satisfy the dynamic changes in the load profile. Usually, the FC power is close to the electric motor power. To supply the FC with hydrogen along the considered range of 1,300 km for buses and 650 km for delivery trucks, this architecture results in more complex and dynamic Balance of Plant (BoP) component operations and might therefore lead to durability issues. It is however the densest power set up due to the energy storage via hydrogen compared to hybrid systems. The dynamic approach is best suited for completely steady power requirements. [BRI11]

In the static FC approach, a FC and a mid-size traction battery that allows the FC to follow a softened power profile are utilized. This interplay opens up opportunities to increase the overall efficiency of operation and durability due to reduction of load changes especially for more dynamic use case load profiles. The FC is designed to meet average load requirements supported by a larger battery which comes with higher weight and costs and thereby worse weight efficiency compared to the dynamic profile.

Plug-in or range extender vehicles are based on the battery as the main energy source which can be charged externally and provides full electric range. Using this configuration, it is possible to establish different battery recharge strategies; in particular the batteries can be recharged when the electric motor does not require any load, i.e. during the stops and at the loading station [BRI11]. In this case, the FC works in optimal operation conditions at a fixed power, avoiding fast changes in the load profile, which comes with a reduction of degradation mechanisms. The FC only covers a fraction of the overall system peak power. This is a major aspect in durability considerations of the FC and a reduction in terms of stack size as well as hydrogen storage amount especially for dynamic use case load profiles. [BRI11]

Static FC, dynamic FC and plug-in or range extender approaches fulfill different use cases. Dynamic FC approaches require the biggest effort in terms of operation strategy and therefore overall system costs in the FC system but static approaches come with larger batteries and thereby worse gravimetric power density. Many sources indicate that static FC approaches may however lead to higher efficiencies and durability depending on the use case (especially use cases with changing load requirements). [JAM18b, HÖF17, MAR16]

Fig. 17 illustrates the efficiency of the FC stack and the FC system when including components of the BoP, Balance of System (BoS) and auxiliaries [HÖF17]. The FC stack has its maximum efficiency between 40–60 % of the load factor [BRI11]. Efficiency drops at deviating load factors which is why, when unsteady driving profiles are presumable, a reasonable sized battery system should be added to operate the FC at maximum efficiency. For driving profiles with a small difference between maximum and average power as in the selected use cases, a dynamic approach with a small-sized traction battery may be beneficial due to the relatively low alteration of power demands and the aim of high durability.

Based on optimal efficiency and the overall FC system costs, the final design of the FCs will be shaped to fit the optimal load requirements of the use cases.

The power of the FC for the selected use cases ranges from 325 kW to 400 kW. Apart from the combination with other forms of energy storage systems like batteries, you may evaluate a combination of multiple smaller stacks to reach the demanded power. Smaller stacks may lead to easier replacement in case of defects but also offer possibilities with regards to productivity improvements and even satisfying multiple different use cases with the same product.

Fig. 18 shows an overview of different available FCEVs which are clustered via the FC Power and the vehicle weight. Different power clusters at 168 kW, 263 kW and 360 kW are shown by the dotted lines. The least common divisor with regards to FC Power is 90 kW and could work as a standalone FC which may be combined to reach the individual power clusters [JAM18b].

Further, Fig. 18 illustrates the different battery outputs in kW. While some manufacturers like Nikola equip their vehicles with more powerful batteries than FCs (Battery: 446 kW; FC: 300 kW), other manufactures like Daimler choose a more powerful FC instead (Battery: 70 kW; FC: 300 kW) [JAM18a, DAI20]. 19 % of the maximum available power of Daimlers approach may be delivered by the battery while 81 % can be delivered by the FC.

Within the selected use case clusters in this study, the required power range among all use cases can be realized by an integrated system of multiple stacks and a battery to cover load peaks and auxiliaries. Assuming applications of 80 % of power supply by FCs and 20 % of direct battery coverage, a 270 kW FC cluster for hub store delivery application and a 360 kW FC cluster for coaches and long distance coaches are estimated. By assuming a 90 kW output per single FC stack, a cluster of either three to four FCs is established to ideally match the demand. For specific use case implementations, a single large FC stack may be beneficial instead and must be considered in greater depth. The load profiles of the selected

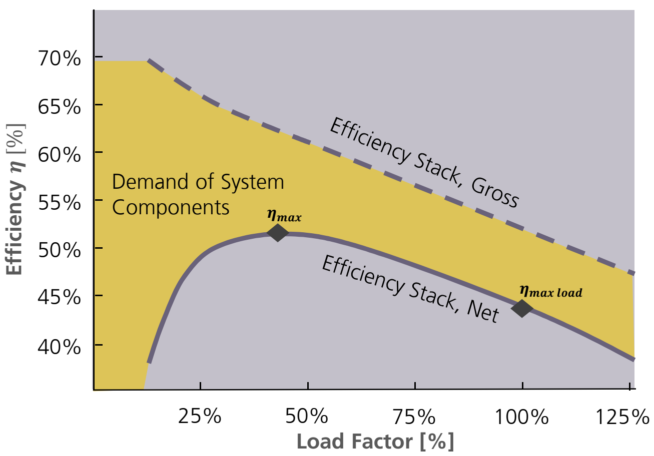

Source: [HÖF17]

Fig. 17: FC Efficiency against Load Factor with and without FC System Components

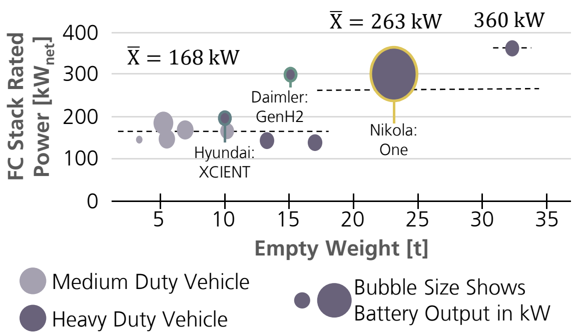

Sources: [DAI20], [HYU20], [JAM18]

Fig. 18: FC Power Specifications for Various Classes of Trucks

use cases with the highest potential are with high shares of constant load requirements but also need to satisfy high durability requirements. In this specific scenario, a dynamic approach with a small battery system may be utilized where the FC system can be operated at best efficiency to enhance durability and reduce costs due to smaller battery systems.

The benchmark of existing specifications serves as the basis to find an estimated number of BPPs, MEAs, etc. to reach 90 kW output power. Depending on the size of the components, a FC stack of 90 kW might consist of 200–400 BPPs in total, each with an anode and cathode side. This assumption leads to a total of 400–800 bipolar half plates per stack. Combining the information, the market demand as a production forecast can be estimated at 600–1,200 BPPs for powering an industrial hub store delivery truck at 270 kW with three FC stacks. Similar, 360 kW for coaches can be reached by four stacks resulting in 800–1,600 BPPs per vehicle. A demand of 1,800 coaches and 1,300 heavy duty hub store delivery trucks seems reasonable in the German market, according to earlier market evaluations. To derive these numbers, newly registered trucks by sector within Germany have been combined with estimations about OEMs to meet emission targets in order to avoid costly fees that stimulate actual sales, and the intensified research ambitions for FC vehicles [WAG20, KA18R, VER14]. Considering a single manufacturer would set production targets to 1,300 hub store delivery trucks and 1,800 long-distance buses per year to serve this demand, the actual number of produced BPPs would add up to at least 2.2 million, complemented by the same amount of MEAs and 4.4 million Gas Diffusion Layers (GDLs) and gaskets.

To sum up, this section outlines the important role of FC operation strategies for the use case applicability. The operation strategy strongly depends on the ratio of maximal and average needed power. For the selected use cases, a dynamic FC approach with a small-size traction battery may be beneficial. A traction battery buffers peak loads, allowing the FC to operate at maximum efficiency [HÖF17, MAR16]. Vehicles for the elaborated use cases can be equipped with a variety of the same FC stack that has a power of about 90 kW [SAT18], i.e. three FCs are considered to cover the estimated demand of 270 kW required for the use case of hub store delivery applications and up to four FCs per cluster applied for a 360 kW vehicle.

INTERIM CONCLUSION

Previous writings and results shape the basis for further considerations of scalable production designs. Indicated by the different requirements of vans, buses or trucks, the need for a wide range of technical solutions for powertrains suitable for their specific use cases is highlighted. Especially long-range buses and trucks are use cases, in which universal advantages of BEVs are unmatched by battery-powered drivetrains. FCEVs can exploit the market potential – namely, cost advantages in case of high range requirements. However, designing scalable production scenarios with mature technology is termed to be a significant lever for market diffusion of PEMFCs.

Any commercialization success of FCEVs is largely dependent on the availability and economic viability of hydrogen refueling. Currently, only 434 HRS's exist worldwide. To close existing gaps in the HRS infrastructure for passenger cars, several strategies have been developed and commitments have been made. While the HRS network for passenger cars is thus projected to be well developed, refueling infrastructure of long-haul heavy duty FCEVs is practically non-existent and needs to be arranged urgently. However, the number of heavy duty trucks and buses is currently significantly lower than the number of passenger cars which increases costs associated with the required hydrogen infrastructure per truck or bus. This makes funding and tax incentives even more important, so that the vehicles do not fully bear these associated infrastructure costs. Considerable funding is available for development and production of electricity-based fuels as well as for the construction of a refueling and charging infrastructure. Thus, chances for significantly lower production costs of hydrogen from renewable energy as well as for refueling infrastructure in the near future seem high.

Additionally, advancement in manufacturing and an up-scaling of production volumes are effective means for manufacturing cost reductions. The main cost drivers and therefore the most important components to focus on are the MEA, BPP, and gaskets. From a technical perspective, the evaluation of each particular vehicle segment in terms of engine power, driving range, and uptime serves as the foundation to conceptualize production line options. For the production concepts in the following chapters, this study focuses on planar FC systems, where MEA, BPP, gaskets, and further components are produced individually and stacked afterwards. Designs with pre-assemblies of single cells are not considered. A second pillar towards scalable production is an estimate of potential units to be sold. Considering all of the named indicators above, coaches and hub store delivery trucks are identified as the most promising applications. Similar driving profiles in terms of routes, range, velocity, and acceleration frequency show synergies among both selected use cases.

In conclusion, technical details towards an adaptable FC-design are derived. Generally, an economic optimum for the distribution of power and capacity between the FC and battery system may be found. This optimum depends not only on the FC and batterie itself but also needs to take all BoP components and the desired use case into account. In order to achieve the required 270 kW or 360 kW, the power supply can be reduced to an integer multiple of 90 kW, operating at maximum efficiency by hybridizing 80 % of the power supply by FCs and 20 % by direct battery coverage. Along with projected market demands, production volumes are derived serving as technical input variables to investigate technological concepts and outline production line options.

TECHNOLOGICAL CONCEPT FOR PEMFC PRODUCTION

In this chapter, a technological concept for manufacturing PEMFCs is developed. A special focus will be paid to the derived use cases. The coach as well as the truck are heavy duty cases which need to operate many thousands of hours and thereby need a higher long term durability compared to light duty vehicles like passenger cars. The durability and the expected part quantities in the middle range will be used as implications on the process by the use case assessment. For further selection, process chains for PEMFC production are introduced with a focus on the main stack components BPP, MEA and gasket. Then, various manufacturing processes for each component are thoroughly reviewed. The specific technologies for each process step are evaluated individually and in the case of the BPP, one manufacturing technology is proposed for each process step. Manufacturing technologies of the MEA and the gasket strongly depend on the FC design which is why they cannot be proposed for each process step. The stack assembly and handling task in between different production steps are addressed before a possible production chain is partly defined. The technological concept for PEMFC production serves as the baseline for a cost evaluation in the subsequent chapter.

PEMFC Production: Process Chain

The production process chain for PEMFCs involves both, manufacturing technology and process technology, which makes it important to have expertise in both domains. Four major process steps, shown in Fig. 19, need be considered to produce a PEMFC stack which consists of hundreds of single PEMFCs. Those steps are the BPP manufacturing, the MEA manufacturing, the gasket assembly and the repetitive stacking of the different components.

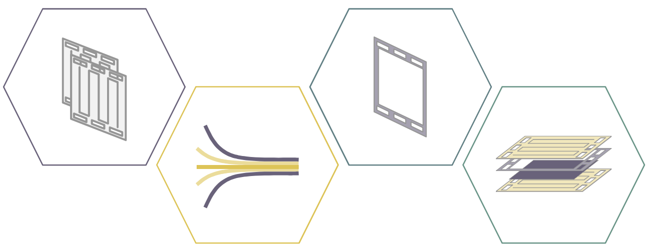

Fig. 19: Main Process Steps of PEMFC Production

Modern BPPs for mass production are manufactured from 75–100 µm thick stainless-steel or titanium sheets [JAM17, JÖR17]. These are normally supplied as coils, which are unwound and fed directly into the production line. The production line for BPP manufacturing needs to conduct four process steps: forming of the flow field, cutting of manifolds and trim, coating of the plates and back to back joining of two plates as shown (see Fig. 20). The sequence of these steps can vary, depending on the technologies used [JAM17].

The MEA consists of different layers. The Proton Exchange Membrane (PEM) as the central layer is covered on both sides by a Catalyst Layer (CL). This sub-assembly is defined as a MEA_{3L}. The GDL lies on the outer surfaces of the CL and defines with the other components the MEA_{5L}. In combination with subgaskets the MEA_{7L} consists of PEM, CLs, subgaskets and GDLs.

The PEM is usually manufactured from an ion-conducting polymer such as Nafion™. The GDL commonly consists of a carbon fiber substrate with a Micro Porous Layer. Both, the PEM and the GDL are generally prefabricated and supplied as sheets or coils. One of the key processes is the application of the CL. There are three basic strategies for the application of the catalyst and several technologies for the application process itself. Regardless of the catalyst application technology, different layers are hot-pressed together and form the MEA_{7L} assembly. In a final step, the sheet is cut into the required sizes. Major possible production routes may be seen in Fig. 20. [JÖR17, SIE15, KAZ08]

In order to form a gasket, sealant may be dispensed either to the BPP or to the MEA. The gasket typically needs curing before cell assembly. A third option is using a prefabricated inlay gasket which is placed between the MEA and BPP while assembling the cell. The gasket is typically applied after manufacturing of the BPP or the MEA (see Fig. 20).

Repetitive stacking is used to combine the different components and to form a functional repetitive unit, the PEMFC. Stacking is typically a pick and place task. There are two major assembly concepts which differ with regards to their validation concepts.

According to mentioned technologies and processes, illustrates a few possible sequences and divides them into the earlier mentioned four major steps BPP manufacturing (purple), MEA_{7L} manufacturing (yellow), gasket assembly (dark grey) and stacking (dark green). The presented process steps are evaluated in the following chapters with regards to their impact on the process chain and their capability to produce PEMFCs according to the earlier described use case.

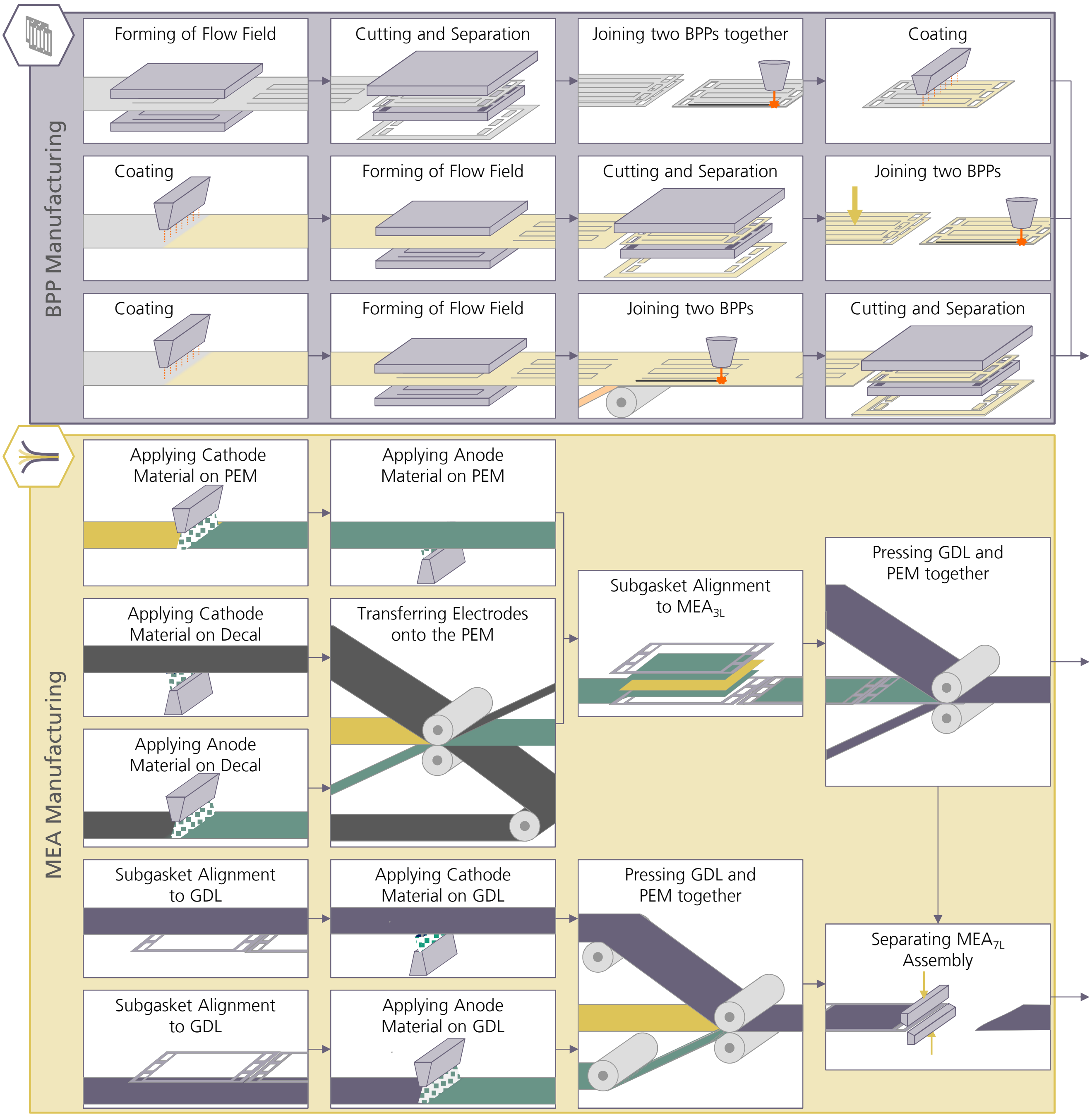
BPP Manufacturing
Forming of Flow Field
Cutting and Separation
Joining two BPPs together
Coating
Coating
Forming of Flow Field
Cutting and Separation
Joining two BPPs
Coating
Forming of Flow Field
Joining two BPPs
Cutting and Separation
MEA Manufacturing
Applying Cathode Material on PEM
Applying Anode Material on PEM
Applying Cathode Material on Decal
Transferring Electrodes onto the PEM
Applying Anode Material on Decal
Subgasket Alignment to MEA3L
Pressing GDL and PEM together
Subgasket Alignment to GDL
Applying Cathode Material on GDL
Subgasket Alignment to GDL
Applying Anode Material on GDL
Pressing GDL and PEM together
Separating MEA7L Assembly

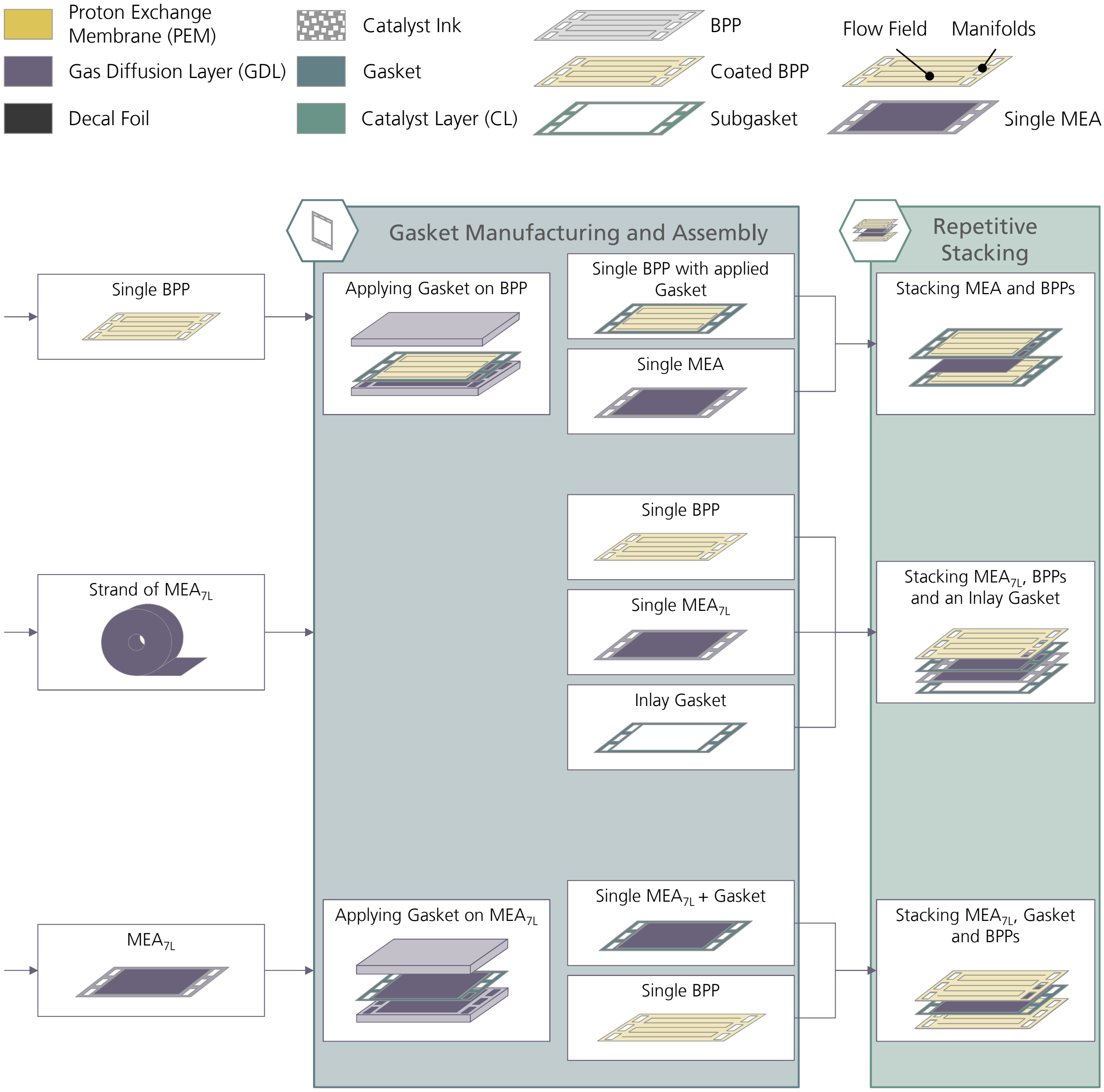

Fig. 20: PEMFC Production Process Chain Overview

BPP Manufacturing

To manufacture the BPPs, there are different considerations that need to be made:

- Design for the BPP
- Material used for the substrate and the coating
- Production technologies utilized for forming, coating, joining and cutting of the BPP
- Underlying business case

For each aspect, there are different alternative options, which –by some extend– also affect each other. The underlying business case has a predominant impact on the selection. A high degree of market penetration is only feasible with technologies, materials and designs that allow high scale production and low costs per stack. The available alternatives are discussed and possible reciprocal effects are described subsequently.

BPP Design

The design of BPPs mainly concerns the thickness of the sheet metal and the flow field design. The thickness of the sheet metal influences the stack weight, handling processes, and material costs. The flow field design affects the forming process and the efficiency of the system.

The thickness of industrially used BPPs is estimated between 75 and 100 µm [JAM17]. As long as the substrate is not damaged during the forming process and the resulting plates are durable, processing of thinner plates leads to a reduced stack weight and stack volume. Thinner plates furthermore provide better cold start capability since the FC system will reach the operating temperature faster with lower mass and volume. However, the thinner the plate, the more complex the handling in an automated production. Furthermore, despite the reduced weight and need for material, the material costs per weight can increase for thinner plates due to a more complex rolling process [GOO20a, GOO20b].

Based on the fluid dynamical consideration of working fluids in anode and cathode sides, BPPs are designed in several types of flow fields, such as serpentine, parallel, interdigitated, pin, spiral, or 3D-fine mesh types [SPI19]. Forming complex geometries with high aspect ratio is generally challenging in many forming processes. In particular, high press force is required for the large flow field area and deep channels. [EBR18, SPI17]

Substrate Material

Currently, stainless steel and titanium are used in BPP applications due to their formability, good electrical conductivity, high thermal conductivity and excellent mechanical properties. Stainless steel (such as 1.4404) is mostly used for automotive application of PEMFCs due to its above-mentioned advantages and compatibility with other processes such as laser welding and coating materials [JAM17, ASR16]. Titanium has a low density, good mechanical properties and high corrosion resistance. However, it has a high material price and limited formability. [SPI18, SHA10]

Potential metals for future applications are Aluminum (e.g. Al6061) or nickel-based materials (e.g. EN1.4539, EN1.4876). Aluminum has many advantages such as low price, low density, and good formability. However, it is very vulnerable to corrosion in the operating environment of FCs. Thereby, an appropriate coating process should be developed. [BOR17] Apart from metallic materials, non-metallic materials such as graphite or carbon based composite materials can be used for BPP substrate. Non-metallic materials have generally excellent corrosion resistance and low bulk resistivity. However, they cannot be utilized in a thin sheet form due to the low mechanical strength, which results in a larger cell pitch and therefore lower power density of the FC systems. [KAR12]

Forming Process

There are two generally used technologies to form BPPs: Embossing and hydroforming. Embossing (see Fig. 21) is a process in which the metal sheet is formed between two dies, one male and one female, which are pressed into each other. For this purpose, a progressive die is used which forms the sheet metal in several subsequent steps. The number of steps depends on the degree of deformation of the flow field. The forming progresses with each closing until the final form is attained. Embossing is one of the most robust forming processes and

Embossing

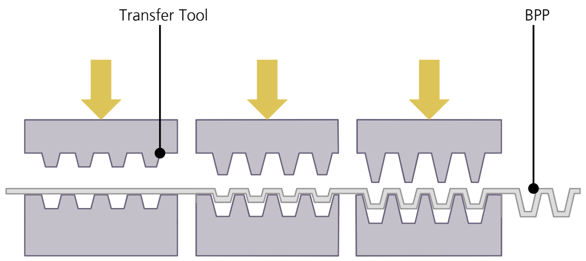

The metal sheet is pressed between two dies and formed respective to the die form. Contrary to a normal embossing process, the process is conducted in two or more steps. At each step, the metal sheet is partially formed until the final form is attained. The holes for the main channels can be punched out with the same tool.

Advantages

- Short cycle time (< 2 second for one stroke)
- Holes for main supply channels can be cut out with the same tool

Disadvantages

- High tooling costs due to the necessity for several die components
- Several forming steps required according to the desired aspect ratio

Sources: [WEI19], [JAM17], [JEN17], [MOH16], [MAH10]

Fig. 21: PEmbossing Process and Evaluation

can easily be automated and combined with other processes. A major advantage is the possibility to cut out the manifolds and the trim within the same tool. Another advantage is the higher formability compared to single-step embossing, which possibly allows to achieve the optimum channel geometry. However, the high forming force may lead to short tool life time. [WEI19, JAM17, JEN17, MOH16, MAH10]

Hydroforming (see Fig. 22) uses just a single die against which the metal sheet is pressed by a fluid. The fluid is under high hydrostatic pressure thus deforming the sheet to the die's geometry. With this process, high aspect ratio, low surface roughness, and small forming tolerances can be attained. [GRÄ20] With the need for just one die, the tooling costs are significantly lower compared to embossing [JAM17]. Additionally, there is only little friction between plate and die, thus the coating of already coated plates is preserved [WEI19]. The disadvantages of hydroforming are the additional trim and cut needed.

The edge of sheet metal is used as a sealing surface during the forming process, but it has to be cut off in an additional step afterwards. Furthermore, it requires an additional cutting process in order to cut out the holes for the main channels. While state of the art hydroforming machines can form two plates in a single cycle, they are still less productive than embossing machines. This is due to the long time needed for pressure build-up. It is not expected that this time can be shortened significantly. However, productiveness could be increased by using more powerful machines which are able to form up to 4 plates per cycle [WEI19, JAM17, HUN12, MAH10].

Also, the high velocity forming and rollforming show a research potential [ZHA17, SHA10]. In a high velocity forming process, the stamp presses in very high speed (50 m/s) and heats up the metal sheets to several hundred degrees by kinetic energy. The material is thereby softened before it is formed. [CEL20] Rollforming is a continuous forming process for flexible materials by using two rolls. In this process, the metal sheet is experiencing forming pressure in thickness direction by two rollers while it is tensioned and moving in rolling direction by the unwinder and rewinder. Thereby, more complex interactions between processing parameters, such as the compressive forming force, tensile force, and feed rate, should be carefully taken into account to produce high quality BPPs. Rollforming is known to have huge economical potential due to increased production rates [BAU19], Additionally, the rubber pad forming process is well suited for the prototyping and small batch production. This process makes use of the elastic behavior of the rubber pad to form metal sheets. Thereby, only one side of metallic stamp is needed to be machined, which can save time and cost compared to the conventional embossing process. Nevertheless, this process cannot be

Hydroforming

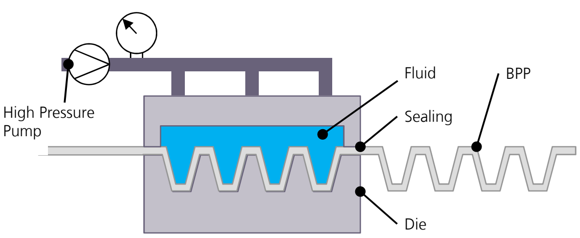

The flow channels of the BPP are formed under a high hydrostatic pressure caused by a pressurized fluid, e.g. oil. The fluid presses the sheet against a die and forms the sheet respective to the die's form.

Advantages

- High aspect ration in one process step
- High repeat accuracy
- Possibility to form coated metal sheets

Disadvantages

- Need for a complementary fine blanking for the main supply channels
- Additional material waste due to the necessary edge trim for sealing the pressurized fluid

Sources: [WEI19], [JAM17], [HUN12], [MAH10],

Fig. 22: Hydroforming Process and Evaluation

adapted to mass production because the rubber pad is subject to high wear, which is why it needs to be changed often. Additionally, rubber pad forming is more difficult to automate due to constructional limitations. [MÜL19]

Coating Material

Most metal BPPs degrade under the operating conditions within a FC. Qualified metals (such as gold) that are resistant against degradation and offer a low contact resistance are too expensive to be used as substrate material in a large-scale production. This is why the above mentioned less expensive substrate materials such as stainless steel are coated with materials that withstand the operating conditions and also have a low interface resistance. [TAW07, WAN06] Gold is the most efficient coating material on BPPs because of its high electrical conductivity and corrosion resistance that are essential parameters. However, the raw material price is high and increases total costs significantly even if the gold is only used as a thin coating [SHA17].

There are different processes and material combinations available. Coating materials that have proven to be suitable include carbon, ceramic, titanium nitride, niobium carbide, and chromium carbon nitride. [IHI20, IMP19, JAM17, ASR16] Metal-based nitride (TiN, CrN) coatings on BPPs provide good corrosion resistance, heat resistance, wear resistance, and good electrical conductivity. [BRY20a, BRY20b, TAW07] Amorphous carbon coating is recently used not only in the research but also in the industry which can effectively reduce the electrical resistance and improve durability of BPPs at low manufacturing cost [ION20, VON20, KRU99, ZHA99].

Coating Process

Coating prevents the metallic BPPs from corrosion in the FC operating condition and provides good electrical conductivity. The mainly used processes are either PVD processes or Chemical

Vapor Deposition (CVD) processes. [TAW07, YOO07]
PVD processes produce a thin film coating that is extremely hard and can be applied on a diverse range of surfaces. The film has a high temperature tolerance and superior ablation resistance. However, it requires high cost due to the intense heating and cooling. On the other hand, CVD produces even and homogeneous coating layers on the irregular surface. This process can be applied to wide range of applications with varying environmental conditions. [AZO19, AZO02] However, it generally requires higher operating temperature compared to PVD process in order to facilitate the reaction of precursors. Furthermore, some precursors and -products are known to be toxic, pyrophoric, or

Physical Vapor Deposition (PVD): Sputtering

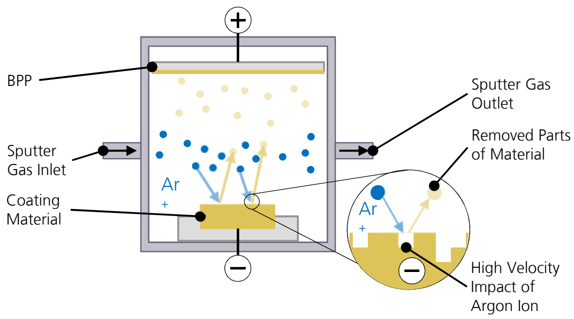

Sputtering is a PVD process in which a high electrical potential accelerates noble gas ions (e.g. argon ions) onto a target consisting of the coating material. Parts of the material are removed by the impact and shot onto the substrate, in this case, the BPP. On impact with the BPP, the material deposits and forms a thin layer.

Advantages

- Wide range of substrate (e.g. metal, alloys, and compounds)
- Evenly distributed coating on flat and on formed surfaces

Disadvantages

- Low sputter deposition rates
- Expensive sputtering targets compared to evaporant sources.

Sources: [ASR16], [LAM13], [SIM89]

Fig. 23: Sputtering Process and Evaluation

corrosive. This might cause problems with material handling and storage. [IND08] Both types of coating processes are able to attain not only very thin but also resistant coatings. Disadvantages for both processes can be the long cycle times and the need for expensive equipment. [JAM17, ASR16] The main cause of long cycle times is due to the vacuum process that can possibly be a bottleneck in the mass production scenario.

PVD processes include sputtering and ion plating. Sputtering (see Fig. 23: is conducted by shooting noble gas ions, such as argon ions, towards a target consisting of the coating material. Upon impact, very small parts of the material are knocked-out of the target and accelerated towards a substrate. The small particles strike the substrate, stick there and form a thin coating. Ion plating (see Fig. 24) uses the already explained sputtering process to clean the substrate's surface. The needed ions arise out of a plasma. After cleaning the substrates surface, the coating material is vaporized and condensed on the substrate's surface to form a thin coating. [GÄR95, SIM89]

CVD (see Fig. 25) in general, is conducted by flooding a chamber with a reactive gas and heating the substrate. A reaction between gas and substrate is triggered which produces a solid material, the coating, on the surface of the substrate and possible byproducts. There are several different CVD process variants respective to the coating material. [ASR16, YAN10]

Apart from that, nitriding can be an alternative process, which is applicable for a wide range of metals. In this process, the nitrogen is diffused on the surface of the substrate material and create a case-hardened surface. This can develop a unique duplex microstructure on the surface enhancing the mechanical properties. [BRA11]

Furthermore, the vacuum-free functionalized carbon deposition process is especially highlighted for the mass production scenario [JAM19].

In this process, the mixture of water and functionalized carbon nanoparticles are firstly dispersed on the surface of BPPs by the ultrasonic spray coating process. Dispersed water is then dried out in the oven so that only functionalized carbon particles can remain on the surface. Finally, the photochemical activation process induces cross-linking of the carbon powders which can function as a coating layer. Different from PVD and CVD coating processes, this process does not require any vacuum process, which can be a bottleneck in the high-volume production. This coating process can be utilized prior to forming as well as afterwards.

Above mentioned processes can be used in the form of single-layer coating, multiple-layer coating, spot coating, or selective coating depending on materials and technical requirements.

Single-layer coating is the simplest type and it can be used when the coating material has good adhesion directly to the substrate material. For example, the gold coating on the stainless steel substrate. However, if these two materials have bad adhesion characteristic, the multiple-layer coating can be

Physical Vapor Deposition (PVD): Ion Plating

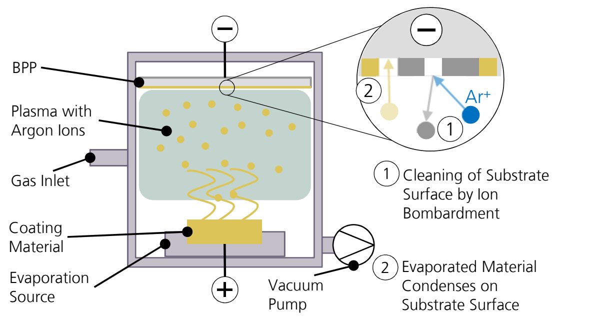

Ion plating is a plasma–assisted PVD process in which the argon ions of plasma are used to clean the surface of the substrate, in this case, the BPP. The cleaning process is similar to the sputtering process, where the coating material is sputtered under ion bombardment. In a second step, the coating material is evaporated by a high–energy source and condenses on the cleaned surface of the substrate.

Advantages

- Good surface coverage and bonding
- Flexibility of ion bombardment level for better adhesion

Disadvantages

- Many process variables
- Excessive substrate heating and residual compressive stress

Sources: [ASR16], [LAM13], [GÄR95]

Fig. 24: Ion Plating Process and Evaluation

Chemical–Vapor–Deposition (CVD)

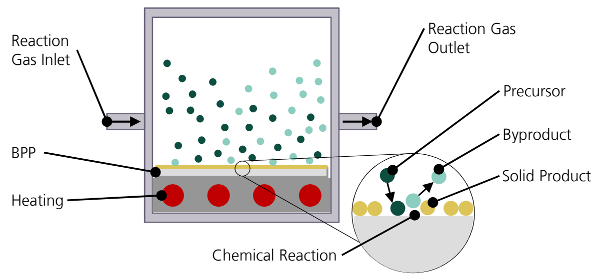

The substrate, in this case, the BPP, is loaded into a chamber, which is flooded with a reactive gas. The substrate is heated in order to enable a reaction between gas and substrate. As a result, a solid component is deposited on the surface of the substrate, which forms a thin coating. The material of the coating depends on the gas substrate combination. There is a variety of processes that follow this operating principle with differences in the used precursor, the chemical reaction, and the solid product that forms the coating. Therefore advantages and disadvantages vary depending on these factors.

Advantages

- Very thin coating can be achieved
- CVD coated plates are resistant to degeneration and have a low interfacial resistance

Disadvantages

- Expensive equipment
- Long cycle times

Sources: [ASR16], [SIM89]

Fig. 25: CVD Process and Evaluation

formulated by adding adhesion layer between coating material and substrate material. TIOX technology developed by Tread Stone is one example, which uses Ti alloy to bond Dopped TiOx semiconductive surface layer to the stainless substrate. [WAN17] Furthermore, the spot coating was developed to reduce the use of expensive coating materials such as noble metals. In this type of coating, the material with good corrosion resistance is deposited on the surface of substrate to prevent corrosion. And then electrically conductive material is deposited in a dot shape to provide pathways to electrons. DOTS technology from Tread Stone is a well-known example. [WAN17] In selective coating, material coating is exclusively applied on the BPP's surface where it has direct contact with GDL. For selective coating, pad galvanization (tampon plating), screen printing, or roller printing process can be used. Prior masking of the recesses is not required. One patent about selective coating claims that an improved adhesion of the coating on the contact surface might be achieved on the basis of a thermoplastic or duroplastic polymer which melts or cross links on drying. This process has a great advantage of minimizing the use of coating material, thereby the material cost. However, it cannot be applied for pre-coating of material because the selective coating is achieved by a different height of formed geometry. [GRA11]

As the demand for FC vehicle continuously increases, appropriate coating processes for mass production are required. Since the production cycle time is more important in mass production, the process which can efficiently reduce production cycle time will be more required such as vacuum-free coating process. Moreover, the amount and cost of used coating material will be also scaled up in mass production, the coating form with less noble metal, such as spot coating or selective coating, will be more preferred. Last but not least, development of cost effective metal alloy which can fulfill technical requirements without coating can be the alternative way. For instance, Posco and Nippon steel have developed stainless steel alloy which can satisfy the requirement of electrical conductivity and corrosion resistance. [THE18, IMA14]

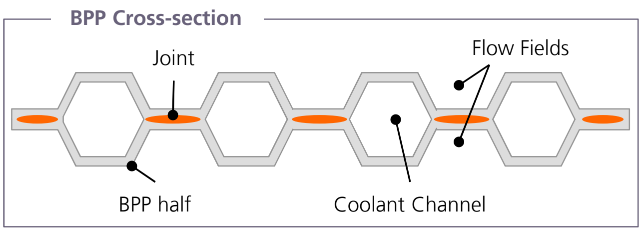

Fig. 26: Illustration of a BPP in Cross-section

Joining Process

Two BPPs are joined back to back in order to obtain a flow field on both surfaces and coolant channels in between the two plates (see Fig. 26). A single BPP is now obtained by placing the formed anode and cathode plates on top of each other and joining them together. By doing so, three channel structures are created that are sealed off from each other. The two channel structures on the outer sides distribute the reactants while the channels on the inner side are used for the coolant distribution. It is important that the coolant channels are sealed perfectly because leakage could lead to chemical reactions with the hydrogen or short circuites. Both could potentially compromise the stack. Furthermore, the sealing conducts the electrical current which is why the resistance needs to be reduced to a minimum. For the above-mentioned reasons, two different technologies can be considered for joining: laser welding and adhesive bonding.

Laser welding (see Fig. 27) uses a highly focused laser beam which melts material of both plates partially in the area the beam is focused on. The molten material of both plates mixes and forms a joint weld pool which then solidifies. Compared to other welding processes, the heat input is considerably lower given to the small circumference of the laser spot. Laser welding can be used to produce high-precision joints in a short time. Process alternatives include for example the use of a scanner for faster guidance of the laser beam. It needs to be taken into consideration that the precision is dependent on the fixture of the plates. [FRA19, JAM17, FRA13] Laser welding provides a number of distinct advantages [BRA16]. It is consistent and repeatable, and does not degrade over time as some adhesively bonded connections do [JAM17]. However, the heat from laser welding may damage the coating material on BPPs if the joining process comes after the coating process.

Using an adhesive boding process (see Fig. 28), the adhesive is applied on the first plate using a roller. Then the second plate is placed atop of the first plate. Both plates are then fixed until the adhesive is cured. The application by roller also allows a continuous process and can be automated to save the process time and cost of manufacturing [JAM17]. Hot melt and epoxide resin might be feasible adhesives. To ensure the electrical conductivity, additives must be mixed into the unprocessed adhesive. For this, gasket titanium nitride and carbon black showed satisfying results. However, the application process poses a challenge. Different factors such as the rheological characteristics of the adhesive mixture, the application procedure itself and the preparation must be taken into consideration. [BEC18, JAM17] Adhesive bonding allows to have small gaps between the plates so that shape deviations can be compensated. Unfavorably adhesively bonded plates leak more often than laser welded plates do. This might be an exclusion criterion given the fact that leaky FCs are a risk for the whole stack. [BEC18, JAM17]

Laser Welding

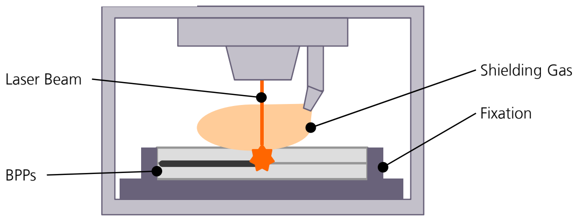

Two BPPs are welded together by a laser beam. The laser melts material of both plates locally. The liquid material diffuses and solidifies, forming a welded joint. In order to prevent oxidization, the process is shielded by a gas. Alternatively the process can be conducted under a vacuum. Because seal tightness is most important for joint BPPs, a precise fixation of the plates is needed.

Advantages

- Fast process with high feed rate (~0.14 m/s)
- Hermetically sealed weld joint
- Heat input limited by precise process control

Disadvantages

- Local structural changes due to heat input possible
- Expensive equipment
- Precise fixture decisive for quality

Sources: [FRA19], [JAM17], [FRA13]

Fig. 27: Laser Welding Process and Evaluation

Adhesive Bonding

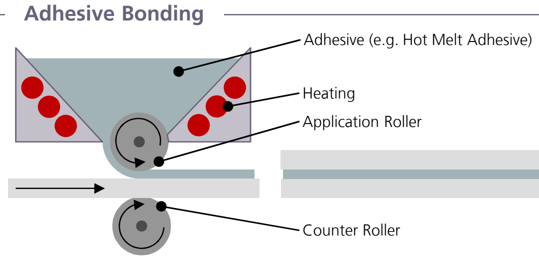

Two BPPs are joint together by an adhesive. The adhesive is applied to a plate with an application roller. The second plate is then pressed onto the first plate and fixated until the adhesive is hardened. Hot melt adhesive or epoxy resin adhesives are possible adhesive materials.

Advantages

- Continuous process possible with a cycle time shorter than two seconds
- No heat input into the plates

Disadvantages

- Adhesive bonds tend to leak more often than laser welded joints
- Surface treatment necessary
- Deformation of the plates due to roller pressure

Source: [BEC18]

Fig. 28: Adhesive Bonding Process and Evaluation

Cutting Process

Separation and cutting of trim and manifolds can be conducted either by shear cutting or laser cutting. In a shear cutting process (see Fig. 29), the material is sheared between two cutting edges. The cutting process can be done within the same embossing machinery as the flow field forming, allowing synergy effects. Alternatively, the cutting can be performed with a second press, which might be beneficial since they can be equipped with a smaller tonnage than forming [JAM17]. The shear cutting process has an advantage of comparatively short cycle time. However, additional costs for tooling are required. [JAM17, HEL06] Laser cutting processes (see Fig. 30) use a highly focused laser beam, which is used to partially heat up the material. The thermal energy melts or even vaporizes the material, which is then blown out by a gas stream. By continuously moving the laser spot or the material, a cut is created. The smallest possible cut width depends on both the beam characteristics and the material characteristics. [JAM17, WET17] Laser cutting can be conducted without a tool. Compared to the shear cutting, laser cutting often requires larger cycle time. Using a scanner based remote system, the cutting process might be shortened, thus compensating this disadvantage. [JAM17, WET17]

Shear Cutting

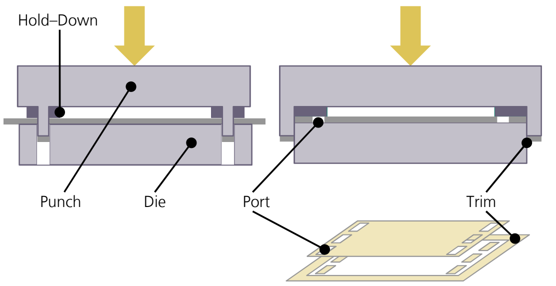

Shear cutting is a process in which parts of the sheet metal are separated from each other. A set off fitting punch and die is needed. The punch presses from above against the material and into the cavities of the die below. Meanwhile, the blank holder assures that only a minimum of deformation takes place. The cutting accuracy can be adjusted by positioning the punch and die or the cutting gap. To further minimize deformation and crack formation, a hold–down device with a knife–edge ring can be used. This is also called fine cutting.

Advantages

- Very short cycle time
- Several cuts can be conducted in one press

Disadvantages

- Tooling costs need to be considered

Source: [HEL06]

Fig. 29: Shear Cutting Process and Evaluation

Laser Cutting

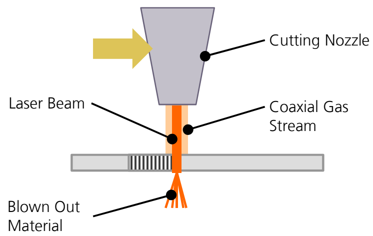

A laser beam is focused on the surface of a sheet metal. The metal absorbs the energy and melts, partly even vaporizes. A coaxial gas stream blows the molten material through the kerf. The cutting nozzle, or sheet metal, is controlled by a CNC controller. For the gas flow, an inert gas enables clean cutting edges, while an active gas increases production. A special form of laser cutting by using highly dynamic mirror deflection systems to control the laser beam is called remote laser cutting.

Advantages

- No tooling costs

Disadvantages

- Expensive equipment
- Conventionally longer cycle times, remote laser cutting could shorten the time drastically

Sources: [FRA14], [HÜG09]

Fig. 30: Laser Cutting Process and Evaluation

Possible Process Chains for BPP Production

Based on presented technical requirements of selected use cases, namely coaches and heavy duty hub store delivery, the possible process chains for BPP production are designed. Both selected use cases require long distance driving and high electrical power. For long distance driving, the exceptional durability of system (longer than 25,000 hours) and each component should be fulfilled, which is closely related to the material selection. Furthermore, the high electrical power output of FCs can be achieved by increasing the active area of the cells or the number of cells per stack. Such considerations are described on each category in more detail and Fig. 31 provides an overview of the selected technologies that are possible within the process chain.

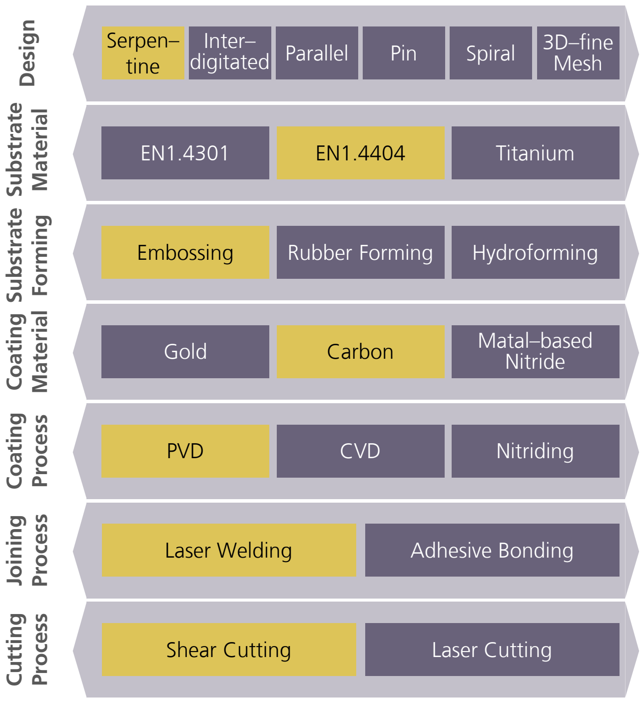

Fig. 31: BPP Process Chain Alternatives and Selection

BPP Design

Sheet metal with a thickness of 100 µm is selected since it is less limp than thinner sheets. Handling of the sheets is therefore easier. The sheets are still thin enough to have a weight advantage. The serpentine flow field, which is the most commonly used type, is selected because this flow field type rarely influences the forming process [NET19].

Substrate Material

For the substrate material, EN1.4404 is selected because it possesses good corrosion resistance and good formability at a low cost [WEI13, KOÇ09]. Furthermore, it is exceptionally well-suited for laser welding processes [JAM17].

Forming Process

Although embossing process may produce lower surface quality than hydroforming and rubber pad forming, it is selected as production concept due to its numerous advantages. It has lower cycle time which is crucial for high volume production. Moreover, it can be easily automated and thereby combined with other processes. [CHE12b].

Coating Material

Carbon is selected as coating material of the production concept. The raw material cost is cheaper than gold, which requires special coating process to reduce the amount of material. Furthermore, the carbon can be coated on various substrate materials such as titanium and stainless steel (EN1.4301 and EN1.4404). In particular, the combination of stainless steel substrate and carbon coating have a cost advantage compared to titanium. Moreover, this combination shows great coating properties such as corrosion current and area specific resistance, which fulfill the technical target of the Department of Energy (DOE) for 2020. [KOP17, YIP13, YIP10, FUK07]

Coating Process

PVD is selected for production concept because of its environmental friendliness and relatively low operating temperature. Additionally, coating layer provides stability in high temperature, good impact strength and excellent abrasion resistance [ASR16]. Furthermore, this process is validated for stainless steel based carbon coating combination [YIP13].

Joining Process

Since no additional joining material is required and it is an economical and fast process, laser welding is chosen. Furthermore, the welded part provides itself as a channel to conduct electrons between BPPs at low resistance. [PAK18, BRA16]

Cutting Process

Shear cutting is chosen because the process can be integrated into the embossing process as a flow field forming operation, allowing to exploite synergy effects.

Outlook

James et al. propose that state-of-the-art BPPs are manufactured by feeding a sheet metal coil into a five stage embossing process, which conducts the forming and the cutting operations. The separated plates are then joined in pairs and back to back by a laser welding operation. In a last step, the joined BPPs are coated within a PVD process. All processes are done on the same production line. Coating and laser welding are limiting the output due to their longer cycle time. [JAM17]

To increase the performance of production process chains for BPPs, some changes need to be done. Instead of coating individual sheets at the end, sheets may initially be coated in a continuous production line before the forming process. Coating could be done within the same line or in a separate line. Some precoated materials are already available on the market such as the BPP material supplied by Sandvik [SAN20]. Outsourcing could lead to reduced investments. This is possible if the coating is resistant against abrasion and if the forming process only involves a minimum of friction between sheet metal and die. This is one reason why, instead of an embossing process, hydroforming could be considered the better process for BPP manufacturing. It must be taken into account that a second machinery is needed to conduct the cutting processes. Also, laser welding might still turn into a bottleneck [GRÄ20, JAM17].

For future development, a continuous process in which the plates are manufactured in one strand might be a game changer. Instead of separating the plates before laser welding, they are separated afterwards. Plates are either joint by combining two strands or by producing two plates side by side and turning one plate onto the other before joining them. However, a continuous process seems possible with using adhesive bonding, as it is already practiced by Toyota. Failing of the adhesive and leakage might still be a problem, though. [WEI19, JAM17]

Key Takeaways for the Manufacturing Industry

- Low-cost high-volume production is required.
- High investments are required for scaling up, but scalable production can tap cost potentials.
- Further researches in substrate and coating materials are required to improve energy density and cost reduction of FC system.
- Opportunities also exist in innovative materials due to the possible use of pre-coated material or alloy metal instead of post-coating process.
- Cycle time reduction should be achieved in every process to avoid excessive parallelization of manufacturing lines in high volume production.

MEA Manufacturing

MEA Production

The MEA comprises of the Proton Exchange Membrane (PEM), the two CLs (anodic and cathodic), a possible subgasket and the GDL. The MEA is built up sequentially and may be named MEA_{3L} (PEM+CL), MEA_{5L} (PEM+CL+GDL) or MEA_{7L} (PEM+CL+GDL+ Subgasket) as described earlier.

The PEM consist of an ionomer, typically of sulfonated tetrafluoroethylene-based fluoropolymer-copolymer and is thereby impenetrable for electrons. The hydrogen ions diffuse through the PEM and react with oxygen to water. The electrons are transferred through the CL, GDL and to the BPP which is why those components need be electrically conductive. The CL typically consist of carbon-based particles with platinum and a specific amount of the same ionomer that is used for the PEM. This way, ionomer, carbon particles and platinum form a three-phase boundary which is where the ionization takes place. The GDL consists of conductive material as well and is functionalized with a hydrophobic polymer like Polytetrafluoroethylene (PTFE). The subgasket is a stabilizing polymer film for easier handling, alignment and provides sealing surface. Furthermore, it enhances the durability of the MEA_{7L}.

Since the MEA is a critical component in limiting the lifetime of a PEMFC stack, high quality components are mandatory. Moreover, the MEA considerably influences the efficiency and stability of a FC [SAN19, BEN10]. A relevant subcomponent for efficiency and costs, already at medium to mid ranged production targets, is the employed catalyst. The amount of catalyst loading has a direct impact on the target of increasing the three-phase boundary (active surface) between catalyst, ionomer and electrically conducting catalyst substrate. Larger amount of active catalyst can optimize the power density and durability but may also lead to an increase in material costs. Maximizing the available catalyst to this reaction is thereby of great interest and may be influenced by different types of production technologies. In most applications of PEMFCs, platinum is used as the catalyst material. Platinum based catalysts show extraordinary catalytic activity for PEMFC reaction.

A multitude of short- and long-term degradation mechanism restrict the applicability for certain use cases in terms of durability aspects. Production technological approaches and design aspects may reduce these degradation mechanisms and are therefore considered in detail in the following. The subgasket will not be discussed in detail but may be integrated before GDL lamination in the process chain. A subgasket may enhance durability of the PEM through additional mechanical stability. The whole MEA_{7L} production not only depends on the coating of the PEM but also on other employed process steps like subgasket alignment and GDL application. Due to the scope of this document, a special focus is put on the individual process chains for catalyst application. The visualizations of the different process chains beneath, show a simplified (continuous) production of the MEA_{7L} including the CL application. To establish a comprehensive production of MEA_{7L} however, every production step needs to be analyzed in detail.

In the following, three production strategies are differentiated according to the substrate on which the CL is applied to in first contact. They are assessed regarding their influence to the characteristics of the final MEA_{7L}. In the direct CCM process chain the catalyst mixture, the so called ink, is applied directly onto both sides of the PEM. After that, the PEM with applied catalysts is placed between two sheets of GDLs. The GDLs are hot-pressed, forming a single MEA_{5L} sheet. Corresponding to the direct CCM is the indirect CCM process, where the CL is coated onto a decal foil and then transferred onto the PEM, after the catalyst mixture has dried. Afterwards, the decal transfer foils have to be removed from the applied CL. Another strategy is the Catalyst Coated Substrate (CCS): the CL is applied on two separate sheets of the GDL. The PEM is then placed between those two GDLs and hot-pressed. [FRÖ15, SIE15, BLA12]

Direct CCM

Direct CCM (see Fig. 32) is a process chain which requires less process steps than indirect CCM and has low costs at high production rates [JAM17]. Using a mixture of solvent and carbon based particles, functionalized with platinum, the thickness of the CL can be controlled very well and a sufficient ionic connection between the PEM and the CL is established. After placing the mixture on the surface of the membrane, the solvent on the other hand may lead to a swelling of the membrane's thickness of up to 30 %. Also wrinkling can occur due to this contact which influences the process stability and the cell's performance. During hot-pressing, the membrane material is heated above its glass transition temperature to establish a well conducting connection. In order not to damage the CL nor the PEM, precise process handling and knowledge is essential. The use of a dry ink may help to overcome a few of these drawbacks [SAN19, SIE15, PAK12, TOW07].

Indirect CCM

The indirect CCM process (see Fig. 33) has certain advantages over the direct CCM technology. It may also be a continuous process which is suitable for high volume production and overcomes the difficulty of the membrane swelling. It is possible to run the indirect CCM process with a single carrier film which

Direct Catalyst Coated Membrane (CCM)

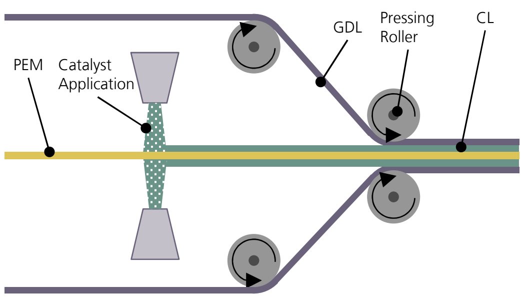

The CLs are coated directly onto the PEM. It may be applied either dry, as a powder, or wet, as a suspension. PEMs are very thin and fragile and tend to expand when in contact with a solvent. After coating, the PEM with the CLs is placed between the GDLs and compressed. Drying of the catalyst ink and additional pressing processes need to be considered.

Advantages

- Short process chain

Disadvantages

- CL solvents may diffuse in order to prevent damages
- PEM tends to expand when in contact with a solvent

Sources: [SIE15], [BLA12]

Fig. 32: Direct CCM Process Overview and Evaluation

Indirect Catalyst Coated Membrane (CCM)

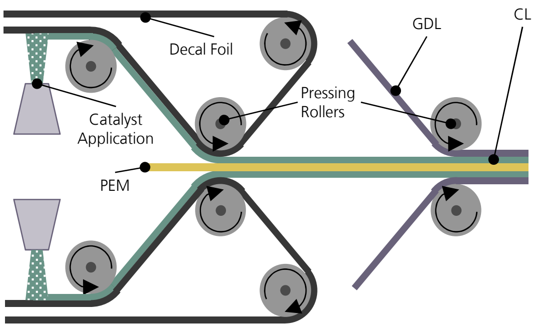

The CLs are applied to a decal foil and then transferred to the PEM. The catalyst is applied wet, as a suspension. After coating, the PEM with the CLs is placed between the GDLs and compressed. Drying of the catalyst ink and additional pressing processes need to be considered.

Advantages

- Best result regarding the cell performance can be achieved
- Sparing application onto the fragile PEM

Disadvantages

- Decal necessary
- Additional waste stream (decal)

Sources: [FRÖ15], [SIE15], [BLA12]

Fig. 33: Indirect CCM Process Overview and Evaluation

limits the additional costs for the decal foil if CL transfer is 100 % efficient. For high production volumes, the material costs account for the largest amount of the total costs, wherein investment costs within the production process have a minor share. [SAN19, JAM17] This technology leads to satisfying cell performance values and is recommended compared to the direct CCM as well as the CCS technology.

CCS

During the so called CCS process (Fig. 34), the CL is applied to the GDL prior to hot-pressing. One of the advantages is, that the CL is not directly applied to the fragile PEM. In a CCS process, the catalyst ink usually has a low viscosity. Due to its small pores and thereby high capillary forces, the GDL may soak up a substantial amount of ink. That amount of ink cannot contribute to the catalytic reaction and furthermore reduces the GDLs performance. To prevent the reduction of the cell's performance, more of the expensive ink needs to be applied compared to the CCM strategies. [FRÖ15, SIE15, BLA12]

Catalyst Application

Not only the process concept where to apply the CL but also the technology how to apply it offers a broad range of possibilities which will be discussed in the following. Depending on the process, the catalyst may be applied either wet, as a so-called catalyst ink, where the catalyst ingredients are mixed with a solvent or dry in form of a powder. Catalyst ink is easier to process but needs an extra drying process and might lead to swelling of the PEM in a direct CCM process. Plain catalyst powder does not need to dry and can be applied to the PEM directly with successive binding steps. [SIE15, BLA12] For aimed catalyst deposition additional deposition methods of the catalyst only can be applied.

With regards to the CL application, continuous coating and intermittent coating is possible. Continuous coating strategies offers faster web speeds and thereby lower cycle times. Dominant MEA designs consist of overlapping layers. Further processing of continuously coated PEM (MEA_{3L}) would therefore need a cutting step, followed by a pick and place process. Whereas intermittent coated PEM (MEA_{3L}) could be further processed by applying the subgasket or the GDL without an intermediate alignment and transferring step. Apart from those design specific restrictions, the drying step need to be taken into account. Corner areas are more likely to form defects during drying which is why continuously coated layers are more homogenous compared to intermittent coated layers. To determine the best suited coating strategy, one need to develop the production alongside the final MEA design and the use case.

Catalyst Coated Substrate (CCS)

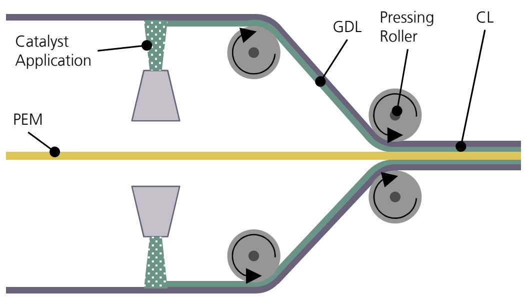

The CLs are coated onto both of the GDLs using either a wet or a dry application process. Afterwards, the PEM is compressed between the GDLs with the coated CLs. Drying of the catalyst ink and additional pressing processes need to be considered.

Advantages

- Short process chain

Disadvantages

- Catalyst ink tends to deposit in the pores of the GDL, where it does not contribute to the cell's performance

Sources: [SIE15], [BLA12]

Fig. 34: CCS Process Overview and Evaluation

Slot Die Coating

One way of applying wet catalyst ink in a continuous production is the slot die coating process (see Fig. 35). The ink is pressed trough a slit onto the substrate, which moves relatively to the die. The thickness of the coating is determined by the velocity difference and the mass flow of the ink. Since the ink is wet, a drying process, e.g. in a convection dryer, needs to be conducted afterwards. The process enables a precise and continuous application but needs a good knowledge of the ink's rheology. Slot die coating is widely used to coat continues surfaces but is still under research for intermittent coating as edges tend to be inhomogeneous in height especially at low viscosities [SIE15, GLÜ13]. Single and double-sided coating technologies are possible variations. By increasing the web speed, high production numbers can be reached with high quality of the coated layers. Slot die coating is therefore a reliable technique for CL application, also for the earlier mentioned use cases. Intermittent coating furthermore is advantageous for dominant MEA designs. This is mainly due to overlapping layers, which require partly uncoated areas of the PEM in order to optimize the catalyst usage.

Slot Die Coating

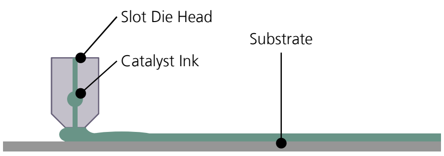

The dispersed catalyst ink is pressed trough a slot onto the substrate which can be, according to the selected manufacturing strategy, the PEM, a decal foil or the GDL. The dispersed catalyst ink needs to dry after application. Therefore a subsequent drying process (e.g. within an oven) is required. Since the ink is applied continuously, a fraction of the material might be wasted because not all of the electrode coating is in use.

Advantages

- Different catalyst ink dispersions processable
- Continuous and intermittent production

Disadvantages

- High complexity when intermittent coating (edges)

Source: [SIE15]

Fig. 35: Slot Die Coating Process Overview and Evaluation

Screen Printing

Screen printing (see Fig. 36) may also be used to apply the CL. It uses a screen with the desired shape of the CLs and a squeegee. The catalyst ink is pushed over the screen by the squeegee and passes through the pores of the screen onto the underlaying substrate. The thickness of the CL can be defined by the distance of the screen to the substrate. Using rotary screen-printing equipment might facilitate a continuous process, depending on the use case. Screen printing is a coating technology which is well known in other coating industries and offers high precision. Disadvantages are a wearing down of the screen due to mechanical stress and the necessity of an additional drying process. Also, the layer quality is highly dependent on the screen quality. [SIE15, BLA12, KAZ08] For high production numbers the wear and cleanliness of the screen limits the applicability. Depending on the MEA_{3L} design, thin CL layers may be needed which could be crucial to fulfill with screen printing. Slot die coating may be more beneficial in this case but technology choices strongly depend on the use case and thereby need to be assessed individually.

Gravure Printing

Another application process for wet catalyst ink is gravure printing (see Fig. 37). This process uses a rotating printing cylinder with gravures, so called cells, on its circumference. The cylinder is submerged partially in a pool of catalyst ink. The ink is collected by the cylinder as it rotates and gets stuck in the cells. Spare ink is wiped off by a doctor blade. The ink in the cells is then pressed onto the substrate where it keeps sticking. This process allows continuous production while also making it possible to shape the CL. The printed layers have a high homogeneity and constant thickness but only low viscous inks may be used and the mechanical stress is higher than compared to other technologies [SAN19, SIE15]. Due to the limitations in CL ink, slot die coating may be more beneficial.

Besides the above-mentioned wet application technologies, flexographic printing, inkjet printing, knife printing, spraying and brushing processes can also be used. [SAN19, SIE15, STR15, GLÜ13, BLA12] Especially inkjet methods offer high potential for future applications due to their fast adaption to new parameters and precise dispensing volume. Possible dry application processes include calendaring, sputtering, and dry spraying. The indirect CCM process in which the catalyst is applied to a decal foil is also often declared a dry application process. [FRÖ15, SIE15, BLA12, KAZ08]

Screen–Printing

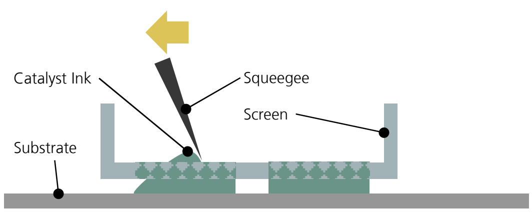

In screen printing, the screen has a porous material structure in the shape of the desired electrodes. The ink particles can pass the screen in this area. The catalyst ink is applied to the screen and pushed over it by a squeegee. The catalyst ink moves through the openings onto the underlying substrate. The thickness of the layer can be adjusted by the distance between the squeegee and the substrate and the volume of the applied ink.

Advantages

- Adjustable and precise CL can be achieved
- Continuous production possible using rotary screen–printing equipment

Disadvantages

- Screen may need to be replaced often because of mechanical stress

Sources: [SAN19], [SIE15], [BLA12]

Fig. 36: Screen-Printing Process Overview and Evaluation

Gravure Printing Process

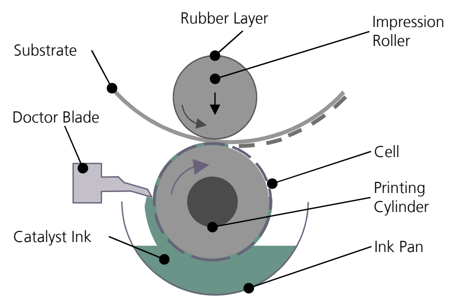

The dispersed catalyst ink is collected by a rotating printing cylinder, which has gravures (cells) on its circumference. The cells display the form of the wanted electrodes. The ink within the cells is transferred onto the substrate, which can be either the PEM, a decal foil or the GDL. Since the thickness and the form of the electrodes is dependent on the gravure, a best fit electrode can be applied by adapting the gravure. As the ink is wet when applied, a drying process needs to be conducted afterwards.

Advantages

- Continuous production
- Very high layer homogeneity

Disadvantages

- Drying process needs to be optimized in relation to the catalyst ink specification
- Mechanical stress is put on the substrate

Sources: [SAN19], [SIE15]

Fig. 37: Gravure Printing Process and Evaluation

Possible Process Chains for MEA Production

The earlier mentioned production strategies investigate only the CL application due to its high potential of lowering production cost through lower catalyst usage and lower cycle times. Drying the CL is a process step which also needs further investigation as inhomogeneous CLs lead to a decreased durability and possibly inefficient production. Apart from this process step, the subgasket may be laminated onto the MEA_{3L}, the GDL needs to be hot-pressed onto the CL and the individual MEA_{7L} then needs to be separated. Employing those steps as well, one may continuously fabricate MEA_{7L}. Many different process chains are possible and subject to different publications and patents.

James et al. describe a direct CCM process developed and used by GORE in which catalyst ink is applied by a slot nozzle onto a substrate and dried afterwards. In a next step the wet PEM is applied along with an expanded PTFE layer onto the dry CL. The membrane material is then dried. After this, the second CL is applied by a slot nozzle and dried afterwards. In a last step, the substrate onto which this sandwich structure is built is being removed. Key technology in this process is the wet application of the membrane material, since most publications describe the membrane as a prefabricated sheet. [JAM17]

A patent submitted by the Toyota Motors Company describes a process in which the CL are applied onto the PEM as a dry powder in rotary screen-printing process. Screen printing is normally conducted with a wet catalyst ink to ensure that the coating adheres to the substrate. However, the patent suggests using a charged drum, similar to the photo conductor drum in an electrophotographic printing process, to transfer the layer onto the PEM. The layer is then pressed onto the PEM by a heating roll. The GDLs are added in a following process. [KAJ13]

Another patent submitted by Hyundai Motor Company describes a CCM process in which the prefabricated PEM is applied to a substrate (a polymer film) using a binder and a hot-pressing process. The catalyst ink is then applied by a bar coating process, which is similar to the slot die process, onto the PEM. The typical shrinking and wrinkling of the PEM, when in contact with the catalyst ink's solvent is avoided by the substrate underneath the PEM. The PEM-Catalyst assembly is then dried in an oven and afterwards separated from the substrate. The product is a so called MEA_{2L}. It now needs to be hot-pressed together with another MEA_{2L} forming a MEA_{3L} with one PEM, consistent of the two earlier functionalized PEMs, between two CLs. In a last step, the GDL is added and the whole assembly is hot-pressed. Alternatively, one of the CLs can be applied to the GDL in a CCS process. [LEE10]

From use case requirement analysis, typical materials, common MEA_{7L} designs and process limitations may be derived, that indirect CCM with slot die coating becomes advantageous. MEA_{7L} design constraints have been identified and taken into account. With decisions on certain process technologies a wide dimension of whole process chains is applicable and must be derived for a certain application and MEA_{7L} design.

Key Takeaways for the Manufacturing Industry

- MEA_{3L} and their components may be produced in continuous roll-to-roll processes.
- One of the key processes is the application of the CL in which three different strategies may be considered.
- Coating and Drying technologies are highly depending on each other.
- For high production volumes, material costs are the major cost driver, especially the catalyst material.

Application of Gaskets

Apart from the BPP and the MEA, the sealing concept has a high impact on the overall design and by that on the whole FC. In addition to the subgasket, the gasket plays an important role for dividing reactant gases. It is the sealant between the BPP and the MEA which also prevents fluids from leaking out of the stack. If the seal is applied onto the BPP, it is often referred to as seal on plate and not as gasket. To fulfill its purpose, the gasket needs to sufficiently seal off independently of the surface roughness, compensate height differences within given tolerances and withstand vibrations, compressions and pressure drops while being utilized in e.g. a coach or truck. Apart from mechanical requirements, chemical stability, especially in acid environments, different moisture levels and high ion concentrations are an important requirement. A broad thermal stability with regards to cold starting of the FC and possible temperature gradients is also essential for a long term durability. Many materials may fulfill the given requirements of which only some are widely available and cost efficient to use. A closer look will be taken at flexible materials due to their proven processability via injection molding, screen printing and dispensing. Those materials may be grouped into their polymerization trigger which could be temperature, light and many more. [FUE11, DIL04]

Curing via temperature is applicable for elastomers like Ethylene Propylene Diene Monomer (EPDM) rubber, fluorinated rubbers and silicones. Thermoplastic elastomers may also be processed via heat but only change in viscosity rather than curing chemically. Other polymers like Polyurethanes (PUR) and Polyolefins (PO) may be cured via UV-light. Both groups offer up- and downsides with regards to availability, curing time and performance. In general, UV-curing polymers are more costly than temperature curing materials due to their photo initiator. They may however cure faster due to their radical polymerization which would lead to a decreased cycle time. Thermoplastic elastomers may also harden quick with fast temperature decrease, available polymers are generally more expensive than other elastomers though. With regards to the use cases and their low to medium sized part quantity, longer drying materials like temperature curing elastomers will be further discussed. The possibly cheapest material would be EPDM rubber followed by silicones and fluorinated rubbers. One suitable material could be room temperature curing silicone due to its broad availability, its good chemical resistance and its processability at moderate temperatures.

Apart from the gasket material, there are several gasket design concepts which differ in the way the gasket is applied and where the gasket is applied to as seen in Fig. 38. Those designs have a big impact on the whole production chain as gasketing changes properties of BPPs and MEAs when applied. [JÖR17]

Firstly, the gasket may be applied as an inlay gasket when assembling the cell. For this, the gaskets are prefabricated and stacked between the MEA and the BPP. Since the production of the gasket is done independently, it has no impact on the quality of the other components. It is however detrimental that the gasket is limp and difficult to pick and place precisely. Another option is the application of the gasket on the BPP as a so called seal on plate. The seal is directly formed on the BPPs by applying the material in its uncured form. The material then

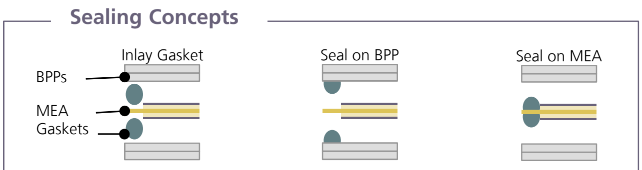

The place the sealing is applied strongly influences the stack design and thereby possible production chains. It may be applied either to parts of the stack like BPP and MEA or is added in between BPP and MEA.

Fig. 38: Visualization of Sealing Concepts

cures and sticks to the BPP. Respective to the application on the BPPs, it is possible to apply the gasket directly to the MEA. The basic procedure is the same: the material is applied and formed in a plastic state and then solidifies and sticks to the MEA. The result is a so called seal on MEA gasket which forms a MEA-gasket-assembly. The curing on top of the material is beneficial for sealing efficiency as the gasket BPP or the gasket MEA interface is perfectly aligned due to the liquid application. This makes the seal on BPP and MEA concept more beneficial for heavy duty use cases as durability generally rises. An even better formed sealing may be achieved by adding the gasket in its plastic form, stacking BPP and MEA and cure the gasket after its adaption to the interfaces. Gasketing should, in this case, take place right before stacking. The following subchapters will take a deeper look into the different concepts. [PEH15, TER15]

Inlay Sealings

Inlay sealings are prefabricated gaskets which are added in between the BPP and the MEA during stacking. The gaskets may be manufactured via injection molding or die cutting. Depending on the process technology, the gasket might need some post processing afterwards such as cutting off excess material and separation. Subsequently the gaskets can be stacked together with the other cell components. It is placed between one BPP and the MEA so that two gaskets are needed for one cell. Almost any polymer may be used for prefabricated gaskets as they need to be either cut out of a sheet or are applied via injection molding. This allows a broad range of polymers and enables usage of EPDM rubber, one of the cheapest materials which might be suitable for gaskets. Injection molding allows the gaskets to be produced in three dimensional shapes which gives more flexibility when designing the BPP and the MEA. The main advantage of this procedure is, that the gasket is fabricated separately from the other components so the gasket production does not influence the quality of the other components and has no influence on the productivity of the other production lines. However, an automated pick and place process for the assembly of the cell might pose difficulties as the gaskets are limp and challenging to handle.

Seal on BPP

Seal on plate gaskets are mainly formed directly onto the already joined BPPs. Possible technologies could be injection molding, screen printing, and dispensing. In case of injection molding, the BPP needs to be positioned in the molding form which is then closed as shown in Fig. 39. The plasticized material is injected into the mold, where it forms the gasket respectively to the molds form. The material cures on the

Seal on BPP / MEA – Injection Molding

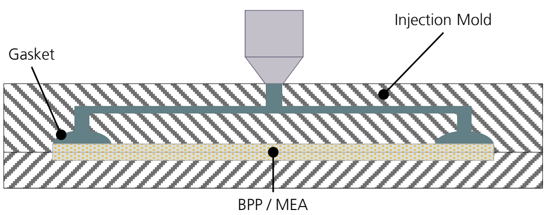

Gaskets on BPP and MEA may be manufactured by placing the substrate in an injection mold. The gasket material is plasticized within an extruder and then injected into the mold, where it forms the gasket onto the substrate and cools down.

Advantages

- High precision and complexity
- Three dimensional production possible

Disadvantages

- Expensive process adaption
- High temperature and pressure inside the tooling
- Possible deformation of joined BPPs inside the tooling
- Long cycle times

Fig. 39: Injection Molding Process Overview and Evaluation

BPP. In case of already joined BPP the gasket should ideally be formed on both sides in one tool leading to lower cycle time. The BPP with the gasket on it, can then be removed from the form. One of the main advantages of injection molding is the ability to form all kind of geometries. Downsides are however the difficult integration in a continuous production line and the process conditions inside the tooling which may cause damage on the coating of the BPP. A faster and continuous production may be achieved when employing screen printing or dispensing. Both technologies make use of BPP carrier which support the fragile structure of the BPP. Screen printing uses a squeegee to press the gasket material in its uncured form through a mesh which only allows throughflow in specific areas. The so called screen resembles the targeted gasket geometry. This process is illustrated in Fig. 40. After the material is applied, it needs to be transferred to its final aggregate state which, depending on the employed material, may be achieved by curing via temperature variation or light. Dispensing on the other hand makes use of different sort of dispensing nozzles which may also be ultrasonic systems or jet nozzles. The basic principle is shown in Fig. 41. The dispensing heads are following a specific geometry while dispensing variable amounts of liquid to deposit a gasket onto the BPP. After deposition, the material needs to be cured, similarly to the screen printing process. Both processes enable relatively high production speeds at good accuracy and leave the possibility

Seal on BPP / MEA – Screen Printing

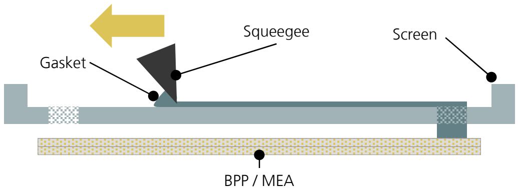

In screen printing, the screen has a porous material structure in the shape of the desired electrodes. The polymer is able to pass the screen in this area. The polymer is applied to the screen and pushed over it by a squeegee. The polymer moves through the openings onto the underlying substrate. The thickness of the layer can be adjusted by the distance between the squeegee and the substrate and the volume of the applied ink.

Advantages

- Cheap design adaptions by adapting the mesh
- High precision though precise mesh
- Low cycle time

Disadvantages

- Screen wear down rate possibly high
- Possible inclusion of air
- Screen size limits substrate size
- Possible deformation of joined BPPs through squeegee pressure

Fig. 40: Screen-Printing Process Overview and Evaluation

Seal on BPP / MEA – Dispensing

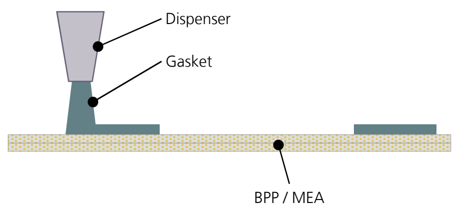

The dispensing process employs a nozzle to deposit plasticized polymer. Dispensing on the other hand makes use of different sort of dispensing nozzles which may also be ultrasonic systems or jet nozzles. The moved dispenser head may easily manufacture multidimensional gaskets and is very flexible to design adaptions.

Advantages

- Design adaptions by changing the dispensing head movements
- High dispensing precision possible
- Easy parallelization possible
- Efficient material usage

Disadvantages

- Low TRL for integration in a continuous material flow

Fig. 41: Dispensing Process Overview and Evaluation

of quick and cheap adaptions. Due to the supporting carrier, the joined BPP must be turned around in order to apply the second gasket which may only be done after curing. Materials need to be adapted to the individual technologies as all of them require a good understanding of the rheology of the material.

Seal on MEA

The MEA-gasket-assembly, much like the seal on plate, may use an injection molding (see Fig. 39), a screen printing (Fig. 40) or a dispensing process (Fig. 41) to form the gasket. The MEA is however more sensitive to mechanical and thermal stress compared to the BPP. A contaminated CL may not perform as well and might wear down faster than clean CLs. In case MEAs are placed inside the injection molding tooling similar to the BPP, the heat and pressure might even lead to irreversible damage of the PEM. Possible alternatives are screen printing and dispensing. Screen printing and dispensing do not apply high pressures and do not need high temperatures to work. The curing however still needs to be assessed as drying times as high as 60 sec with dry surrounding might lead to irreversible deformations of the PEM and delamination of the CL.

Possible Process Chain Integration for Gasket Application

The gasket application may be carried out at different points along the cell production process chain, depending on the chosen gasket concept. The inlay sealing has to be inserted during the final assembly of the cell. Typically, the seal on plate gasket is formed on the BPPs after they are joined and coated. This mainly bases on the assumption, that the gasket channel is also used for joining the BPP and that the coating may not cover the gasket. There are however concepts of partial coatings which would allow a coating after gasketing. The functionalized BPPs may then be packaged and sold or forwarded to the final assembly of the FC. Similarly, the seal on MEA gasket is formed after all parts of the MEA are stacked and hot-pressed together. The seal on MEA gasket can then be assembled together with the BPPs to form the cell. The assembly processes will be discussed further in the chapter "Assembly of the Stack". Apart from the discussed concepts, the gasket may also be applied to either the BPP or the MEA which are first stacked and cured afterwards. In this case, the plasticized gasket material is cured via temperature after the stacking process. This formed in place gasket adapts better to interferences and might result in a superior sealing performance, depending on the employed materials.

Key Takeaways for the Manufacturing Industry

- The gasket is an essential part of every FC and should therefore be taken into account when designing the FC especially due to their implication on FC design and production processes.
- Three technologies are available for gasket manufacturing which are injection moulding, screen printing and dispensing. All offer a different set of advantages and disadvantages and choices strongly depend on each case.
- When technologies are suitable combined, a process with low cycle times and high quality products for long term durability may be established.
- Seal on BPP or MEA appears to be advantageous to inlay gaskets.

Assembly of the FC Stack

After the production of BPPs, gaskets and MEAs, the next step is to assemble them into a functional arrangement, a so called FC stack. This is achieved by alternately layering BPPs and MEAs on top of each other. After multiple pick and place operations, the stack is compressed to ensure adequate sealing of the system and to achieve a low electrical contact resistance between the layered components of the stack. High precision with regards to positioning in the earlier stacking process is one key parameter for sufficient sealing and low contact resistance. A controlled environment during assembly may be beneficial due to the high sensitivity of the MEA to temperature and humidity fluctuations and its resulting change in dimensions.

The following chapters analyze how FC parts can be stacked, compressed and tensioned, as well as how the FC design influences stacking. Further, different EoL tests and FC conditioning are addressed.

The typical arrangement of the individual processes during assembly is shown in Fig. 42.

After a possible pre-stacking of BPPs and MEAs, they are stacked, compressed and tensioned. In the next process step, the entire stack may be tested with regards to leakage and electrical insulation. After it has been verified that the stack is functional, it needs to be electrochemically prepared for later usage via conditioning with reactant gases. A possible electrochemical testing, involving hydrogen, may be carried out prior to or after conditioning. These processes usually take place at individual stations. Depending on the cycle times, processes may be used in parallel.

Fig. 42: Process Steps of FC Stack Assembly

Giving this overview, the individual assembly processes are discussed in more detail.

Stacking & Pre-stacking

The stacking procedure is more or less independent for the use of the FC stack, although the number of cells influences the overall performance of the stack. Depending on the stack design, different numbers of cells as well as different geometries of BPPs and MEAs need to be stacked. Depending on the BPP and MEA manufacturing process, different sub-assemblies need to be handled and stacked, which are listed below:

- Two main components are stacked alternately: BPP, MEA_{7L}
- Three main components are provided for stacking: BPP, GDL, MEA_{5L}
- Four main components are provided for stacking: BPP, GDL, gasket, MEA_{3L}
- MEA_{7L} can be connected to BPP in a pre-process, which leads to a single cell unit as one component for the stacking.

Apart from the repetitive components (BPPs and MEAs), end plates, current taps, bracing elements and connectors are also provided for stacking and need to be added to produce a complete FC stack.

During the stacking, the components with different geometries and stiffnesses are placed on top of each other by grippers. The more individual parts need to be stacked, the longer the entire stacking process takes. Pre-stacked components however need to be stacked in an earlier production process which results in a cycle time shift and might offer advantages with regards to productivity but could result in more complex handling operations. To optimize the processing time during stacking, multiple separate grippers which grip and deposit parts may be installed asynchronously. Due to high flexibility of gripping systems, different stack sizes and geometries can be assembled in one stacking line. However, the technological possibilities of the stacking process should be kept in mind, when FC designs are developed.

Pre-stacking individual cells with later stack manufacturing (Assembly Version A, see Fig. 43) compared to stacking with individual BPPs and MEAs (Assembly Version B, see Fig. 44) result in different production concepts which will be assessed further below.

The assembly process in Version A is divided into two parts: pre-stacking and stacking. During pre-stacking, the MEA is stacked between two BPP halves. The individual components are provided by feeders in a batch-wise manner, or by a conveyor belt. Subsequently, the cell is joined, locked into position and tested. If the cell has no leakage and no short circuit, it is passed on to the stacking station. In the stacking station, the tested cells are stacked to form a finished stack. Good electrical contact between the anodes and cathodes BPP needs to be ensured with e.g. an electrically conductive adhesive. The finished stack is again compressed, tensioned and conditioned as seen in Fig. 43. Due to the single cell testing the assembled stack has a lower possibility of malfunctioning. One possible error however, could be insufficient alignment of the cells themselves. Version A has a higher cycle time compared to Version B due to the pre-testing of the cells and the repetitive compression process in the pre-assembly and the assembly.

When assembling according to Version B, all components are positioned on top of each other at once. The components again are provided by feeders in a batch-wise manner, or by a conveyor belt. Afterwards, the stack is compressed, tensioned and forwarded to the test station. At the test station, a complete stack is tested for leaks and short-circuit connection.

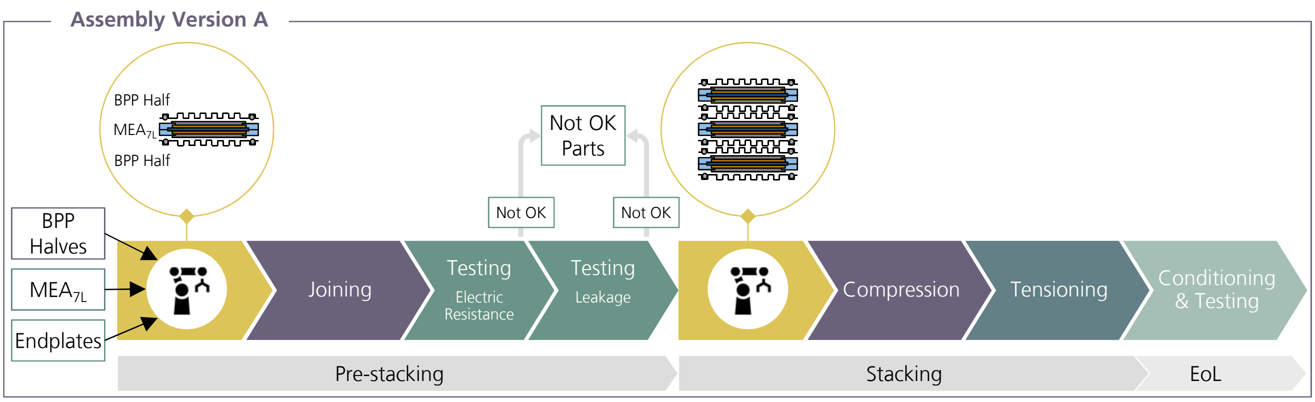

Advantages

- Better error management
- The stack does not have to be disassembled to look for errors

Disadvantages

- Alignment problems of the cells themselves
- Pre–checking takes a lot of time
- Higher cycle time of the overall process
- Compression step must be repeated

Fig. 43: Single Cell Assessment Assembly Process Chain for BPP Halves

Compared to Version A, one final test results in a much lower cycle time per cell for testing. The process is shown in Fig. 44. Due to the missing tests of the single cells, the possibility of malfunctions inside the stack is higher though. In case of a defect, the whole stack would need to be disassembled and the faulty cell would need to be detected. Testing in version B generally indicates errors in the stack, but cannot give the information, which single cell is defective. Therefore, this process chain is only recommendable if the manufacturing processes of BPP, gasket and MEA are well known and little prone to errors.

The main difference between both concepts lies in the order of processes with regards to the testing. Whilst Version A assesses the single cell, Version B tests the stack. Pre-stacking first stacks a single cell, which consists of two BPP halves a MEA and a seal in between. This version is therefore more suitable, if BPP halves are not joined in earlier production steps. If BPP halves are joined in previous processes, the single cell consists of a BPP, a MEA and gaskets, which makes the test procedure of a single cell impossible and would therefore be more suitable for Version B [BOB20, H2M20, WAL20]. Precise positioning of components when layering is of high importance for both approaches. To achieve precise positioning, the individual parts may either be aligned by mechanical structures like tensioning rods or other sort of supporting stack structures. In addition, optical systems may be added to the stacking machinery to check every stacked component on its precise placing.

Compression

Compression is needed to maximize contact surfaces between BPP, GDL and CL for low electrical resistance as well as for sufficient sealing. However, a compression force that is too high may destroy the stack.

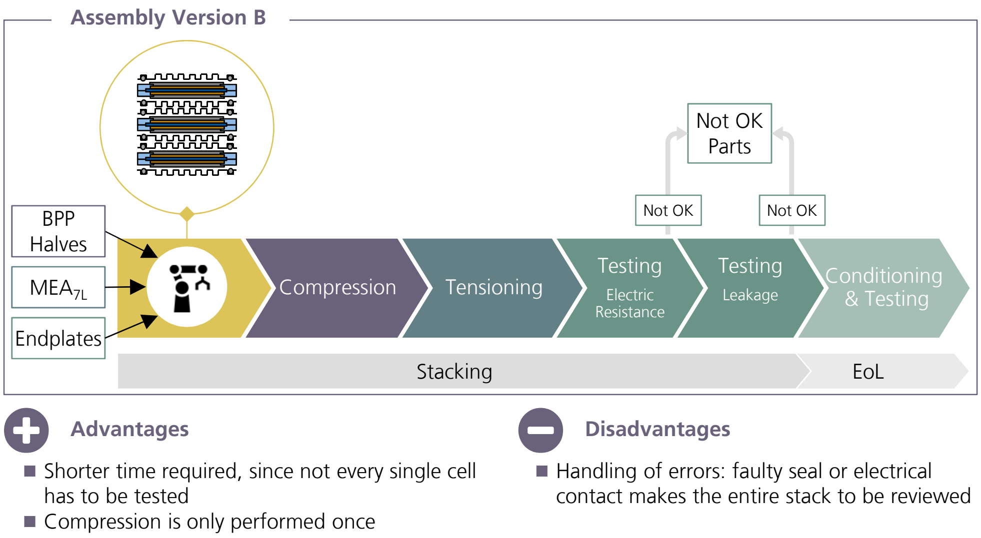

Fig. 44: Stack Assessment Assembly Process Chain for BPPs

GDL is a very porous component (60–70 % porosity) and should be compressed by around 10 % so that an electrical contact to the BPP and the CL is ensured. If it is compressed too much, the porosity of GDL is reduced, which limits the mass transport and thereby has negative effect on the cell performance. GDL is typically made of carbon fiber, depending on the type of GDL, may be brittle and poorly resistant to mechanical stress. PEM and gasket are other compressible components, that are much less compressible than GDL. In the case of seals, imprecise positioning of the gasket creates the risk of seal slipping and thereby the risk of blocking the flow field channels or manifolds. The gasket needs compression though to properly seal. In addition, BPPs made from graphite composites are brittle, a compression and bracing can lead to cracks and breaks in the BPP. [MIL15]

For stack compression a compression force of 2,000–3,000 kPa is required. Compression can be performed with several devices e.g. hydraulic presses, pneumatic presses, screw presses or servohydraulic presses. Due to mechanical relaxation processes in the stack the compression process must be performed over a period of several minutes in order to reach a stable tension state. There are several versions of how the pressure can be built up, e.g. in stages or with vibration. The optimal contact pressure needs to be calculated for each stack depending on the contact surfaces of the single components.

Tensioning

After compression, the stack is tightened with tensioning elements. This process is relevant to maintain the compression and thereby its function over the whole lifespan of the stack. Uneven tensioning leads to a lower lifetime of the FC stack as BPPs, gaskets and MEAs are unevenly stressed which could result in internal or external leakage of process gases. There are several ways to brace a stack, the most common is using tension bars. Depending on the stack design, the tension bars go through the stack or are located on the outside of the stack. They connect the two end plates to another and thereby keep the stack clamped. Mechanical alignment through the rods may be possible using methods like guiding constructions that facilitate positioning and are not part of the stack.

Tension Rods

Advantages

- Used for alignment when stacking
- Clamping against the end plates by means of screw nuts
- Non–destructive dismantling possible

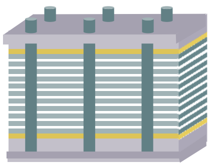

Disadvantages

- Defined screwing sequence in steps required, otherwise the membrane and / or GDL may be crushed
- Inhomogeneous pressure distribution possibly
- Thick end plates are used to compensate for uneven compression
- The clamping force is only present on a limited number of points around the perimeter

Tension Bands

Advantages

- Can be cheaper in mass production
- Use of thinner end plates is possible
- Weight reduction is possible

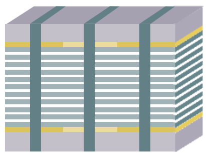

Disadvantages

- Complex machine structure/ process due to limited accessibility during pressing
- Non–destructive dismantling is not possible when welding
- Tightening becomes more complicated

Fig. 45: Two of the most popular Tension Methods: Tensioning Bands and Tensioning Rods

A second common method of tightening stacks is tensioning with bands which are placed around the stack. Both ends of the bands are then connected. In some stack designs, the band ends are welded which makes it difficult to disassemble the stack if necessary. Tensioning bands might therefore be a better choice for the stacking concept version A due to lower possibilities of stack errors after tensioning. A main advantage of the tensioning bands are the low price and weight compared to other systems. Furthermore, mixed concepts including bands with rod are available. This enables a tightening of the band if necessary. Other concepts work with clamping plates. A comparison of tension rods and tensions band is shown in Fig. 45.

Leakage and Insulation Testing

After staking, either single cells or a complete stack, the assembly is tested. The testing ensures correct manufacturing via physical validations. In a first step, the FC can be investigated with respect to its electrical conductivity. Electrical connections between two BPPs (electrical short circuit) indicate that the gasket/subgasket does not work properly or that the MEA has pin holes. These small holes can arise as a mistake in membrane manufacture. When testing the entire stack, the electrical isolation of every single cell has to be tested. Otherwise a short circuit cannot be located. Typically, the determination of the gasproof sealing follows the electrical testing.

In all technical systems, 100 % leak tightness is not achievable. It is reasonable to define a maximum acceptable leakage rate (limiting leakage rate) for the respective application. Depending on the defined limiting leakage rate, a selection of suitable test methods and procedures can be made. Attention must also be paid to the pressure load during operation and the choice of test gas, which is used for testing. In addition, a distinction between integral and local testing can be made.

With the integral test, the total sum of all existing leaks can be determined. It is not possible to quantify or localize these leaks though. With localizing testing, the exact location of a leakage is determined, but a quantification of the leakage rate is only possible to a limited extent.

The test spectrum ranges from the simpler bubble test to more advanced test methods with detection gases. For FCs, DIN EN 62282-2-100 proposes a gas leakage test for the routine testing of FC modules using the through-flow test or the pressure decay test.

Pressure decay test (max. leakage rate 10^{-4}–10^{-3} mbar L/s):
In the pressure decay test, the system is pressurised with gas while the outlets of the stack are closed. Typical gases are Air or Nitrogen. Then the part is disconnected from the gas supply and after a stabilisation time, its internal pressure is monitored. The pressure drop is measured over time. If the pressure drops as slow as expected, the component may be error-free.

Trough-flow-test (max. leakage rate 10^{-3} mbar L/s):
This test method measures the flow rate of gas over time with the stack outlets open. The test gas flow rate is measured with a flow meter and then compared to an acceptance range.This test method is similar to the pressure decay test and typical gases are Air or Nitrogen. The difference is that the gas flow rate is measured over time with the outlets opened to the atmosphere.

Sniffing test (max. leakage rate 10^{-6}–10^{-7} mbar L/s):
The FC system is pressurised with a specific test gas like Helium. Afterwards a detector is used to measure the specific test gas on the outside to detect leaks. The detector is moved around the part while measuring and may thereby detect site specific leaks. The speed, the distance to the part and the sensitivity of the probe determines the accuracy of the leak detection.

Accumulation test (max. leakage rate 10^{-6} mbar L/s):
The FC system is placed in a test chamber, which is under atmospheric pressure. The system is filled with test gas. The exit of the test gas is prevented by closing the system outlet. If there is a leak, test gas accumulates in the test chamber. After the test gas has accumulated during the test period, the helium concentration is detectedby a gas sensor and the leakage rate can be determined.

Vacuum chamber test (max. leakage rate 10^{-10} mbar L/s):
The vacuum chamber test works analog to the accumulation test but the test chamber is not filled with gas but rather evacuated. This method enables to only measure the test gas without any other impurities and thereby enables the highest measurement resolution.

Depending on the assembly concept, testing may be carried out with the whole stack or with single cells [KUM20, CHE12a].

Conditioning and Testing

In order to maintain optimum performance during operation of the stack, conditioning is required. There are three main functions of the conditioning, which all in cooperate the MEA: humidification, removal of residual solvents and other impurities resulting from the manufacturing of the MEA, and removal of anions from the catalyst to activate the reaction areas. State of the art procedures require from 1 h up to 15 h of FC operation while achieving varying degrees of FC stack functionality. When conditioning according to the protocol, the temperature, current/voltage and gas flow rate are variable in stages [TIN09, SCH06].

Key Takeaways for the Manufacturing Industry

- Stacking is generally a pick and place process in which the stack components are positioned on top of one another.
- The stacking process strongly depends on whether BPPs are joined prior to stacking.
- When it comes to stacking, the speed, a high degree of automation, and the accuracy are decisive.

Possible Process Chains for Stack Assembly

The process steps of assembling BPP, MEA and gasket vary in terms of the order of testing and stacking and are assessed in the two concepts shown. Functional inclusion of assembly inside the whole PEMFC production chain is a bigger challenge though. Especially when cycle times from earlier continuous processes need to be met, the discontinuous assembly process may form a crucial bottleneck for scaled up productions. The relevant process steps for fluent transversion of manufactured parts will be discussed in the following chapter.

Interconnections of Multiple Process Steps

To design an optimal PEMFC production concept, the overall PEMFC process chain may be divided into sub-processes like BPP manufacturing which itself consists of many different processes like forming, cutting and joining as described above and as shown in Fig. 46. To develop an automated production chain, the single processes need to be connected to ensure seamless material flow. A well-developed material flow allows for high efficiency with regards to automatization of the overall production concept.

Connected process chains usually employ different sorts of gripping systems and carriers. Those handling systems will not be assessed further during this publication due to a high dependency on their field of use and their variety. This chapter proposes a generic method for analyzing interconnections in a simplified way, illustrated by the example of BPP manufacturing. The method consists of the following three basic steps which will be addressed separately in the following: production requirement analysis, process chain boundary conditions and technology evaluation. Production Requirement Analysis Requirements derived from utilized production technologies are mandatory to be considered and require individual determination for every process step itself. Forming and cutting of metallic BPP halves will be used as an example. After separating the BPP halves from the coil, they need to be transported as single parts or batchwise, which either way is a discrete transportation. The first requirement is therefore the ability to transport single or grouped BPP halves. The second

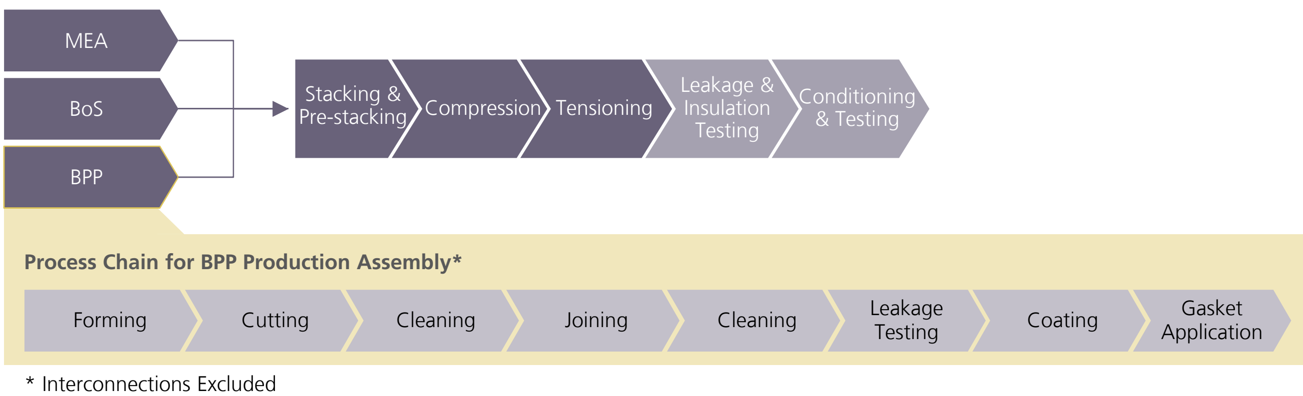

Fig. 46: Overall FC Production Chain

requirement results from the approximate material thickness of BPP halves (~100 µm), which tend to be limp and therefore need some kind of supporting structure. Transporting the flexible single BPP while stabilizing it is therefore of great interest. There are also none-mandatory requirements that may be considered like marking techniques for quality assurance or quality aspects like controlled environments with regards to particles and pollution as well as vibrations.

Process Chain Boundary Conditions

As discussed earlier, individual process steps may be chosen not only due to their technological suitability but also due to economic factors, including parameters like cycle time and overall equipment effectiveness. A similar approach may be chosen when assessing interconnection technologies. Based on assumptions from the production processes described earlier, interconnections may not be slower than a few seconds per piece in order to keep the velocity of the complete process chain and to achieve target quantity. The required cycle times can be reached batchwise or in a continuous production. The decision is highly influenced by the possible necessity of high peak production volumes or by high flexibility in between manufacturing steps.

Technology Evaluation

After assessing the requirements, possible technologies can be evaluated by comparing their individual suitability. As mentioned in the requirement analysis, low structural stiffness of BPPs is one of the issues that influences the choice of interconnecting technologies in production processes. A possible interconnecting technology would therefore need to transport the BPP half without damaging it but also adapt to the fast process speeds of the formed BPP halves. Additionally, the position accuracy has to be guaranteed when the products are forwarded to the next processing step. Depending on the local proximity to the next process step, BPP halves may be stored in magazines or be transported individually. In some production steps, BPP halves may be joined, cleaned and coated. Areas of fixation on the BPP half should be precisely chosen as joining for example needs specific accessible areas on the part's surface. Possible technologies may employ air or magnets in order to enable touchless transport. A variety of gripper solutions is available.

For the development of an overall concept, all of the interconnections within a production line have to be considered. A technological solution is mainly specifically tailored to the use case and needs profound knowledge of the overall process chain to gain a seamless implementation and thereby high degrees of technological and economical efficiency.

Key Takeaways for the Manufacturing Industry

- Interconnecting of individual process steps, but also of whole process chains, depends on technological and economical requirements which need to be analyzed prior to an evaluation of possible technologies.
- Production requirements may be derived from type and form of the produced product like weight and stiffness.
- Technical requirements of the interconnecting technologies may be derived from use cases and strategic goals.

Possible Process Chain for PEMFC Production

There is a variety of process combinations, all able to manufacture FCs with a decent performance. While the process steps required to produce an FC stack can often be determined without uncertainty, the difficulty arises in defining the specific process chains and the process-step-specific technology selection. However, scalability and stack quality are crucial in FC production in order to reduce costs and provide long term durability, which is why there is ongoing development of the production technology. The objective of this study is the derivation of a reference process chain for the production of an FC stack. For this purpose, concrete application cases were

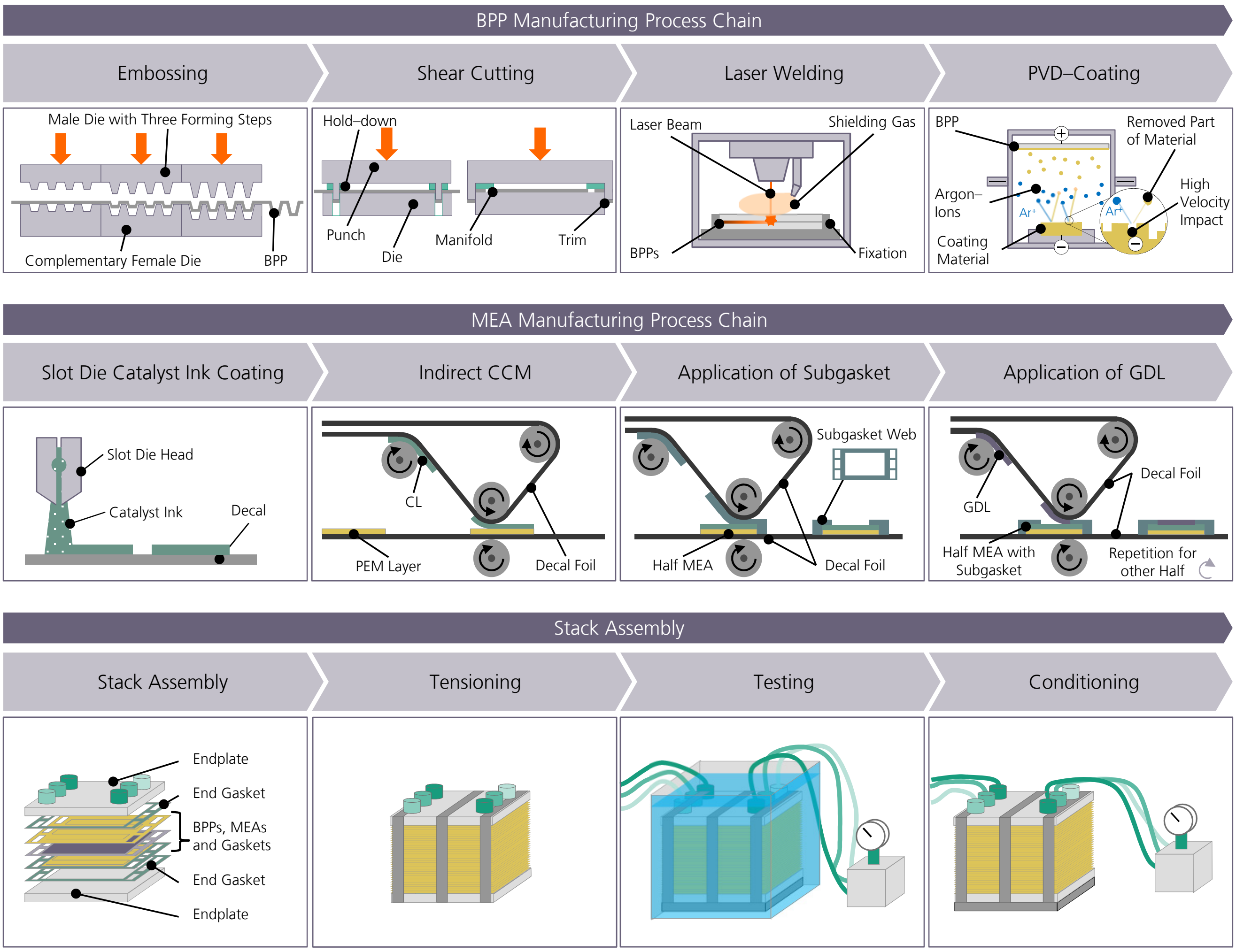

Sources: [FRA19], [WEI19], [JAM17], [JEN17], [ASR16], [MOH16], [FRA13], [LAM13], [MAH10], [HEL06], [SIM89]

Fig. 47: Reference Process Chain

initially considered and a specific use case was selected. In the context of the presentation of the necessary process steps for the production of individual FC components, individual technologies were already selected for the specific use case. Fig. 47 provides an overall overview of the selected technology alternatives for a reference process chain. The BPP production chain can be specified in more detail compared to the MEA chain due to the fewer possibilities of substantial design variations of the BPP´s and thereby higher correlation to the case. The MEA process chain was analyzed with regards to the catalyst application concept and technologies. Further process steps include the application of subgaskets and GDL. Employing a decal foil as carrier is one possibility and is shown in Fig. 47. Follow-up processes like hot-pressing and cutting is not investigated at this point. The gasket assembly also has a high dependency on the PEMFC design. Typically, the gasket is applied to the BPP technology may not be chosen due to its strong dependance on the PEMFC design. Stacking may be used which leads to a stack as shown Fig. 47. Handling, consistent of many different possible technological solutions, is not shown due to its complexity.

ECONOMIC ANALYSIS OF FC PRODUCTION

To increase the attractiveness of FCEVs, reducing TCO is crucial in addition to driving forth technical improvements. Focus is put on costs of FC stacks, as part of TCO. Stack costs depend on product and process design as well as on production quantity. For a fixed design, eligible process alternatives need to be compared regarding their manufacturing and material cost influence. Any decision on the process type depends on the designated annual production rate. In case of fixed production processes, a favorable annual production rate needs to be determined.

Fraunhofer IPT has developed a dynamic cost estimation tool, that enables a thorough analysis of the cost distribution, cost drivers and dependencies as well as an evaluation of manufacturing and material cost of FC stacks for different designs, manufacturing processes and annual production rates and thereby can be a valuable assistance tool for companies that are planning a specific production line.

Description of Dynamic Cost Estimation Tool

The FC stack tool includes MEA with GDL, BPP, gaskets, current collectors and endplates. Other parts such as compression bands and stack housing as well as BoP components as air loop, fuel or coolant loops, controllers and sensors, battery and electric motor are currently excluded. Furthermore, no mark-up rate is included in the cost estimation.

The total costs is the sum of direct material costs and manufacturing costs. The material costs are a function of material type, material mass, volume prices and learning curve. The learning curve is used to incorporate the tendency of material cost on a per-unit basis to decrease with increasing purchasing volumes. The manufacturing costs depend on the design features of parts, time to generate required part features, machine type incl. tools and machine rate. The machine rate is the hourly cost based on amortization of capital and operation cost (maintenance, electricity e.g.).

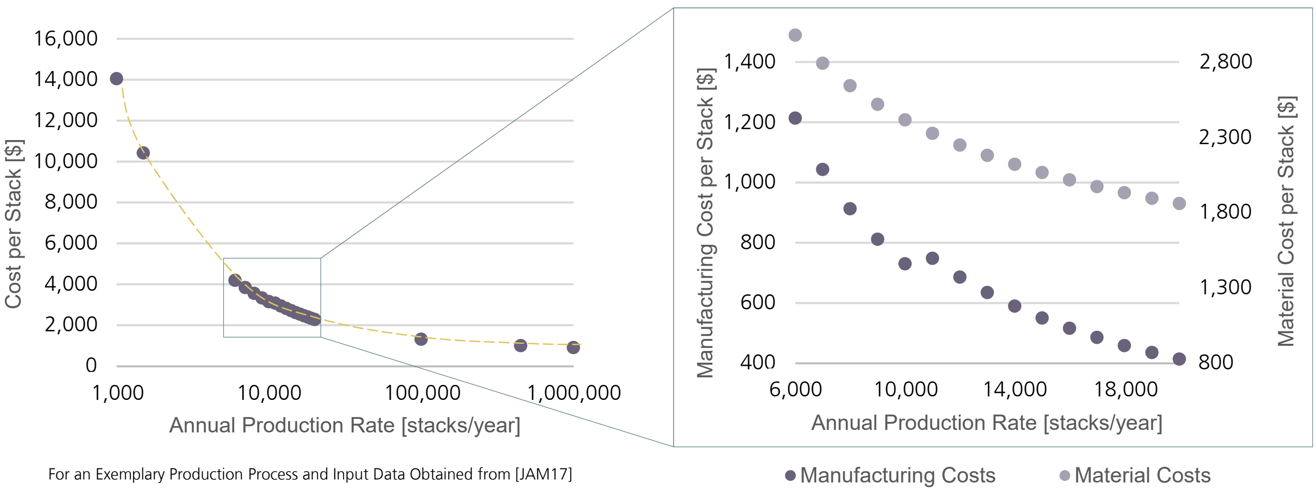

Fig. 48: Total Cost as a Function of the Annuals Production Rate

Thus, required input variables are material and labor cost related quantities such as material purchasing price per weight and hourly labor costs per worker. Next to these physical design quantities, performance quantities such as the electric power required per stack, geometrical quantities such as area of a BPP and active to total area ratio need to be inserted into the calculation tool.

Discussion of Influences on Stack Costs and Potential Levers for Cost Reductions for an Exemplary Process

The tool is able to produce models given design and process variants as well as different production scenarios. We hereafter only produce a limited number of evaluations for an exemplary production process in more detail.

The particular visualizations and conclusions displayed in the following are based on calculation results of the tool, chosen design quantities (electric power of 100 kW per stack and stack power density of 10 kW/m^2) and process and machine data taken from a study of the DOE [JAM17]. MEA group in this case includes the manufacturing steps catalyst preparation and ink application, CCM acid washing due to special catalysts, hot-pressing CCM and GDL manufacturing, cutting and slitting and MEA sub gasket manufacturing. The BPP manufacturing here includes BPP stamping with cutting, coating and laser welding. Under the term endplate, here compression molding of the end plate, current collector manufacturing and end gasket screen printing are summed up. As mentioned above, the tool input data needs to be adapted to the particular processes, that the user is interested in. Thus, the following results are specific to the addressed process (and chosen design) and are no universally valid insights.

For this exemplary production process, total costs per stack are examined as a function of the annual production rate (see Fig. 48). Here, high costs occur for small annual production rates in the order of a thousand stacks per year. A scale up results in significantly lower production costs. At an annual production rate of 10,000 stacks, the price per stack is about one fifth of the costs at 1,000 stacks.

Fig. 48 furthermore shows, that the course of the cost curve is not steady and costs do not continuously decrease with an increase in production rate which can be seen at a higher resolution and when splitting up manufacturing and material costs. When displaying the total costs split up into material and manufacturing costs, this behavior can be clearly attributed to the manufacturing costs curve. The sudden increase in the total manufacturing costs is due to the necessity of an additional machine for example, which is needed at a certain threshold in annual production rate. As a result, machine utilization reduces and stack cost increases. Due to the superposition of the effects of different machine capacities for the numerous processes, the determination of an optimal production rate in a given range of planned annual production rate is not trivial.

Furthermore, different process steps see scaling in a different way. In Fig. 49. the total cost per stack for various annual production rates are shown for separate part groups. For all production rates in the investigated range, the BPP for example makes up for a rather small share of cost. The cost distribution and development show that although a reduction of costs with increased production rate takes place, for this example design and process type, the BPP costs are a small lever in reducing the overall costs for low production rates. For larger production rates, the share of BPP costs increases. This is due to the made assumptions and resulting scale effects already for small production rates. For an annual production rate of 1,000,000 stacks compared to 10,000 stacks, the share increases from about 10 % to 40 % and therefore should be considered a lever for cost reduction in large scale production. The cost distribution might look different in case other assumptions are made for the input data for the tool.

The total cost of stacks can be split into material and manufacturing costs (see Fig. 50). For the design and processes investigated here, manufacturing costs for an annual production of 10,000 stacks make up about 23 % of the total cost while for an annual production of 100,000 stacks the manufacturing costs share reduces to about 13 %. For higher production rates, no significant further reduction of manufacturing costs can be observed and the cost of material is predominant. Regarding separate parts or part groups, respectively, we refer to Fig. 50: a significant cost reduction through optimizing production processes can be achieved for MEA production volumes between 10,000 and 100,000 stacks per year for this stack design as an example and the assumed production processes. Here especially manufacturing costs decrease strongly. The share of manufacturing costs of the BPPs also decreases, but still makes up for about 27 % for production rates between 100,000 and 1,000,000 stacks per year. Here, further reduction of manufacturing costs should be analyzed.

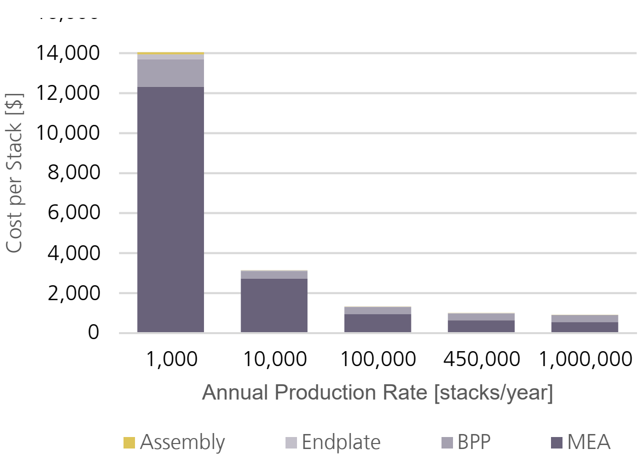

For an Exemplary Production Process and Input Data Obtained from [JAM17]

Fig. 49: Total Cost per Stack as a Function of annual Production Rate and Part

As stated above, for the displayed process in this example, at higher production rates, material costs are predominant. But, the reduction of manufacturing costs for low production rates is a large lever for the reduction of the overall stack costs. As can be observed in Fig. 51 the by far largest share of manufacturing costs at 10,000 stacks a year can be attributed to the manufacturing processes of the MEA part group. However, the MEA part group is dominated by material costs, where the BPP costs can be reduced by optimizing the production process.

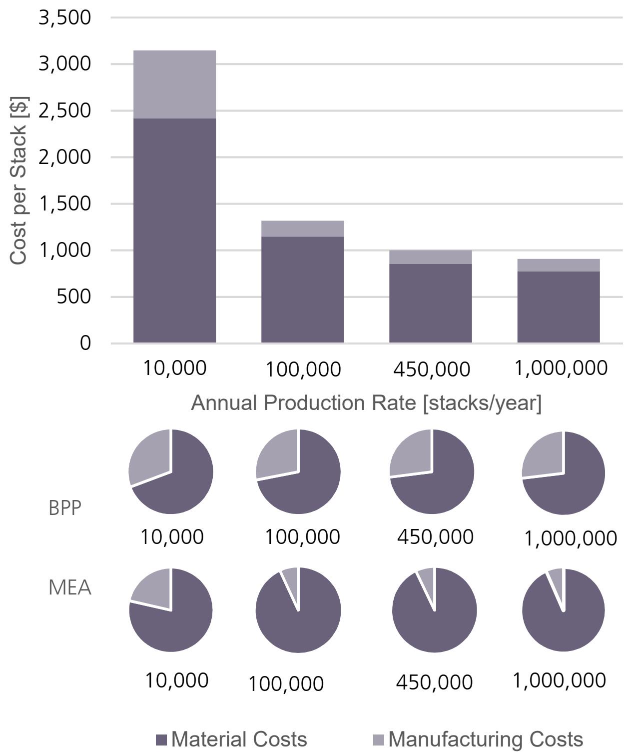

For an Exemplary Production Process and Input Data Obtained from [JAM17]

Fig. 50: Share of Material and Manufacturing Costs as a Function of Annual Production Rate

For any reduction of manufacturing costs for certain sub process steps and parts of the stack, which are identified as levers for cost reduction, alternative production processes should be assessed. This approach is demonstrated in Fig. 52. Here cost estimations for two alternative BPP manufacturing processes, which were implemented in the calculation tool, are shown. Highly automated processes such as hydroforming and embossing both scale significantly with increasing production quantities. For the assumptions and input data here used, the embossing process shows to be more expensive for all production rates.

Outlook

The developed dynamic cost estimation tool has several functionalities to assist in manufacturing planning of economic FC stacks. Firstly, by displaying the costs as a function of production quantity, sensitivities in upscaling can be easily identified. Thus, the optimal process chain and technology for a certain envisaged quantity can be identified or for a fixed process chain favorable quantity can be determined. Secondly, total costs of various alternative processes can be compared to each other as well as a baseline scenario such as the "Toyota Mirai" or "DOE" process. Total FC stack costs can also be compared to competing technologies such as ICE or electrical drive systems. Through these functionalities, companies that are planning a specific production line are able to implement their individual planned processes and get insight on total cost, cost distribution and dependency on production quantity.

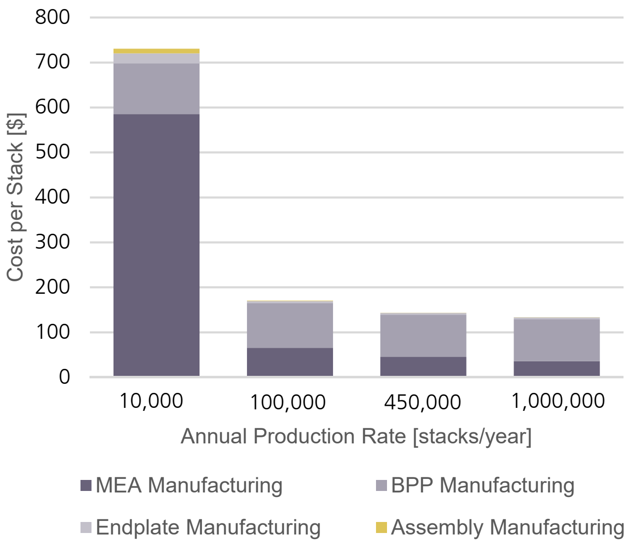

For an Exemplary Production Process and Input Data Obtained from [JAM17]

Fig. 51: Manufacturing Costs per Part as a Function of Annual Production Rate

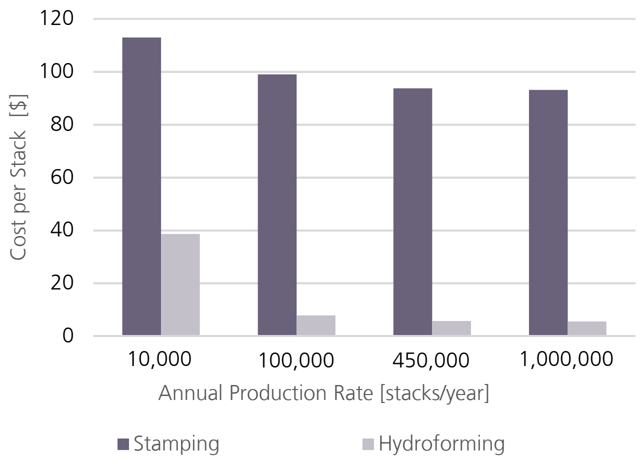

For an Exemplary Production Process and Input Data Obtained from [JAM17]

Fig. 52: Manufacturing Costs of BPP as a Function of Annual Production Rate for Different Processes

THE ROLE OF FRAUNHOFER IPT

Despite recent developments in FC technology, FCs have not yet reached the technological and economical maturity which is required for serial production and economic competitiveness. Further research is needed to reach a sufficient TCO level as well as high technical reliability, low maintenance efforts, long life-time and a higher TRL (see Fig. 53). Many of these challenges are linked to production technology of the FCs. To support the shift from small manufacturing operations to large-scale FC production facilities, Fraunhofer IPT develops solutions to overcome production-technological challenges.

Gaining control over the pending technological challenges is a key factor for the up-scaling of the FC production and thereby making the FC a competitive alternative to other energy storage and drivetrain solutions.

In BPP production, precise forming of the thin plates still has to be realized for high production rates. The joining of two adjacent BPP halves requires advanced clamping technology to control positioning and thermally induced distortion. Based on experiences in sheet metal processes, handling solutions and laser applications, Fraunhofer IPT is a strong partner for the development of manufacturing processes of BPP.

For MEA production, Fraunhofer IPT uses its expertise in rollforming processes to optimize the continuous manufacturing processes. Production of the MEA requires know-how in coating of high viscosity fluids like the CL ink, but also laminating of several layers and subgasket printing. In addition, Fraunhofer IPT gained important insight in applying force and heat over a variable length which is beneficial in all sorts of hot-pressing applications. Depending on the design of the final MEA, Fraunhofer IPT offers support in the single production steps and the layout of production lines.

Being a component between BPP and MEA, the gasket has to fit to both parts in terms of design, material and function. Fraunhofer IPT is working on the assessment of different technologies for the gasket application, in theoretical and experimental approaches. For the production of the FC's components, Fraunhofer IPT offers detailed technology benchmarking and process chain optimization as well as solutions for tooling and equipment development.

During the assembly, single cells are layered on top of each other repeatedly to build the final stack. Regarding the precise handling required to layer the components properly,

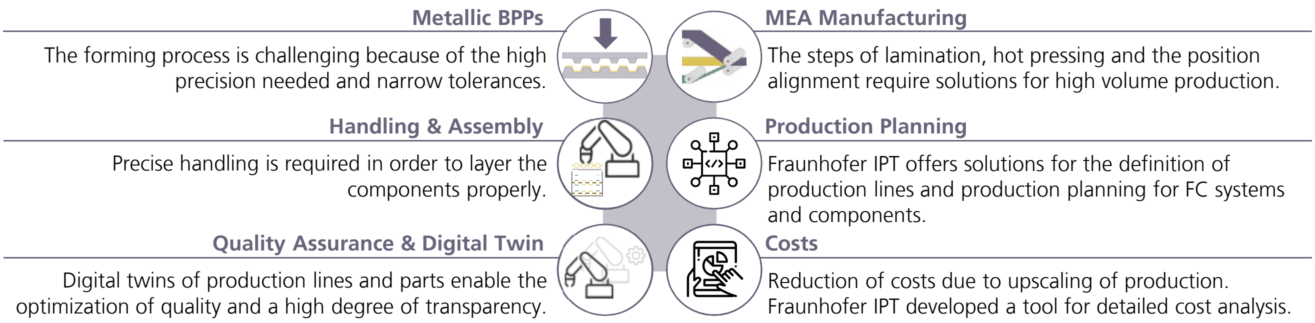

Fig. 53: The Role of Fraunhofer IPT - Surpassing Production-Technological Challenges

Fraunhofer IPT provides expertise in handling technology, gripper equipment and position measurement which is also of great importance for the processing of thin films in MEA production. Exact alignment of different layers like the GDL is needed for high FC efficiency.

With measures of quality control, high precision measurement and digital twins for production processes, Fraunhofer IPT applies knowledge to the optimization of quality and production processes. Fraunhofer IPT continues researching to master the required and critical processes for technology development of FCs. Furthermore, the developed solutions will provide support to utilize the potential for economies of scale for industrial series production of the FC stack, its components, and associated peripheral systems.

CONCLUSION

The increasing demand for zero emission applications shapes an industry around new energy storage technologies. Especially in the mobility sector, innovative powertrain-concepts enrich the landscape of future sustainable technologies.

Among powertrain-concepts including flywheel, SSB or SC, it is the LIB and FC technology that captures special interest. From a technical perspective, LIBs are a mature and broadly applied technology. Their characteristic nonlinear behavior of investment costs as a result of the gravimetric energy density however leads to restrictions in range. This underlines the beneficial linear relation of investment costs, driving range and possible use cases for FCs. Triangulating the advantage from a market perspective, extended range applications among dynamic payloads and extended uptime show potential to meet unmatched market demand. These are requirements which are particularly pronounced in the commercial vehicle sector.

Identifying specific, suitable market applications for FCs to scale production volume to mitigate initial high investments is a major lever to tap the market potential. Companies willing to enter the market should keep key considerations in mind when assessing the market, as exemplary outlined within this study. First, the necessary infrastructure for refueling has to be considered. Commercial applications can be operationalized independently from publicly accessible supplies of hydrogen. In terms of necessary investments, it is possible for FC-fleet operators to build up stations in their hubs on their own. Also, design considerations can further enhance production scalability, and it is argued that hybrid options are most feasible so FCs can run at optimum efficiency. Finally, transparency about production options and costs is necessary to realize cost-efficiency. Within this study, different process line options have been compared regarding advantages in cost, quality and ease of production. A dynamic cost estimation tool was developed for the further assessment of the scalability of production processes. The tool offers functionalities with relevance for manufacturing planning and optimization of the economies of scale in FC stack production.

Practical applications of the cost tool indicate four essential process steps: BPP manufacturing, MEA manufacturing, application of gaskets and the stack assembly. Because of cost-constraints and application-restraints, all of these processes can be adjusted by the selection of materials and production technologies. The description and assessment of production technologies is done for a planar FC design in which the FC stack is assembled with the single components MEA and BPP with an applied gasket. Within the application, material characteristics, such as good corrosion resistance and good formability among a low price lead to the selection of EN 1.4404 (steel) substrate and carbon coating. The materials predetermine the selection of production technology, complemented by selection criteria in terms of operational efficiency and flexibility. Fraunhofer IPT reference production line included PVD, embossing and laser welding as the major technical levers for production.

While materials for MEA do not need forming but rather coating and pressing, they still heavily influence the choice of technologies. Because membranes are easily damaged by solvents from inside the catalyst ink, the proposed manufacturing line employs indirect CCM. This strategy uses a pre-coating system via slot die onto a film which is then transferred onto the membrane. For the chosen use cases, gaskets may best be applied via dispenser for improved durability and high accuracy. The functionalized BPP is then stacked with the MEA during the assembly and tested afterwards via insulation and leakage testing.

As shown in the economical assessment, an upscaling is required to achieve a feasible production and thereby a fast market diffusion. Possible technological solutions have been illustrated and assessed in this study while many technologies unfold their maximum efficiency when perfectly aligned within the production chain and precisely tailored onto the FC design which is determined by the use case. According to first estimations, current production technologies have to be further developed and new innovations are required to meet target production costs published and demanded by political institutions. Solutions from the sector of mechanical and plant engineering are therefore needed for the economic competitiveness of FC and the realization of their advantages in zero emission mobility.

By this study it is therefore important to sense and seize external advances in production technology and market developments as they are major contributors to the market diffusion. However, the final FC design needs to be tailored to the individual use case selected which always has some kind of implication on the production chain. Further improvements and enhancements of production technologies based on the outlined scope of this study need to follow.

LIST OF FIGURES

ACRONYMS

AC	Alternating Current
BEV	Battery Electric Vehicle
BoP	Balance of Plant
BoS	Balance of System
BPP	Bipolar Plate
CCM	Catalyst Coated Membrane
CCS	Catalyst Coated Substrate
CL	Catalyst Layer
CO_2	Carbon-Dioxide
CVD	Chemical Vapor Deposition
DC	Direct Current
DOE	Department of Energy
ECF	Energy Climate Fund
EEG	German Renewable Energy Sources Act
EoL	End of Line
EPDM	Ethylene Propylene Diene Monomer
FC	Fuel Cell
FCE	Fuel Cell Electric
FCEV	Fuel Cell Electric Vehicle
GDL	Gas Diffusion Layer
HRS	Hydrogen Refueling Station
HTG	Handling, Transfer, and Gripping
ICEV	Internal Combustion Engine-based Vehicle
KBA	Kraftfahrt-Bundesamt
LIB	Lithium-Ion Battery
MEA	Membrane Electrode Assembly
NHS	National Hydrogen Strategy
NIP	National Innovation Programme for Hydrogen and Fuel Cell Technology
OEM	Original Equipment Manufacturer
PEM	Proton Exchange Membrane
PEMFC	Proton Exchange Membrane Fuel Cell
PO	Polyolefines
PTFE	Polytetrafluoroethylene
PUR	Polyurethanes
PVD	Physical Vapor Deposition
REDII	Renewable Energy Directive
SC	Supercapacitor
SSB	Solid-State Battery
TCO	Total Cost of Ownership
TRL	Technology Readiness Level
VECO	Vehicle Energy Consumption Calculation Tool

BIBLIOGRAPHY

[ANT19] Antoni, L. et al.: AFC TCP Survey on the number of fuel cell electric vehicle, hydrogen refueling stations and targets. Fuel Cell Vehicles as of End 2018. 2019. Available online: https://www.ieafuelcell.com/fileadmin/publications/2019-04_AFC_TCP_survey_status_FCEV_2018.pdf

[ASR16] Asri, N. F. et al.: Coating of stainless steel and titanium bipolar plates for anticorrosion in PEMFC: A review. In: International Journal of Hydrogen Energy. 2016, 42 (14); pp. 9135–9148

[AZO19] Azom: Chemical Vapor Deposition - What is a CVD Coating? 2019. Available online: https://www.azom.com/article.aspx?ArticleID=17531

[AZO02] Azom: Physical Vapour Deposition (PVD) - An Introduction. 2002. Available online: www.azom.com/article.aspx?ArticleID=1558

[BAL18] Ballard: Ballard Announces Planned Deployment of 500 Fuel Cell Commercial Trucks in Shanghai. 2018. Available online: https://www.ballard.com/about-ballard/newsroom/news-releases/2018/02/14/ballard-announces-planned-deployment-of-500-fuel-cell-commercial-trucks-in-shanghai

[BAR19] Baronas, J. et al.: Joint Agency Staff Report on Assembly Bill 8: 2019 Annual Assessment of Time and Cost Needed to Attain 100 Hydrogen Refueling Stations in California. 2019. Available online: https://ww2.energy.ca.gov/2019publications/CEC-600-2019-039/CEC-600-2019-039.pdf

[BAT16] Batelle Memorial Institute: Manufacturing Cost Analysis of PEM Fuel Cell Systems for 5- and 10-kW Backup Power Applications. 2016. Available online: https://www.energy.gov/sites/prod/files/2016/12/f34/fcto_cost_analysis_pem_fc_5-10kw_backup_power_0.pdf

[BAU20] Baum, C. et al.: Future Energy Storage Systems. Discussion Paper. 2020. Available online: https://doi.org/10.24406/ipt-n-590461

[BAU19] Bauer, A. et al.: Manufacturing of Metallic Bipolar Plate Channels by Rolling. In: Journal of Manufacturing and Materials Processing. 2019, 3 (2)

[BEC18] Reckers, M. et al.: Abschlussbericht. Verbundvorhaben "Low Cost BiP: Klebfügen metallischer Bipolarplatten für PEM-Brennstoffzellen unter den besonderen Anforderungen des automotive Betriebs". Förderkennzeichen: 03ET6029. Laufzeit des Vorhabens: 1. Mai 2014 bis 31. Oktober 2017 (nach Verlängerung). 2018. Available online: https://doi.org/10.2314/GBV:1026023513

[BEN10] Bendzulla, A.: Von der Komponente zum Stack: Entwicklung und Auslegung von HT-PEFC-Stacks der 5 kW-Klasse. Dissertation. RWTH Aachen University. 2010. Available online: https://core.ac.uk/download/pdf/34890454.pdf

[BLA12] Bladergroen, B. et al.: Overview of Membrane Electrode Assembly Preparation Methods for Solid Polymer Electrolyte Electrolyzer. In: Kleperis, J.; Linkov, V. (Eds.): Electrolysis. IntechOpen, London. 2012; pp. 45–60

[BOB20] Bobka, P. et al.: Fast and precise pick and place stacking of limp fuel cell components supported by artificial neural networks. In: CIRP Annals. 2020, 69 (1); pp. 1–4

[BOR17] Borup, R. et al.: (Metal) Bipolar Plate Testing. DOE 2017 Bipolar Plates Workshop. 2017. Available online: https://www.energy.gov/sites/prod/files/2017/05/f34/fcto_biploar_plates_wkshp_borup.pdf

[BRA16] Branson Ultrasonics Corporation: Laser Welding Technical Information. How Laser Welding Works. 2016. Available online: https://www.emerson.com/documents/automation/technical-brief-laser-welding-technical-information-branson-en-us-160146.pdf

[BRA11] Brady, M. P. et al.: Nitrided Metallic Bipolar Plates. In: Satyapal, S. (Ed.): FY 2010 Progress Report for the DOE Hydrogen Program. 2011; pp. 925–929. Available online: https://www.hydrogen.energy.gov/pdfs/progress10/v_l_1_brady.pdf

[BRI11] Briguglio, N. et al.: Fuel Cell Hybrid Electric Vehicles. In: Soylu, S. (Ed.): Electric Vehicles - The Benefits and Barriers. IntechOpen, London. 2011; pp. 93–118

[BRY20a] BryCoat Inc.: BryCoat Titanium Nitride (TiN) Coatings. 2020. Available online: https://www.brycoat.com/surface-engineering/brycoat-pvd-coating-solutions/brycoat-titanium-nitride-tin-coatings/

[BRY20b] BryCoat Inc.: Chromium Nitride (CrN) PVD Coating. 2020. Available online: https://www.brycoat.com/surface-engineering/brycoat-pvd-coating-solutions/chromium-nitride-crn-pvd-coating/

[CEL20] Cellimpact: Cell impact forming. 2020. Available online: https://www.cellimpact.com/technology/high-velocity-forming

[CHE12a] Chen, R. et al.: Modular, High-Volume Fuel Cell Leak-Test Suite and Process (Phase I). Final Technical Report. 2012. Available online: https://www.osti.gov/servlets/purl/1036158

[CHE12b] Chen, T.-C. et al.: Analysis of Stainless Steel Bipolar Plates Micro-Stamping Processes. In: Electrical Review. 2012, 88 (9b); pp. 121–126.

[DAI20] Daimler AG: Daimler Trucks presents technology strategy for electrification – world premiere of Mercedes-Benz fuel-cell concept truck. 2020. Available online: https://media.daimler.com/marsMediaSite/en/instance/ko.xhtml?oid=47453560&relId=1001&resultInfoTypeId=175&ls=L2VuL2luc3RhbmNlL2tvLnhodG1sP29pZD00NzQ2OTQ2MSZyZWxJZD02MDgyOSZmcm9tT2lkPTQ3NDY5NDYxJmJvcmRlcnM9dHJ1ZSZyZXN1bHRJbmZvVHlwZUlkPTQwNjI2JnZpZXdUeXBlPWxpc3Qmc29ydERlZmluaXRpb249UFVCTElTSEVEX0FULTImdGh1bWJTY2FsZUluZGV4PTAmcm93Q291bnRzSW5kZXg9NSZmcm9tSW5mb1R5cGVJZD00MDYyOA!!&rs=0#toRelation

[DEL16] Delgado, O. et al.: Estimating the fuel efficiency technology potential of heavy duty trucks in major markets around the world. 2016. Available online: https://theicct.org/publications/estimating-fuel-efficiency-technology-potential-heavy-duty-trucks-major-markets-around

[DHL20] DHL Paket GmbH: Preferred Day: Delivery on the desired day. 2020. Available online: https://www.dhl.de/content/dam/images/pdf/GK/Services/dhl-wunschtag-infoblatt-en-05-2020.pdf

[DIL04] Dillard, D. A. et al.: Seals and Sealants in PEM Fuel Cell Environments: Materials, Design, and Durability Challenges. In: Shah, R. K.; Kandlikar, S. G. (Eds.): Fuel cell science, engineering and technology 2004 presented at the Second International Conference on Fuel Cell Science, Engineering and Technology, June 14 - 16, 2004, Rochester, New York, USA. ASME, New York. 2004; pp. 553–560

[DUR13] Duran et al.: A Statistical Characterization of School Bus Drive Cycles Collected via Onboard Logging Systems. In: SAE International Journal of Commercial Vehicles. 2013, 6 (2)

[EBR18] Ebrahimzadeh, A. A. et al.: Numerical investigation of dimensions and arrangement of obstacle on the performance of PEM fuel cell. In: Heliyon. 2018, 4 (11)

[EHR19] Ehret, O.: Hydrogen and fuel cells: Eight important questions and answers for the media. 2019. Available online: https://www.now-gmbh.de/content/service/3-publikationen/1-nip-wasserstoff-und-brennstoffzellentechnologie/hydrogen-and-fuel-cells_important-questions.pdf

[EIS10] Eisenführ, F. et al.: Rationales Entscheiden. 5., überarb. und erw. Aufl. Springer, Berlin. 2010

[EUR20a] European Alternative Fuels Observatory: Locations of fuel stations. 2020. Available online: https://www.eafo.eu/fuel-map

[EUR20b] European Environment Information and Observation Network (Eionet): CO2 emissions from passenger transport. 2020. Available online: https://www.eea.europa.eu/media/infographics/CO2-emissions-from-passenger-transport/view

[EUR19] European Commission: Refueling Protocols for Medium and Heavy-Duty Vehicles. 2019. Available online: https://cordis.europa.eu/programme/id/H2020_FCH-04-2-2019/fr

[EUR18] Proposal for a Regulation of the European Parliament and of the council setting CO2 emission performance standards for new heavy-duty vehicles. 2018. Available online: https://eur-lex.europa.eu/resource.html?uri=cellar:f38df734-59da-11e8-ab41-01aa75ed71a1.0001.02/DOC_1&format=PDF

[EUR70] Richtline des Rates zur Angleichung der Rechtsvorschriften der Mitgliedsstaaten über den zulässigen Geräuschpegel und die Auspuffvorrichtung von Kraftfahrzeugen. 70/157/EWG. 1970. Available online: http://data.europa.eu/eli/dir/1970/157/2013-07-01

[EVO18a] EvoBus GmbH: Technische Daten. Die ComfortClass 500. 2018. Available online: https://www.germany.setra-bus.com/content/dam/sbo/markets/common/buy/services-online/download-technical-brochures/images/content/comfort-class-500/s-cc500-2-de-07-18.pdf

[EVO18b] EvoBus GmbH: Technische Daten. Die TopClass 500. 2018. Available online: https://www.germany.

setra-bus.com/content/dam/sbo/markets/common/buy/services-online/download-technical-brochures/images/content/top-class-500/s-tc500-2-de-07-18.pdf

[EVO12] EvoBus GmbH: Specifications. The TopClass 400. 2012. Available online: https://www.setra-bus.com/fileadmin/media/07_Downloads/Broschueren_english/2012_Broschueren_TD_en/2012_en_TD_TC400.pdf

[FED20] Federal Ministry for Economic Affairs and Energy: The National Hydrogen Strategy. 2020. Available online: https://www.bmwi.de/Redaktion/EN/Publikationen/Energie/the-national-hydrogen-strategy.pdf?__blob=publicationFile&v=4

[FRA19] Fraunhofer-Institut für Lasertechnik ILT: Jahresbericht 2018. 2019. Available online: https://www.ilt.fraunhofer.de/content/dam/ilt/de/documents/Jahresberichte/JB18/TF2/HZ_JB18_S80_Laserstrahlschwei%C3%9Fen_von_Bipolarplatten.pdf

[FRA14] Fraunhofer-Institut für Werkstoff- und Strahltechnik IWS: Remote-Laserstrahlschneiden metallischer Werkstoffe. remocut®M. 2014. Available online: https://www.iws.fraunhofer.de/content/dam/iws/de/documents/publikationen/infoblaetter/400-5b_remote_metalle_de.pdf

[FRA13] Fraunhofer-Institut für Lasertechnik ILT: Jahresbericht 2012. 2013. Available online: https://www.ilt.fraunhofer.de/content/dam/ilt/en/documents/annual_reports/ar12/JB12_S75.pdf

[FRA09] Fraunhofer-Institut für Grenzflächen- und Bioverfahrenstechnik IGB: Kein Durchlass für Ethanol – Neue Kompositmembran für Brennstoffzelle. 2009. Available online: https://www.igb.fraunhofer.de/de/presse-medien/presseinformationen/2009/kompositmembran-fuer-brennstoffzelle.html

[FRÖ15] Frölich, K.: Der Decal-Prozess zur Herstellung katalysatorbeschichteter Membranen für PEM-Brennstoffzellen. Dissertation. Karlsruher Institut für Technologie. 2015.

[FUE20] Fuel Cells and Hydrogen Observatory: Cumulative data on installed HRS. 2020. Available online: https://www.fchobservatory.eu/observatory/technology-and-market/hydrogen-refueling-stations/cumulative-data

[FUE11] Fuel Cell and Hydrogen Energy Association: Recommended Standard Test Methods for Fuel Cell Gasket Materials. 2011

[FUK07] Fukutsuka, T. et al.: Carbon-coated stainless steel as PEFC bipolar plate material. In: Journal of Power Sources. 2007, 174 (1); pp. 199–205

[GÄR95] Gärtner, H.: Ionenplattieren. In: Kienel, G.; Röll, K. (Eds.): Vakuumbeschichtung. Verfahren und Anlagen. Springer, Berlin. 1995; pp. 107–126

[GLO20] Global Automotive & Transportation Research Team at Frost & Sullivan: Strategic Collaborations Towards Technology Development Transforming The Global Fuel Cell Vehicles Market, 2020–2030. Establishing a Robust Refuelling Infrastructure and Lowering the Cost of H2 Production to Drive Growth Opportunities. 2020

[GLÜ13] Glüsen, A. et al.: Slot-Die Coating: A New Preparation Method for Direct Methanol Fuel Cells Catalyst Layers. In: Journal of Fuel Cell Science and Technology. 2013, 10 (4)

[GOO20a] Goodfellow: Rostfreier Stahl - Werkstoff Nr. 1.4404 – Folie 0,05 mm. Fe/Cr18/Ni10/Mo 3. As of 13.11.2020. 2020. Available online: http://www.goodfellow.com/de/

[GOO20b] Goodfellow: Rostfreier Stahl - Werkstoff Nr. 1.4404 - Folie 0,1 mm - Fe/Cr18/Ni10/Mo 3. As of 13.11.2020. 2020. Available online: http://www.goodfellow.com/de/

[GRÄ20] Gräbener Maschinentechnik GmbH & Co. KG: Ihre Fertigungstechnik für metallische Mikrostrukturen. Vom Prototyping über die Kleinserie bis hin individuellen Fertigungslinie für das Formen, Schneiden und Schweißen. 2020. Available online: https://www.messe.de/apollo/hannover_messe_2020/obs/Binary/A1004026/25782_43532_1574 41642586924400_aeid_205__265_atomfeld_205_265-13946531574420357.pdf

[GRA11] Grafl, D. et al.: Contact Plate for Fuel Cells. US 8,053,141 B2. 2011

[H2M20] H2 MOBILITY Deutschland GmbH & Co. KG: H2 tanken. Wasserstoffmobilität beginnt jetzt. 2020. Available online: https://h2.live/

[HAL19] Hall, D. et al.: Estimating the infrastructure needs and costs for the launch of zero-emission trucks. 2019. Available online: https://theicct.org/sites/default/files/publications/ICCT_EV_HDVs_Infrastructure_20190809.pdf

[HEL06] Hellwig, W.: Spanlose Fertigung: Stanzen. Grundlagen für die Produktion einfacher und komplexer Präzisions-Stanzteile. 8., aktualisierte und erg. Aufl. Mit 187 Abbildungen und 48 Tabellen. Vieweg & Sohn Verlag, Wiesbaden. 2006

[HÖF17] Höflinger, J. et al.: FCREEV. Ein batterieelektrisches Fahrzeug mit Brennstoffzellen-Range-Extender. In: MTZ - Motortechnische Zeitschrift. 2017, 78 (5); pp. 18–25

[HOK19] HoKyun Ju, S. et al.: Apparatus for Rapidly Stacking Fuel Cell Stack Using Automatic Stacking and Pressurization of Fuel Cell Components. US 2019/0252712 A1. 2019

[HÜG09] Hügel, H. et al.: Laser in der Fertigung. Strahlquellen, Systeme, Fertigungsverfahren. 2., neu bearb. Aufl. Mit 400 Abbildungen. Vieweg + Teubner, Wiesbaden. 2009

[HUN12] Hung, J.-C. et al.: Fabrication of micro-flow channels for metallic bipolar plates by a high-pressure hydroforming apparatus. In: Journal of Power Sources. 2012, 206; pp. 179–184

[HYD20] Hydrogen Council: Path to hydrogen competitiveness. A cost perspective. 2020. Available online: https://hydrogencouncil.com/wp-content/uploads/2020/01/Path-to-Hydrogen-Competitiveness_Full-Study-1.pdf

[HYD17] Hydrogen Europe: Hydrogen Transport & Distribution. 2017. Available online: https://hydrogeneurope.eu/hydrogen-transport-distribution

[HYU20] HYUNDAI SUISSE: Die ersten schweren Brennstoffzellen-Nutzfahrzeuge Hyundai XCIENT Fuel Cell sind unterwegs nach Europa. 2020. Available online: https://aktuell.hyundai.ch/die-ersten-schweren-brennstoffzellen-nutzfahrzeuge-hyundai-xcient-fuel-cell-sind-unterwegs-nach-europa/

[IHI20] IHI HAUZER TECHNO COATING B.V.: Bipolar Plate Coatings. 2020. Available online: https://www.hauzertechnocoating.com/wp-content/uploads/2020/09/24477_hz_folder_bipolar_plate_coatings_lr.pdf

[IMA14] Imamura, J. et al.: Stainless Steel Foil for Bipolar Plates of PEFCs NSSMC-NAR-316BC. Technical Report. 2014. Available online: https://www.nippon-steel.com/en/tech/report/nssmc/pdf/106-18.pdf

[IMP19] Impact Coatings AB: Ceramic Maxphase™ for Fuel Cells. 2019. Available online: https://impactcoatings.com/wp-content/uploads/2017/08/Ceramic_MaxPhase.pdf

[IND08] Indium Corporation: Chemical Vapor Deposition vs. physical Vapor Deposition. 2008. Available online: https://www.google.com/url?sa=t&rct=j&q=&esrc=s&source=web&cd=&ved=2ahUKEwiYz5bZgPrsAhUNGuwKHXS9CX8QFjABegQIAxAC&url=https%3A%2F%2Fdocuments.indium.com%2Fqdynamo%2Fdownload.php%3Fdocid%3D1957&usg=AOvVaw2zeBVsTrSwbSgJsWbKkLch

[ION20] ionbond: Fuel Cell Carbon Technology. 2020. Available online: https://www.ionbond.com/fileadmin/ionbond/global/Factsheets/EN/Fuel_Cell/Ionbond_Factsheet_Fuel_Cell_Carbon_EN_OS.pdf

[JAM19] James, B. D.: 2019 DOE Hydrogen and Fuel Cells Program Review Presentation. Fuel Cell Systems Analysis. 2019. Available online: https://www.hydrogen.energy.gov/pdfs/review19/fc163_james_2019_o.pdf

[JAM18a] James, B.: 2018 Cost Projections of PEM Fuel Cell Systems for Automobiles and Medium-Duty Vehicles. 2018. Available online: https://www.energy.gov/sites/prod/files/2018/04/f51/fcto_webinarslides_2018_costs_pem_fc_autos_trucks_042518.pdf

[JAM17] James, B. D. et al.: Mass Production Cost Estimation of Direct H2 PEM Fuel Cell Systems for Transportation Applications: 2017 Update. 2017. Available online: http://www.sainc.com/assets/site_18/files/publications/sa%202017%20transportation%20fuel%20cell%20cost%20analysis.pdf

[JEN17] Jendras, P. et al.: Strömungssimulation zur Optimierung von Flussfeldern in PEM-Brennstoffzellen. 9. Anwendertreffen SAXSIM –Chemnitz, 28. März 2017. 2017. Available online: https://monarch.qucosa.de/api/qucosa%3A20723/attachment/ATT-0/

[JAM18b] James, B. et al.: Fuel Cell Vehicle Cost Analysis. In: Satyapal, S. (Ed.): FY 2017 Progress Report For The DOE Hydrogen And Fuel Cells Program. 2018. Available online: https://www.hydrogen.energy.gov/pdfs/progress17/v_e_5_james_2017.pdf

[JÖR17] Jörissen, L. et al.: Polymerelektrolytmembran-Brennstoffzellen (PEFC) Stand und Perspektiven. In: Töpler, J.; Lehmann, J. (Eds.): Wasserstoff und Brennstoffzelle. Springer, Berlin, Heidelberg. 2017; pp. 263–313.

[KAJ13] Kaji, Y. et al.: Verfahren und Vorrichtung zur Herstellung von Membranelektroden für Brennstoffzellen. DE 102 43 100 C5. 2013

[KAR12] Karimi, S. et al.: A Review of Metallic Bipolar Plates for Proton Exchange Membrane Fuel Cells: Materials and Fabrication Methods. In: Advances in Materials Science and Engineering. 2012.

[KAZ08] Kaz, T.: Herstellung und Charakterisierung von Membran-Elektroden-Einheiten für Niedertemperatur Brennstoffzellen. Dissertation. Universität Stuttgart. 2008

[KLU19] Kluschke, P. et al.: What is the design of a potential HDV HRS network in Germany in 2050? In: AVERE – The European Association for Electromobility (Ed.): Proceedings of the 32nd Electric Vehicle Symposium 2019. Available online: https://www.google.com/url?sa=t&rct=j&q=&esrc=s&source=web&cd=&ved=2ahUKEwjGm93T8urrAhVQDewKHYl0DccQFjAAegQIBBAB&url=https%3A%2F%2Fpapers.evs32.org%2Fdownload.php%3Ff%3Dpapers%2Fevs32-830037.pdf&usg=AOvVaw1c1rJf-KSasBCIKqiv5OtX

[KUN17] Kunith, A.: Elektrifizierung des urbanen öffentlichen Busverkehrs. Technologiebewertung für den kosteneffizienten Betrieb emissionsfreier Bussysteme. Springer, Wiesbaden. 2017

[KOÇ09] Koç, M. et al.: PEMFC Metallic Bipolar Plates: Effect of Manufacturing Method on Corrosion Resistance. In: ECS Transcations. 2009, 25 (1); pp. 1773–1782

[KOP17] Kopasz, J. P. et al.: 2017 Bipolar Plate Workshop Summary Report. 2017. Available online: https://publications.anl.gov/anlpubs/2017/11/137641.pdf

[KRA18] Kraftfahrt-Bundesamt: Fahrzeugzulassungen (FZ). Neuzulassungen, Besitzumschreibungen, Außerbetriebsetzungen von Kraftfahrzeugen und Kraftfahrzeuganhängern. Jahr 2017. FZ 7. 2018. Available online: https://www.kba.de/SharedDocs/Publikationen/DE/Statistik/Fahrzeuge/FZ/2017/fz7_2017_pdf.pdf?__blob=publicationFile&v=9

[KRU99] Krumpiegl, T. et al.: Amorphous carbon coatings and their tribological behaviour at high temperatures and in high vacuum. In: Surface and Coatings Technology. 1999, 120-121; pp. 555–560

[KUM20] Kumaraguru, S. P. et al.: System and Method for MEA Conditioning in a Fuel Cell. US 10,784,527 B2. 2020

[KUR16] Kurzweil, P.: Brennstoffzellentechnik. Grundlagen, Materialien, Anwendungen, Gaserzeugung. 3. Auflage. Springer, Wiesbaden. 2016

[LAM13] Lampert, C.: Vacuum Deposition and Coating Options. 2013. Available online: https://www.pfonline.com/articles/vacuum-deposition-and-coating-options

[LEA19] Leaver, J.: Hydrogen and New Zealand's Heavy Vehicle Fleet. 2019. Available online: https://unitec.researchbank.ac.nz/bitstream/handle/10652/4719/Leaver%2c%20J.%20%282019%29.pdf?sequence=4&isAllowed=y

[LEE10] Lee, K. S. et al.: Method of Manufacturing Membrane-Electrode Assembley for Fuel Cell. US 7,837,819 B2. 2010

[LUD20] Ludwig-Bölkow-Systemtechnik GmbH: Statistics: Hydrogen Infrastructure. 2020. Available online: https://www.h2stations.org/statistics/

[LUD17] Ludwig-Bölkow-Systemtechnik GmbH: Sharp growth of hydrogen refuelling station numbers in Europe within the next 10 years. 2017. Available online: http://www.lbst.de/news/2017_docs/LBST%20Markt%20Trend%20Wasserstofftankstellen%202017_EN%20(2).pdf

[MAH10] Mahabunphachai, S. et al.: Effect of manufacturing processes on formability and surface topography of proton exchange membrane fuel cell metallic bipolar plates. In: Journal of Power Sources. 2010, 195 (16); pp. 5269–5277

[MAR16] Marcinkoski, J. et al.: Driving an Industry: Medium and Heavy Duty Fuel Cell Electric Truck Component Sizing. In: World Electric Vehicle Journal. 2016, 8 (1); pp. 78-89

[MEH03] Mehta, V. et al.: Review and analysis of PEM fuel cell design and manufacturing. In: Journal of Power Sources. 2003, 114 (1); pp. 32–53

[MIL15] Millichamp, J. et al.: Mechanisms and effects of mechanical compression and dimensional change in

polymer electrolyte fuel cells – A review. In: Journal of Power Sources. 2015, 284; pp. 305–320
[MOH16] Mohammadtabar, N. et al.: Feasibility study of a double-step hydroforming process for fabrication of fuel cell bipolar plates with slotted interdigitated serpentine flow field. In: The International Journal of Advanced Manufacturing Technology. 2016, 85 (1-4); pp. 765–777
[MÜL19] Müller, C. et al.: Analysis of Forming Technologies for the Production of Bipolar Plates. In: Unwerth von, T.; Drossel, W.-G. (Eds.): Konferenzband der ersten FC³ Fuel Cell Conference Chemnitz. 26. und 27. November 2019. Universitätsverlag Chemnitz, Chemnitz. 2019; pp. 113–122. Available online: https://nbn-resolving.org/urn:nbn:de:bsz:ch1-qucosa2-362327
[NET19] Neto, D. M. et al.: Numerical Study on the Formability of Metallic Bipolar Plates for Proton Exchange Membrane (PEM) Fuel Cells. In: Metals. 2019, 9 (7)
[NEU20] Neuhausen, J. et al.: Making zero-emission trucking a reality. Truck Study 2020: Routes to decarbonizing commercial vehicles. 2020. Available online: https://www.strategyand.pwc.com/de/de/studien/2020/green-trucking/truck-study-2020.pdf
[NOW20] NOW GmbH: Development of a hydrogen refuelling station network for fuel cell vehicles in Germany. 2020. Available online: https://www.now-gmbh.de/en/national-innovation-programme/aufbau-wasserstoff-tankstellennetz
[PAK18] Pakamanesh, M. R. et al.: Optimization of pulsed laser welding process parameters in order to attain minimum underfill and undercut defects in thin 316L stainless steel foils. In: Optics & Laser Technology. 2018, 99; pp. 30–38
[PAK12] Pak, C. et al.: High Performance Membrane Electrode Assemblies by Optimization of Processes and Supported Catalysts. In: Minic, D. (Ed.): Hydrogen Energy - Challenges and Perspectives. IntechOpen, London. 2012; pp. 259–278
[PEH15] Pehlivan-Davis, S.: Polymer Electrolyte Membrane (PEM) Fuel Cell Seals Durability. Dissertation. Loughborough University. 2015. Available online: https://repository.lboro.ac.uk/account/articles/9232517
[REU17] Reuter, B. et al.: New Bus ReFuelling for European Hydrogen Bus Depots. Guidance Document on Large Scale Hydrogen Bus Refuelling. 2017. Available online: https://www.fuelcellbuses.eu/sites/default/files/documents/NewBusFuel_D4.3_Guidance-document-for-large-scale-hydrogen-refuelling_final.pdf
[REX17] Rexeis, M. et al.: VECTO tool development: Completion of methodology to simulate Heavy Duty Vehicles' fuel consumption and CO2 emissions. Upgrades to the existing version of VECTO and completion of certification methodology to be incorporated into a Commission legislative proposal. Specific Contract N° 34020112014/695203/SERJCLIMA.C.2. Framework contract CLIMA.C.2/FRA/2013/0007. By order ofEUROPEAN COMMISSIONDG CLIMA. Report No. I 15/17/Rex EM-I 2013/08 1670 from 30.10.2017. 2017. Available online: https://ec.europa.eu/clima/sites/default/files/transport/vehicles/docs/sr7_lot4_final_report_en.pdf
[RIC17] Ricardo Energy & Environment: Heavy Duty Vehicles Technology Potential and Cost Study. Final Report for the International Council on Clean Transportation (ICCT). 2017. Available online: https://theicct.org/sites/default/files/publications/HDV-Technology-Potential-and-Cost-Study_Ricardo_Consultant-Report_26052017_vF.pdf
[ROD18] Rodríguez, F. et al.: Fuel consumption testing of tractor-trailers in the European Union and United States. 2018. Available online: https://theicct.org/sites/default/files/publications/EU_HDV_Testing_BriefingPaper_20180515a.pdf
[SAM19] Sampietro, J. L. et al.: Optimal Sizing of Storage Elements for a Vehicle Based on Fuel Cells, Supercapacitors, and Batteries. In: Energies. 2019, 12 (5)
[SAN20] Sandvik AB: Sandvik Sanergy® LT pre-coated strip steel for bipolar plates for PEM FC. 2020. Available online: https://www.materials.sandvik/en/products/strip-steel/strip-products/coated-strip-steel/sandvik-sanergy-lt/
[SAN19] Santangelo, P. E. et al.: Review of Catalyst-deposition Techniques for PEMFC Electrodes. In: Tecnica Italiana - Italian Journal of Engineering Science. 2019, 63 (1); pp. 65–72

[SHA17] Sharretts Plating Company: Benefits of Gold-Plated Electrical Contacts. 2017. Available online: https://www.sharrettsplating.com/blog/gold-plated-electrical-contacts/

[SCH06] Schrooten, J. A. et al.: Performance Enhancing Break-In Method for a PEM Fuel Cell. US 7,078, 118 B2. 2006

[SHA10] Shang. J.: et al.: Commercialization of Fuel Cell Bipolar Plate Manufacturing by Electromagnetic Forming. In: Daehn, G. (Ed.): High speed forming 2010: proceedings of the 4th international conference: March 9th - 10th, 2010, Columbus, Ohio, USA. IUL, Dortmund. 2010; pp. 47–56

[SIE15] Siegel, F.: Tiefdruckverfahren zur Herstellung von Katalysatorschichten für (PEM) Brennstoffzellen. Dissertation. Technische Universität Chemnitz. 2015. Available online: https://monarch.qucosa.de/api/qucosa%3A20464/attachment/ATT-0/

[SIM89] Simon, H. et al.: Angewandte Oberflächentechnik für metallische Werkstoffe. Eignung, Verfahren, Prüfung. 2., durchges. Aufl. Hanser, München. 1989

[SON12] Son, C.-Y. et al.: Evaluation of the formability of a bipolar plate manufactured from aluminum alloy Al 1050 using the rubber pad forming process. In: Proceedings of the Institution of Mechanical Engineers, Part B: Journal of Engineering Manufacture. 2012, 226 (5); pp. 909–918

[SPI19] Spiegel, C.: Building a Micro DMFC Design. 2019. Available online: https://www.fuelcellstore.com/blog-section/fuel-cell-basics/building-a-micro-dmfc-design

[SPI18] Spiegel, C.: Considerations for Stainless Steel Bipolar Plate Manufacturing: Part 2. 2018. Available online: https://www.fuelcellstore.com/blog-section/fuel-cell-materials-blog/considerations-for-stainless-steel-bipolar-plate-manufacturing-part-2

[SPI17] Spiegel, C.: Flow-Field Design. 2017. Available online: https://www.fuelcellstore.com/blog-section/flow-field-design

[STR15] Strong, A. et al.: Depositing Catalyst Layers in Polymer Electrolyte Membrane Fuel Cells: A Review. In: Journal of Fuel Cell Science and Technology. 2015, 12 (6)

[SUS19] Sustainable Bus: Hydrogen at scale for transit. What does it mean to operate fuel cell buses? 2019. Available online: https://www.sustainable-bus.com/news/hydrogen-at-scale-for-transit-what-does-it-mean-to-operate-fuel-cell-buses/

[TAW07] Tawfik, H. et al.: Metal bipolar plates for PEM fuel cell—A review. In: Journal of Power Sources. 2007, 163 (2); pp. 755–767

[TER15] Terry, F.: Untersuchungen zur Alterungsbeständigkeit von Dichtungen in PEM-Brennstoffzellen. Dissertation. Universität Ulm. 2015

[THA10] Thanasilp, S. et al.: Effect of MEA fabrication techniques on the cell performance of Pt–Pd/C electrocatalyst for oxygen reduction in PEM fuel cell. In: Fuel. 2010, 89 (12); pp. 3847–3852

[THE18] The International Stainless Steel Forum: New Application Awards 2018. 2018. Available online: https://www.worldstainless.org/files/issf/non-image-files/PDF/ISSF_New_Applications_Award_2018.pdf

[TIN09] Tingelöf, T. et al.: A rapid break-in procedure for PBI fuel cells. In: International Journal of Hydrogen Energy. 2009, 34 (15); pp. 6452–6456

[TOW07] Towne, S. et al.: Fabrication of polymer electrolyte membrane fuel cell MEAs utilizing inkjet print technology. In: Journal of Power Sources. 2007, 171 (2); pp. 575–584

[TÜV19] TÜV SÜD AG: Highest Increase of Hydrogen Refuelling Stations in Germany Worldwide in 2018 Again. 2019. Available online: https://www.tuvsud.com/en/press-and-media/2019/february/highest-increase-of-hydrogen-refuelling-stations-in-germany-worldwide-in-2018-again

[VER14] Verband Deutscher Verkehrsunternehmen e. V. (VDV): 2013/2014. Jahresbericht. 2014. Available online: https://www.mobi-wissen.de/files/jahresbericht-2013-2014.pdf

[VON20] VON ARDENNE: Vacuum Coating Technology & Equipment. Contact & Protection Coatings for Metal Bipolar Plates. 2020. Available online: https://www.vonardenne.biz/fileadmin/user_upload/VAOP/druckschriften/www/pdf/Bipolar_Plates_Vacuum_Coating_SPA_eng.pdf

[WAG20] Wagner, I.: Projected market demand for lithium-ion batteries used in electric vehicles in 2030, by application. 2020. Available online: https://www.statista.com/statistics/888258/market-demand-for-lithium-ion-batteries-in-electric-vehicles-by-application/

[WAL20] Walter, A.: Assembly Device for Stacking a Fuel Cell Stack. US 2020/0036026 A1. 2020

[WAN17] Wang, C.: Corrosion Resistant Coating of Metal Bipolar Plates for PEM Fuel Cells. Workshop on Research and Development Needs for Bipolar Plates for PEM Fuel Cell Technologies. 2017. Available online: https://www.energy.gov/sites/prod/files/2017/05/f34/fcto_biploar_plates_wkshp_wang.pdf

[WAN06] Wang, S.-H. et al.: Performance of the gold-plated titanium bipolar plates for the light weight PEM fuel cells. In: Journal of Power Sources. 2006, 162 (1); pp. 486–491

[WAT20] WaterstofNet: NIKOLA Two: hydrogen electric day cab. 2020. Available online: https://fuelcelltrucks.eu/project/nikola-two/

[WEI19] Weiler, T.: Innovationspotentiale in der Brennstoffzellenfertigung. Promotionsvortrag. RWTH Aachen University. 2019. Available online: https://www.researchgate.net/publication/339953484_Innovationspotentiale_in_der_Brennstoffzellenfertigung

[WEI13] Weissbecker, V. et al.: A Comprehensive Corrosion Study on Metallic Materials for HT-PEFC Application. In: ECS Transactions. 2013, 58 (1); pp. 693–704

[WET17] Wetzig, A. et al.: Latest Developments of Laser Cutting. In: Laser Institute of America (Ed.): ICALEO 2016, 35th International Congress on Applications of Lasers & Electro-Optics. Online resource: October 16-20, 2016, San Diego, California, USA. Laser Institute of America, Orlando. 2017

[WIL17] Wilberforce, T. et al.: Developments of electric cars and fuel cell hydrogen electric cars. In: International Journal of Hydrogen Energy. 2017, 42 (40); pp. 25695–25734

[YAN10] Yan, X.-T. et al.: Chemical Vapour Deposition. An Integrated Engineering Design for Advanced Materials. Springer, London. 2010

[YIP13] Yi, P. et al.: Cr–N–C multilayer film on 316L stainless steel as bipolar plates for proton exchange membrane fuel cells using closed field unbalanced magnetron sputter ion plating. In: International Journal of Hydrogen Energy. 2013, 38 (3); pp. 1535–1543

[YIP10] Yi, P. et al.: Performance of a Proton Exchange Membrane Fuel Cell Stack Using Conductive Amorphous carbon-coated 304 stainless steel bipolar plates. In: Journal of Power Sources. 2010, 195 (20); pp. 7061–7066

[YOO08] Yoon, W. et al.: Evaluation of coated metallic bipolar plates for polymer electrolyte membrane fuel cells. In: Journal of Power Sources. 2008, 179 (1); pp. 265-273

[ZHA17] Zhang, P. et al.: Deformation in Micro Roll Forming of Bipolar Plate. In: Journal of Physics: Conference Series. 2017, 896

[ZHA99] Zhang, S. et al.: Improving the adhesion of amorphous carbon coatings on cemented carbide through plasma cleaning. In: Surface and Coatings Technology. 1999, 113 (1-2); pp. 120–125

Fraunhofer Institute for
Production Technology IPT
Steinbachstrasse 17
52074 Aachen
Germany
Phone +49 241 8904-0
info@ipt.fraunhofer.de
www.ipt.fraunhofer.de

Authors
Dr.-Ing. Christoph Baum
Dr.-Ing. Dipl.-Wirt. Ing. Henning Janssen
Prof. Dr.-Ing. Christian Brecher
Prof. Dr.-Ing. Dipl.-Wirt. Ing. Günther Schuh

Martin Aretz, Carolin Hamm, Rainer Horstkotte,
Marlin Kersting, Sangwook Lee, Angela Massonet,
Clemens Müller, Maximilian Nadicksbernd, Ulla Panchenko,
Leonard Schenk, Paul Scholz, Toni Voebel

Your Contact
Clemens Müller
Business Unit Manager Energy Storage Systems
Phone +49 241 8904-469
clemens.mueller@ipt.fraunhofer.de

Project Management of the Study
Paul Scholz
Phone +49 241 8904-315
paul.scholz@ipt.fraunhofer.de

Carolin Hamm
Phone +49 241 8904-737
carolin.hamm@ipt.fraunhofer.de

ISBN 978-3-00-067727-4
DOI: 10.24406/IPT-N-633591